AD NUMBER

AD839883

NEW LIMITATION CHANGE

TO

Approved for public release, distribution unlimited

FROM

Distribution authorized to U.S. Gov't. agencies and their contractors; Administrative/Operational use; 3 Sep 1968. Other requests shall be referred to AFAPL, Air Force Systems Command, Wright Patterson Air Force Base, OH 45433 Attn: Flight Vehicle Power Branch Aero Space

AUTHORITY

AFAPL ltr, 12 Apr 1972

AFAPL-TR-68-115

SILVER-ZINC ELECTRODES

And

SEPARATOR RESEARCH

J. A. Keralla

Delco-Remy Division, General Motors Corporation

TECHNICAL REPORT AFAPL-TR-68-115

3 September 1968

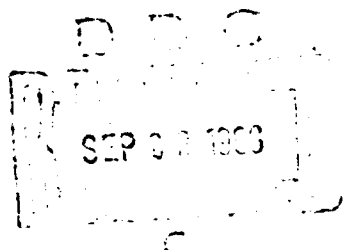

AFAPL-TR-68-115

SILVER-ZINC ELECTRODES

And

SEPARATOR RESEARCH

J. A. Keralla

Delco-Remy Division, General Motors Corporation

TECHNICAL REPORT AFAPL-TR-68-115

3 September 1968

Air Force Aero Propulsion Laboratory

Air Force Systems Command

Wright Patterson Air Force Base, Ohio

REPRODUCTION QUALITY NOTICE

This document is the best quality available. The copy furnished to DTIC contained pages that may have the following quality problems:

- Pages smaller or larger than normal.
- Pages with background color or light colored printing.
- Pages with small type or poor printing; and or
- Pages with continuous tone material or color photographs.

Due to various output media available these conditions may or may not cause poor legibility in the microfiche or hardcopy output you receive.

☐ If this block is checked, the copy furnished to DTIC contained pages with color printing, that when reproduced in Black and White, may change detail of the original copy.

839883

NOTICE

FOREWORD

This report was prepared by Delco-Remy Division of General Motors Corporation, Anderson, Indiana, on Air Force Contract Nr. AF33(615)-3487, under Task Nr. 314522 of Project Nr. 3145, "Silver-Zinc Electrodes and Separator Research." The work was administered under the direction of the Static Energy Conversion Section, Flight Vehicle Power Branch, Aero Space Power Division, Aero Propulsion Laboratory; Mr. J. E. Cooper was task engineer for the laboratory.

The assistance of Dr. T. P. Dirkse, Professor of Chemistry, Calvin College, Grand Rapids, Michigan, as consultant on this project is greatly appreciated.

This report was submitted by the authors on 31 August 1968.

J. A. Keralla
Engineer - Power Systems
Delco-Remy Division, GMC

ABSTRACT

Carbowaxes in a molecular weight range of 1000 give comparable cycle life with Emulphogene BC-610. As carbowaxes are linear polyethyleneoxide polymers and as Emulphogenes contain a polyethylene oxide chain, it is surmised that the polyethyleneoxide structure is active in promoting cycle life.

The addition of .25% Pb in ZnO tends to reduce agglomeration of the formed zinc and to prolong cycle life.

The limit of .010% Fe in ZnO is tolerable for satisfactory cycle life.

The use of CaO in the negative material to produce insoluble sites for zincate stoppage is not satisfactory.

Some evidence of pore sizes of various separator membranes have been found through electron microscope studies.

Increasing the stoichiometric ratio of formed zinc is not practical in terms of redesigning the present cell because of increased volume with a small increase in cycle life.

The 90 Mrad precrosslinked Bakelite 0602 polyethylene base, radiation grafted methacrylic acid membrane is suitable for use as a separator in secondary silver-zinc batteries.

TABLE OF CONTENTS

LIST OF FIGURES

LIST OF FIGURES (Continued)

LIST OF FIGURES (Continued)

LIST OF TABLES

I. INTRODUCTION

The objectives of this program are to provide design criteria for long life (5000 cycles), light weight (25 wh/#) silver-zinc batteries for military aerospace applications. Effort will be concentrated on the zinc electrode and separator since these are recognized as the major causes of premature failure of the silver-zinc battery.

The specific items presently under study in this contract are:

A. Surfactant Additions
B. Fundamental Studies on Surfactants
C. Particle Size & Morphology of Zinc Oxides
D. Zinc Electrode Fabrication Techniques
E. Influence of Membrane Separator Characteristics
F. Sites for Zinc Oxide Overgrowths
G. Development of Failure Analysis Techniques
H. Sizes of Zincate Ion and Soluble Silver Species in KOH
I. Membrane Pore Size Measurements in KOH
J. Stoichiometric Ratio of Formed Zinc
K. Alternate Method of Surface Area Measurement
L. Separator Development

This report covers the second years' work on most of the above items. Most of the cells were cycled at 60% depth-of-discharge at the two-hour cycle program of 35 minutes discharge and 85 minutes charge. In the separator testing program, 40% and 25% depth-of-discharge were also employed.

II. FACTUAL DATA

A. Surfactant Additions

One-hundred-and-eight 25 a.h. cells have been constructed in two groups of 54 cells. One group having 2% cotton fibers in the negative material along with various concentrations of carbowaxes of three different molecular weight ranges. The second group of 54 cells is the same, but does not contain 2% cotton fibers in the negative material. The following table shows the concentration and cycle life obtained at 60% depth of discharge.

Table I

Cells	Moiecular Weight	Carbowax Concentration	Initial Capacity	Cycles Without 2% Cotton	Cycles With 2% Cotton
6	6000	.3%	24 a.h.	156	148
6	6000	.6%	23	132	148
6	6000	1.0%	23	132	148
6	1000	.3%	22 a.h.	204	132
6	1000	.6%	22	204	156
6	1000	1.0%	22	204	156
6	200	.3%	22 a.h.	120	108
6	200	.6%	23	108	108
6	200	1.0%	22	98	108
6	Controls		21.0	84	

The cause of failure in all cells was loss of negative plate capacity. The use of cotton fibers in the negative electrode does not appear to improve cell cycle ability. The carbowax mecular weight range of 1000 appears to have a strong effect on increasing cycle life. Table II shows the appearance of cell components after cycle testing. Figures 1, 2 and 3 show the photomicrographs of negative plates containing 1% carbowax in the three molecular weight ranges.

TABLE II

Study: Surfactants

Note: All cells contained 8 positive plates 4" x 2-1/2" x .015" with 12g silver; 7 negative plates 4" x 2-1/2" x .050" with 20g ZnO and 2% H_2O. The separator system was one layer of acrylonitrile monower & four layers of reinforced cellulosic material. Electrolyte was 90cc, 50% KOH.

Cell No.	Surfactant	Condition of Positive Plate	Condition of Separation	Condition of Negative Plate				Cause of Failure
				Extent Formed	Treeing	Material Creeping	Material Washed Out	
1-6	.7% LSA	Good-well formed	Good-no pin holes or tears	90% ZnO	None	None	10-20%	Shedding of material and subsequent loss of plate capacity
7-12	1.1% LSA	"	"	"	"	Light-though 2 layers	20-30%	
13-18	1.1% LSA + 5% $ZnSO_4$	"	1st layer deteriorated-rest o.k.	75% ZnO	Light	Medium-around 4 layers	40-50%	"
19-24	1.1% LSA + 1% FC95	"	"	75% ZnO	Medium	"	20-30%	"
25-30*	None	"	"	"	"	"	50-60%	"
31-36	.3% carbowax 6000	"	Good	75%-90% ZnO	None	Light-2 layers	40-50%	"
37-42	.6% carbowax 6000	"	"	"	"	"	"	"
43-48	1% carbowax 6000	"	"	"	"	"	"	"
49-54	.3% carbowax 6000 + 2% cotton fibers	"	"	"	"	"	"	"
55-60	.6% carbowax 6000 + 2% cotton fibers	"	"	"	"	"	"	"
61-66	1% carbowax 6000 + 2% cotton fibers	"	"	"	"	"	"	"
67-72	.3% carbowax 1000	"	1st layer deteriorated-rest o.k.	70% ZnO	Medium	Medium-4 layers	50-60%	"
73-78	.6% carbowax 1000	"	"	"	"	"	"	"
79-84	1% carbowax 1000	"	"	"	"	"	"	"
85-90	.3% carbowax 1000 + 2% cotton fibers	"	Good	"	None to light	"	50%	"
91-96	.6% carbowax 1000 + 2% cotton fibers	"	"	"	"	"	"	"
97-102	1% carbowax 1000 + 2% cotton fibers	"	"	"	"	"	"	"
102-107	.3% carbowax 200 + 2% cotton fibers	"	"	90% ZnO	None	2 layers	40-50%	"
108-113	.6% carbowax 200 + 2% cotton fibers	"	"	"	"	"	"	"
114-119	1% carbowax 200 + 2% cotton fibers	"	"	"	"	"	"	"
120-125	.3% carbowax 200	"	"	"	Heavy	Medium-4 layers	30-40%	"
126-131	.6% carbowax 200	"	"	"	"	"	"	"
132-137	1% carbowax 200	"	"	"	"	"	"	"

(*) Control cells

Thirty 25 a.h. cells were constructed containing various percentages of LSA (lignosulfonic acid) $ZnSO_4$, and FC95 incorporated in the negative plate. Table III shows the cells with the percentages of additives and the number of cycles obtained at 60% depth-of-discharge.

Table III

No. of Cells	Percent Additive	Initial Capacity	Cycles
6	.7% LSA	23 a.h.	108
6	1.1% LSA	24	108
6	5% $ZnSO_4$+ 1.1% LSA	24	96
6	5% $ZnSO_4$+ 1% FC95	23	96
6	Controls	24	148

The cause of failure was loss of negative plate capacity. Table II shows the appearance of cell components after cycle testing. Figure 4 shows a photomicrograph of a negative plate containing 1.1% LSA after 108 cycles. Figure 5 shows a negative plate containing 5% $ZnSO_4$ and 1.1% LSA after 96 cycles.

B. Fundamental Studies on Surfactants

The sixth Quarterly Report on "Adsorption of Organic Materials on Zinc Electrodes" from the University of Texas is attached.

C. Particle Size and Morphology of Zinc Oxides

Fifteen samples of zinc-oxide powders have been submitted by the New Jersey Zinc Company for evaluation in 25 a.h. cells. Ten of these samples contain percentage ranges of metals previously tested and are considered to be most

advantageous to prolonging cycle life with the exception of iron additions. These samples containing iron were tested to determine allowable limits of iron in ZnO as impurity that is not detrimental to cycle life. The limits ranged from a high of .07% to a low of .0003%.

In addition, three repeat samples of ZnO reported in the Sixth Quarterly Technical Report were tested.

Table IV shows the percentage of additives in the various ZnO samples, and the number of cycles obtained at 60% depth-of-discharge.

Table IV

No. Cells	ZnO Sample	Additive	Initial Capacity	Cycles
6	243-127-2	.0008% Pb .0003% Fe	23.5 ah	202
6	243-107-4	.028% Pb .0003% Fe	24	214
6	243-107-2	1.02% Pb .0003% Fe	21	221
6	243-107-3	2.42% Pb .0004% Fe	22.5	214
6	243-131-1	.0006% Fe	23.5	178
6	243-131-2A	0.0086% Fe	20	168
6	243-131-2B	.0092% Fe	24	120
6	243-135-1	.26% Pb .010% Fe	23	192
6	243-139-1	.07% Al .0010% Fe	23	156
6	243-139-2	.92% Al .0008% Fe	24	167

Table IV (Cont'd.)

No. Cells	ZnO Sample	Additive	Initial Capacity	Cycles
6	243-107-1*	.25% Pb	23 a.h.	221
6	243-99-1*	.07% Fe	0	0
6	243-41-1*	.30% Al	24	170
6	Controls (KADOX-15)	- - - -	24	170
6	243-115-1 Blue Powder	.14% Fe	0	0
6	243-119-1 Zinc Dust	.0001% Fe	23	168
6	243-123-1 Flaked Zinc Dust	.003% Fe	23	204
6	Controls (KADOX-15)	- - - -	24	130
6	243-111-1	.027% As	20	80
6	243-103-1	.089% Mn	23	130

*repeat samples

The cause of failure was due to loss of capacity of the negative electrode. The cells containing lead and flaked zinc dust, and in combination with iron (.010%) gave the largest cycle life. Cells containing an excessive (over .010% apparently) amount of iron did not cycle; in fact, the zinc oxide did not reduce to zinc on initial formation due to the lowered Zn/ZnO potential.

Table V shows the appearance of the cell components after testing. Figures 6 through 24 show photomicrographs of negative plates representative of the ZnO samples after completion of the indicated cycles.

TABLE V

Study: Particle Size and Morphology of Zinc Oxides

Note: Same as Table II

Cell No.	ZnO Sample	Additive	Condition of Positive Plate	Condition of Separator	Condition of Negative Plate				Cause of Failure
					Extent Formed	Treeing	Material Creeping	Material Washed Out	
1-6	243-127-2	.0008% Pb .0003% Fe	Formed	Good	50%	None	Medium-around 3 layers	35-45%	Loss of negative capacity
7-12	243-107-4	.028% Pb .0003% Fe	"	"	"	"	"	"	"
13-18	243-107-2	1.02% Pb .0003% Fe	"	"	"	"	"	30-40%	"
19-24	243-107-3	2.42% Pb .0004% Fe	"	"	"	"	"	"	"
25-30	243-131-1	.0006% Fe	"	"	"	"	"	"	"
31-36	243-131-2A	.0086% Fe	"	"	"	"	"	"	"
37-42	243-131-2B	.0092% Fe	"	"	"	"	Light-around 2 layers	25-30%	"
43-48	243-135-1	.26% Pb .010% Fe	"	"	"	"	"	30-40%	"
49-54	243-139-1	.07% Al .0010% Fe	"	"	"	"	"	"	"
55-60	243-139-2	.92% Al .0008% Fe	"	"	"	Light	Medium-around 3 layers	35-45%	"
61-66	243-107-1	.25% Pb	"	"	"	None	"	40-50%	"
67-72	243-99-1	.07% Fe	"	"	0%	None	None	None	Fe lowered Zn/ZnO Potential
73-78	243-41-1	.30% Al	"	"	50%	"	Light-2 layers	40-50%	Loss of negative capacity
79-84*	KADOX-15	None	"	"	"	"	Medium-3 layers	50-60%	"
85-90	243-115-1	.14% Fe.	"	"	25%	"	None	None	Fe lowered Zn/ZnO Potential
91-96	243-119-1	Zinc Dust	"	"	"	"	Heavy-3 layers	40-50%	Loss of negative capacity
97-102	243-123-1	Flaked Zinc Dust	"	"	50%	"	"	"	"
103-108*	KADOX-15	None	"	"	"	"	Light-3 layers	"	"
109-114	243-111-1	.027% As	"	"	"	"	None	20-30%	"
115-120	243-103-1	.089% Mn	"	"	"	"	"	"	"

(*) Control Cells

Based on the performance of these samples, as well as those previously reported in AFAPL-TR-67-107 the following three batches of 25# each were obtained from the New Jersey Zinc Company:

1. .25% Pb doped ZnO
2. High conductivity ZnO with .3% Al
3. Flaked zinc dust

The iron content as impurity was held to .004% where feasible.

These samples have been received, and cells are under construction containing these materials for cycle testing.

The Sixth Quarterly Report from the New Jersey Zinc Company is attached.

D. Zinc Electrode Fabrication Techniques

In an effort to determine if an electrodeposited zinc electrode would increase cycle life of the cell system, six 25 a.h. cells were constructed using electrodeposited negative plates at three different depths-of-discharge as shown in Table VI.

Table VI

No. Cells	Initial Capacity	Cycles at 60% DOD	Cycles at 40% DOD	Cycles at 25% DOD
2	20 a.h.	96		
	18	96		
2	22		228	
	28		228	
2	29			700*
	29			700*
Controls				
1-6	28.5	204	400**	850
		204	400**	850

(*) Failure due to shorts
(**) Test stopped

The main cause of failure was due to loss in negative plate capacity. The plated negatives, upon inspection, showed the same pattern of shedding and agglomeration as did the regular production plates.

Additional cells containing plated negatives were constructed, and three cells have completed cycle test at 60% DOD reaching 168 cycles before failure. The control cells on this test reached 144 cycles. The cause of failure was loss of negative plate capacity in all cases. The plated negative photomicrographs are under preparation, but will be included in a forthcoming report.

E. Influence of Membrane Separator Characteristics

The Quarterly Report of the NARMCO Division of Whittaker Corporation is attached.

F. Sites for Zinc Oxide Overgrowths

Early work reported in AFAPL-TR-67-107 utilized low concentrations (1%-3% by weight) of CaO in the negative active material. However, this did not improve or prolong the life of the negative plate. It was thought that higher percentages of CaO and lower concentrations of KOH might yield the desired results, with an acknowledged lower energy yield. The following table shows the concentration used and cycle life obtained with CaO in the negative active material.

Table VII

No. Cells	% CaO	% KOH	Initial Capacity	# Cycles at 60% DOD	# Cycles at 25% DOD
6	30%	45%	24 a.h.	84	not run
3	30%	15%	0.75	0	0
3	30%	20%	1.05	0	0
3	30%	25%	1.8	0	0

Table VII (Cont'd.)

No. Cells	% CaO	% KOH	Initial Capacity	# Cycles at 60% DOD	# Cycles at 25% DOD
3	20%	15%	1.25 ah	0	0
3	20%	20%	2.5	0	0
3	20%	25%	5.0	0	0
3	10%	15%	7.0	0	1
3	10%	20%	13.0	0	382
3	10%	25%	13.0	0	1000
3	Controls	15%	12.0	0	382
3	"	20%	12.0	0	500
3	"	25%	20.0	not run	900

It is readily seen that many of the above cells would not cycle at any reasonable depth of discharge due to low capacity. The cells containing 30% CaO in the negative mix in 45% KOH were the only group to cycle at 60% DOD, and this for only 84 cycles. Figure 25 shows a photomicrograph of a negative plate containing 30% CaO, and Figure 26 shows the control negative after 84 cycles.

The remaining combinations of CaO and KOH concentrations were only capable of cycling at 25 DOD.

G. Development of Failure Analysis Techniques

No work has been done this year other than the use of techniques already established, and to take many more microphotographs of failed plates. Much of the contemplated work is waiting on cycle life improvement possibilities.

H. Sizes of Zincate Ion and Soluble Silver Species in KOH

This work is still underway, and should be completed in time for the next Quarterly Report.

I. Membrane Pore Size Measurements in KOH

Three types of separators and a porous Dow Corning

disk of glass were submitted for the determination of their pore sizes. These materials were VF WP millipore, VM WP millipore, 2.2XH polyethylene, plain unradiated polyethylene, and a porous glass disk.

The pores of the VF millipore (black dots shown in the photos), Figure 27, are in the 80-120 angstrom range. If the large white areas of the picture are the pores, then their pore size ranged from 600-2000 angstroms. Again, Figure 28, the pores of the VM millipore material would be 170-250 angstroms for the black dots and 1300-4000 angstroms for the white areas. The Dow Corning glass disk had pores in the 50-75 angstrom range, Figure 29. The 2.2XH polyethylene separator pore size was 40-100 angstroms, Figure 30. The plain unradiated polyethylene surface was basically smooth and without detail.

The VF WP millipore material was manufactured by the Millipore Corp., Bedford, Mass. According to their literature, this material is made of mixed esters of cellulose in a white plain surface with a mean pore size of 100 angstroms plus or minus 20 angstroms. Its porosity is 70%. The second material (VM WP millipore) was also made of mixed esters of cellulose but had a mean pore size of 500 angstoms plus or minus 30 angstroms according to the manufacturer's specifications. The third type of separator was 2.2XH polyethylene, a radiated grafted polyethylene sheet made by Radiation Applications Inc. The mean pore size of this separator, as claimed by the manufacturer, was 40 angstroms or less. Also, a plain sheet of RAI's polyethylene was submitted so that its surface could be ascertained. The disk of Dow Corning glass was reputed to have pore sizes of 36-54 angstroms.

Direct one-step carbon replicas were made of the millipore type materials in a vacuum evaporator shadow caster. Gold or chromium was pre-shadowed on small strips of the separators and then 100-200 angstrom thick carbon was put down on the surfaces in a continuous film. Small pieces of

this replicated material were placed on 1/8 inch specimen grids of 200 mesh and into an acetone reflux colume equipped with a cold finger. After three hours in the reflux column, the original cellulose material was dissolved away leaving a clean direct replication of the material's surface.

A two stage replica technique was used for the polyethylene and the porous glass. Two drops of Ladd's replication solution were placed on an inch strip of Ladd's plastic replicating tape and this tape was placed on the surface of the polyethylene and left to dry. When dry, the replicating tape was peeled carefully from the polyethylene and fastened to a glass slide with scotch tape. A carbon replica was then made of the surface of the plastic tape by the vacuum evaporator and reflux column techniques.

The replicas were viewed with an RCA EMU-3F electron microscope and the images were recorded on Kodak electron image photographic plates. The total magnification of the prints was based upon a replica of a 28,800 lines per inch grating.

Several attempts were made to pot some of the materials in epoxies and to slice ultra thin sections of the cross-sectional areas with a Porter Blum ultramicrotome. This technique did not work - primarily because the polyethylene would not be cut by our diamond knife. The epoxy would not saturate or permeate the sample so there was little bonding of the epoxy to the polyethylene.

Figure 27 shows the surface of the VF WP millipore material at 150,000 X magnification. This separator should have pores of about 100 angstroms in diameter. The size of the small black dots in this photo is about 100 angstroms. According to the manufacturer's specifications, this material is 70% porous; however, these dots do not cover 70% of the surface area. If the large white areas are the pores, then their pore size would range from 600-2000 angstroms and still they would not occupy 70% of the area.

Figure 28 shows the small black dots of the VM WP millipore separator to be in the 170-250 angstrom range. Its magnification was also 150,000 X. Now if the white areas were the pores, the dimensions of these would be 1300-4000 angstroms. Again its porosity according to the manufacturer was supposed to be 72%.

The porous glass made by Dow Corning is pictured in Figure 29 at 300,000 X. The small black and gray projections represent the pores which range from 50-75 angstroms. Figure 31 is another view of the porous glass.

The surface of the 2.2XH polyethylene separator at 61,000 X looked like that pictured by Figures 30 and 32. Replica number 30 was not pre-shadowed with a metal; replica number 32 was shadowed with chromium. At this magnification the pores cannot be seen. Figures 33 and 34 show parts of "5" and "6" respectively at 300,000 X. The pores in the separator are represented by the small round projections which are similar to those of the porous glass. The diameters of these pores range from 40-100 angstroms.

The actual pore size openings of the separator surfaces are represented in the photos. The shape and size of the pores as they proceed through the interior of the separators could not be determined using our known techniques.

J. Stoichiometric Ratio of Formed Zinc

Groups of three 25 a.h. cells were constructed with weight ratios of formed zinc material to silver in 2:1, 3:1 and 4:1. Cycling was done at temperatures of 30°F, 40°F, 75°F and 110°F, and at 40% DOD and 60% DOD. The results of these cells are shown in Table VIII.

Table VIII

Ratio	Initial Capacity	Temperature	Cycles at 40% DOD	Cycles at 60% DOD
2:1	24 a.h.	30°F	12	2
2:1	23	40	84	0
2:1	26	75	380	184
2:1	23	110	410	175

Table VIII (Cont'd)

Ratio	Initial Capacity	Temperature	Cycles at 40% DOD	Cycles at 60% DOD
3:1	24 a.h.	30°F	50	3
3:1	22	40	60	0
3:1	22	75	460	204
3:1	24	110	349	204
4:1	25 a.h.	30	2	2
4:1	25	40	60	0
4:1	25	75	435	220
4:1	25	110	336	210

The cause of failure was due to loss of capacity at the zinc electrode. In general, the failures at low temperatures were due to the inability of the zinc electrode to accept the recharge in 85 minutes charge time.

Figure 35 shows a photomicrograph of a negative plate with a 2:1 construction. Figure 36 shows a photomicrograph of a negative plate with a 3:1 construction. Figure 37 shows a photomicrograph of a negative plate with a 4:1 construction.

Ratios above 2:1 show a little increase in cycle life at room temperatures, but the resulting increase in volume area does not warrant a cell design change.

K. Alternate Method of Surface Area Measurement

The summary report by Prof. T. P. Dirkse, Calvin College is attached.

L. Separator Development

The initial study by RAI, Inc., was to prepare experimental batches of membranes from three different polyethylene base materials; namely, Bakelite 0602, Phillips 1712 and USI 280. The three base materials were crosslinked to 90 Mrads,

and radiation grafted with acrylic and methacrylic acid. The samples were of 100' lengths, about 1-1/2 mils thick and had a resistance of about 30-90 milliohm inches^2.

Five 25 a.h. cells were constructed with 2, 3 and 4 layers each from the three base material samples, and cycled at 60% depth-of-discharge. The results are listed in Table IX.

Table IX

No. Cells	RAI Membrane	Initial Capacity	Cycles: Acrylic Acid Graft	Cycles: Methacrylic Acid Graft
10	4 Layers Bakelite 0602	24 a.h.	60(5)*	116(5)*
10	3 Layers Bakelite 0602	26	60(5)*	116(5)*
10	2 Layers Bakelite 0602	24	60(2)[1], 76(3)[1]	50(1)[1], 80(4)[1],
10	4 Layers Phillips 1712	30	40(5)*	140(3)[1], 112(2)[1],
10	3 Layers Phillips 1712	30	48(1)[1], 60(4)[1],	103(5)[1]
10	2 Layers Phillips 1712	30	60(5)[1]	36(5)[1]
10	4 Layers USI 280	30	48(1)[1], 60(4)*	140(5)*
10	3 Layers USI 280	30	48(3)[1], (2)*	56(3)[1], (2)*
10	2 Layers USI 280	30	36(5)[1]	24(5)[1]
3	Controls 4 Layers FSC	22	120(3)*	
3	Controls 3 Layers FSC	25	123(3)*	
4	Controls 2 Layers FSC	31	76(4)[1]	

* = Capacity Failure () = No. of Cells ()[1]=Failure by shorts

Table X shows the appearance of the cell components. The results of the teardown inspection revealed that in all cases, the zinc electrode had material bunching along the center and bottom portions of the grid showing the effect of heavy agglomeration. There was no indication of zinc creepage on any layer of membrane with the acrylic acid graft. With the methacrylic acid graft, however, there was zinc creepage around the layers. This occurred only in the Bakelite 0602 and Phillips 1712 base materials.

Cells containing two layers of Bakelite material, both acrylic and methacrylic acid graft, delivered as many cycles as the control cells containing two layers of FSC. Cells containing three and four layers of the Bakelite methacrylic acid graft cycled nearly as well as the control cells. Although cells containing four layers of Phillips 1712 and USI 280 methacrylic acid graft did obtain more cycles than the controls, the two layer samples did not perform as well as either the two layer Bakalite or control cells.

On the basis of this test, 500 foot lots of Bakelite acrylic and methacrylic acid radiation graft, crosslinked at the 90 Mrad level were prepared by RAI, Inc. A third sample, containing chemically grafted methacrylic acid was also furnished.

Groups of eighteen 25 a.h. cells were constructed with each of the three membrane samples. The eighteen cell group contained 5, 4 and 3 layers of each membrane. These cells were cycled at 60%, 40% and 25% depth-of-discharge. In addition, cells containing 4 layers of each membrane are presently under cycle test at the indicated depth-of-discharge at the Quality Assurance Laboratory, Crane, Indiana. This is done so that a comparison of cycle life can be made with cells containing 4 layers of separation.

Table XI shows the initial capacity and cycle life obtained at the various depths of discharge for these cells containing the three membrane samples. The control cells contained 4 layers of cellulosic membrane.

TABLE X

Study: Separators

Note: All cells were constructed as in Table I except for separator combinations. All cells contained one layer of acrylonitrile monomer next to the positive plate. Electrolyte concentration was 40% KOH. MA = methacrylic acid graft. AA = acrylic acid graft. The general condition of the RAI separator after cycle life was good.

Cell No.	O.C. Voltage	Number and Kind of Separators*	Condition of Positive Plate	Extent Formed	Treeing	Creeping	Penetration	Washout	Cause of Failure
		Bakelite MA							
1-5	1.80	4L	Buckled	Zinc 90%	None	Light 3L	None	65%-75%	Loss of negative capacity
6-10	1.82	3L	+ ZnO	"	"	"	"	"	
11-15	0.30	2L	Deposit	Oxide 90%	"	None	"	20%	Shorts
		Phillips MA							
16-20	1.12	4L	"	"	"	Light 3L	"	65%-75%	"
21-25	0.70	3L	"	"	"	Light 2L	"	"	"
26-30	0.00	2L	"	"	"	None	"	30%	"
		USI MA							
31-35	1.82	4L	"	50%-50%	"	"	"	50%-60%	Loss of capacity
36-40	1.8-0.5	3L	"	Oxide 90%	"	"	"	"	Loss of cap. & shorts
41-45	0.00	2L	"	"	"	"	"	10%-20%	Shorts
		Bakelite AA							
46-50	1.82	4L	"	Zinc 90%	"	"	"	65%-75%	Loss of capacity
51-55	1.82	3L	"	"	"	"	"	"	"
56-60	0.00	2L	"	Oxide 90%	"	"	"	"	Shorts
		Phillips AA							
61-65	1.82	4L	"	Zinc 90%	"	"	"	50%-60%	Loss of capacity
66-70	0.00	3L	"	Oxide 90%	"	"	"	"	Shorts
71-75	0.00	2L	"	"	"	"	"	"	"
		USI AA							
76-80	1.82	4L	"	Zinc 90%	"	"	"	"	Loss of capacity
81-85	0.50	3L	"	Oxide 90%	"	"	"	"	Shorts
86-90	0.50	2L	"	"	"	"	"	"	"
		Cellulosic							
91-93*	1.84	4L	Good	Zinc 60%	"	Light 3L	"	"	Loss of capacity
94-96*	1.84	3L	"	"	"	Light 2L	"	"	"
97-100*	0.00	2L	Discharged	Oxide 90%	"	Heavy 2L	Yes	"	Shorts

* Control Cells. The first layer of cellulosic material was deteriorated in these cells.

The failure mode is by loss of negative material and/or short circuiting. All cells in this test are considered to have failed by short circuiting if the open circuit voltage is below 1.52V after a weeks' charged stand time after completion of cycle testing.

TABLE XI

A. 90 Mrad Methacrylic Acid Radiation Graft Membrane

	Controls	3 Layers	4 Layers	5 Layers
Initial Capacity	22 a.h.	27 a.h.	28 a.h.	27 a.h.
Cycles @ 60% DOD	156(4)*	120(6)*	72(3)*	132(2)* 96(2)* 108(2)*
40% DOD	288(2)* 312(2)*	180(1)[1] 288(2)[1] 276(2)[1] 288(1)*	253(3)*	120(2)* 216(3)* 240(1)*
25% DOD	396(2)*[1] 480(1)[1] 528(1)[1]	432(1)[1] 444(1)[1] 456(2)[1] 492(1)[1] 601(1)[1]	400(1)* 428(2)	553(1)* 600(5)[c]

B. 90 Mrad Acrylic Acid Radiation Graft Membrane

Initial Capacity	Same as A	25 a.h.	28 a.h.	25.5 a.h.
Cycles @ 60% DOD	"	48(2)[1] 72(3)[1] 72(1)*	84(3)*	48(2)[1] 72(4)[1]
40% DOD	"	144(1)[1] 156(1)* 180(1)[1] 204(1)[1] 240(2)*	144(2)* 144(1)[1]	120(3)* 156(3)*
25% DOD	"	408(1)* 468(1)[1] 492(2)[1] 517(2)*	324(2)* 300(1)*	336(2)* 408(1)* 468(2)*

TABLE XI (Cont'd.)

C. 90 Mrad Methacrylic Acid Chemical Graft

	Controls	3 Layers	4 Layers	5 Layers
Initial Capacity	24 a.h.	22 a.h.	20 a.h.	23 a.h.
Cycles @ 60% DOD	144(1)* 168(3)*	48(2)[1] 84(2)[1] 96(2)[1] 96(3)*	2(3)*	Awaiting Test
40% DOD	Awaiting Tests ----------			
25% DOD	Awaiting Tests		348(1)* 400(2)	Awaiting Test

* = Failure () = No. of Cells ()[1] = Failure by shorts
()[C] = Cycling

Table XII shows the number of cells that failed by short circuiting with the number of layers of membranes tested at the indicated depths-of-discharge.

TABLE XII

	3L MA	3L AA	3L CMA
60% DOD	0	5	6
40% DOD	5	3	2
25% DOD	6	2	Awaiting Test
	4L MA	**4L AA**	**4L CMA**
60% DOD	0	0	Awaiting Test
40% DOD	0	1	Awaiting Test
25% DOD	0	0	0
	5L MA	**5L AA**	**5L CMA**
60% DOD	0	6	Awaiting test
40% DOD	0	0	"
25% DOD	Awaiting Test		"

TABLE XII (Cont'd.)

Control Cells

60% DOD	0
40% DOD	0
25% DOD	3

MA = Methacrylic Acid
AA = Acrylic Acid
CMA = Chemically Grafted Methacrylic Acid

Table XIII shows the appearance of the cell components after cycle testing. The main difference here in the polyethylene treated membranes and the cellulosic controls are:

1. The cellulosics will deteriorate (rot) while the polyethylenes will not.

2. The zinc material will creep around layers in big splotches in and on the cellulosics, while in the polyethylenes the same material will penetrate in one or two areas in each layer about the size of a dime if it does occur. In many instances, the penetration can not be seen, yet cell shorts have occurred.

3. The cellulosics will swell to over twice the original thickness, while the polyethylenes will not. In fact, there appears to be a "deswelling" causing a stretching of the membrane across the plate. This is probably what is making the positive plates buckle, and, since pressure is reduced in the perpendicular direction to the face of the plate, this is causing increased shedding of the negative material.

Figure 38 shows the appearance of the negative plate material after the indicated cycle failure due to loss of negative plate capacity. These plates are from cells containing 3 and 5 layers of the radiated methacrylic acid graft. The control plate is in the center from a cell containing

TABLE XIII

Study: Separators

Note: Same as Table X

Number and Kind of Separator**	Depth of Discharge	Cell No.	O.C. Voltage	Condition of Positive Plate	Condition of Negative Plate: Extent Formed	Treeing	Creeping	Penetration	Wash Out	Cause of Failure
3 Layers MA	60%	1-6	1.83V	Buckled	60% Zinc	None	None	None	60%	Loss of neg.cap.
" " "	40%	7-12	1.54	+ZnO	90% Oxide	"	"	All layers	"	Shorts
" " "	25%	13-18	0.70	Deposit	" "	"	"	" "	"	"
4 Layers MA	60%	19-21	1.82	"	60% Zinc	"	"	2 layers	70%	Loss of neg.
" " "	40%	22-24	1.82	"	" "	"	"	3 layers	"	capacity
" " "	25%	25-27	1.77	"	" "	"	"	3 layers	"	"
5 Layers MA	60%	28-33	1.83	"	" "	"	"	3 layers	60%	"
" " "	40%	34-39	1.82	"	" "	"	"	None	"	"
" " "	25%	Still cycling, except for one cell which will be examined with the group								
3 Layers AA	60%	46-51	0.50	Buckled	90% Oxide	None	None	None	50%	Shorts
" " "	40%	52-57	1.77	+ZnO	" "	"	"	"	"	Loss of capacity
" " "	25%	58-63	1.59	Deposit	" "	"	"	3 layers	80%	and shorts
4 Layers AA	60%	64-66	1.82	"	60% Zinc	"	"	" "	60%	Loss of capacity
" " "	40%	67-69	1.60	"	50%-50%	"	"	None	"	"
" " "	25%	70-72	1.80	"	"	"	"	All layers	80%	"
5 Layers AA	60%	73-78	0.90	"	90% Oxide	"	"	None	50%	Shorts
" " "	40%	79-81	1.76	"	60% Zinc	"	"	"	70%	Loss of capacity
" " "	25%	82-87	1.80	"	" "	"	"	3 layers	80%	"
Control Cells*	60%	88-91	1.83	Good	" "	Medium	4 layers	None	50%	"
	40%	92-95	1.82	"	" "	Heavy	"	"	"	"
	25%	96-99	0.80	Discharged	90% Oxide	"	"	"	"	Shorts

* The cellulosic membranes were in general badly deteriorated in cells at 40% & 25% DOD; at 60% DOD, the first layer only was deteriorated.

** The MA and AA radiated grafted membranes were in very good condition at all depths-of-discharge.

4 layers of cellulosic membrane material. In all cases after cycle failure, the negative material resulted in this configuration. Figure 39 shows the average number of cycles obtained by cells in each membrane category at various depths of discharge.

In general, from the cycle data obtained to date, the 90 Mrad crosslinked polyethylene methacrylic acid radiation grafted membrane gave longer cycle life, layer for layer, than did the acrylic acid grafted membrane, at each depth-of-discharge. In addition, 3 layers of the methacrylic acid graft is as good as or better than the separator for the control cells. The best cycles obtained so far are with the 5-layer methacrylic acid graft at 25% depth-of-discharge. It is believed that loose element pack construction could be a factor in some early cycle failures at all depths-of-discharge. All cells now under construction have proper shimming.

While the test results are not complete with cells containing the chemically grafted methacrylic acid membranes, the results that are available indicate that this method of grafting at this time is not as desirable as the radiation graft. The cells containing these membranes are not included in Table XIII because all cycle tests are not complete.

An additional 5000 feet of 90 Mrad crosslinked polyethylene methacrylic acid radiation graft will be furnished by RAI, Inc. to demonstrate reliability of uniformity in thickness, acceptable resistance to zincate and silver ion penetration, low electrical resistance and in good workmanship.

The material received to date from RAI, consisting of both 100-foot and 500-foot samples of the radiation grafted methacrylic and acrylic acid membranes, have been in excellent condition, and a degree of uniformity has been maintained thus far. It is anticipated that cycle life will improve with this membrane, and it can be used as a separator system for secondary silver-zinc batteries.

III. GENERAL DISCUSSION

Carbowaxes in the molecular weight range of 1000 give good cycle life by comparison with cells containing Emulphogene BC-610. Carbowaxes are linear polyethyleneoxide polymers and since the Emulphogenes contain a polyethylene oxide chain, it is surmised that the polyethyleneoxide structure is active in promoting cycle life.

The additions of various percentages of LSA and $ZnSO_4$ are not consistently capable of increasing negative plate cycle life, and no further work will be done with these compounds.

In the various ZnO powders produced by the New Jersey Zinc Company, the addition of Pb and Al in .25% to .3% concentrations showed promise of increasing the cycle life of the negative plate. Additional large batch (25#) samples were forthcoming, and 25 a.h. cells are under cycle test now with these compounds. Limits on the concentration of Fe in the ZnO were established, and a maximum limit of .010% Fe appears to be tolerable in ZnO for battery usage, although a limit of .004% Fe is called for where possible.

The photomicrographs of the negative plates, containing these and other additives, are presented for comparison purposes. Those containing the Pb additives seem to show the least agglomeration tendency, and as a result, produce the most cycles on the average.

Additional work will be done with the flaked zinc dust compound. Initial test results showed good cycle life at 60% DOD (200+ cycles). It is possible that additional cycles can be had if different plate making techniques are employed. Work in this area is presently underway.

These compounds are also being tested with polyethylene treated separators, as well as cellulosic separators. It is anticipated that increased cycle life at 60% DOD will result in the use of these improvements to the negative material.

In the area of zinc fabrication techniques, work on the electroplated zinc negative was started, and initial results show that the cycle life capability of this negative plate is about equal to the pressed powder plate. Work is continuing in this area.

The use of CaO as an additive to the negative material to produce insoluble sites for zincate captive is not satisfactory. No further work will be done with the insoluble oxide.

Attempts have been made to characterize pore sizes of several materials using the electron microscope and surface replication techniques. The results are somewhat inconclusive because of lack of certainty as to what are pores in the electromicrographs. Resolution of the problem might be made by work on cross-sections; however, attempts to prepare satisfactory cross-sections have not been successful.

Work has been completed on the study of stoichiometric ratios of formed zinc. There are indications that an increase of the stoichiometric ratio of formed zinc leads to a modest increase in cycle life at 60% depth-of-discharge and room temperature. The increase is not sufficient to offset the additional volume required for the extra zinc.

Work on the development of an inert separator material has proven successful in that cycle life results are obtained that equal or better the cellulosic control membrane. Inspections after cycle life show the material to be unaffected by electrode or electrolyte environment.

Studies on base polymer material, precrosslink dosage, grafting techniques and the graft monomer have resulted in producing a membrane of uniform characteristics. Three polyethylene base materials were used; i.e., Bakelite 0602, Phillips 1712, and USI 280, and precrosslinked

at 90 Mrad. Two monomers, acrylic and methacrylic acid were radiation grafted and 100 ft. samples were furnished for cycle test at 60% depth-of-discharge. The results indicated that the Bakelite 0602 base polyethylene grafted with methacrylic acid produced the best cycle life, and was fairly equal to the controls.

Additional 500 ft. samples containing the 90 Mrad precrosslinked film with radiation grafted methacrylic and acrylic acid were furnished. A third sample of 90 Mrad precrosslinked film was chemically grafted with methacrylic acid.

The results show that the radiation grafted methacrylic acid membranes yield longer cycle life than the acrylic acid grafted membrane, and are equal to, and in some cases better than the control membranes. The importance of the data here is that 3 layers of the methacrylic acid grafted membrane was as good as 4 layers of the cellulosic membrane in nearly all depths-of-discharge. This indicates that a higher energy yield can be expected since less space and weight is required with this membrane system and, as cell manufacturing techniques improve with the use of this membrane, it is expected that no more than three layers would be required for many applications of this cell system.

While the test results on the chemically grafted membranes are not completed, early results are not favorable, and this method of grafting will not be studied further on this program.

At the present time, it appears that controls used in the manufacture of the 90 Mrad precrosslinked Bakelite 0602 polyethylene base, radiation grafted methacrylic acid membrane, are adequate to produce a membrane having uniform chemical and physical characteristics.

An additional 5000 ft. sample of the above membrane will be produced for the purposes of reliability, and also for further cell test work.

With proper cell construction, and allowing proper spacing between the finished element and container wall, the above membrane is suitable for use as a separator material in secondary silver-zinc batteries.

IV. RECOMMENDATIONS

Additional work on fabrication techniques of the zinc electrode, using material furnished by the New Jersey Zinc Company, is necessary.

A reliability study of the manufacturing processes of polyethylene based, precrosslinked, and radiation grafted membranes should be accomplished. Good advances have been made in this program with this membrane, and good controls that have been established here should be permanently nailed down through the use of automatic handling devices and in-house radiation facilities.

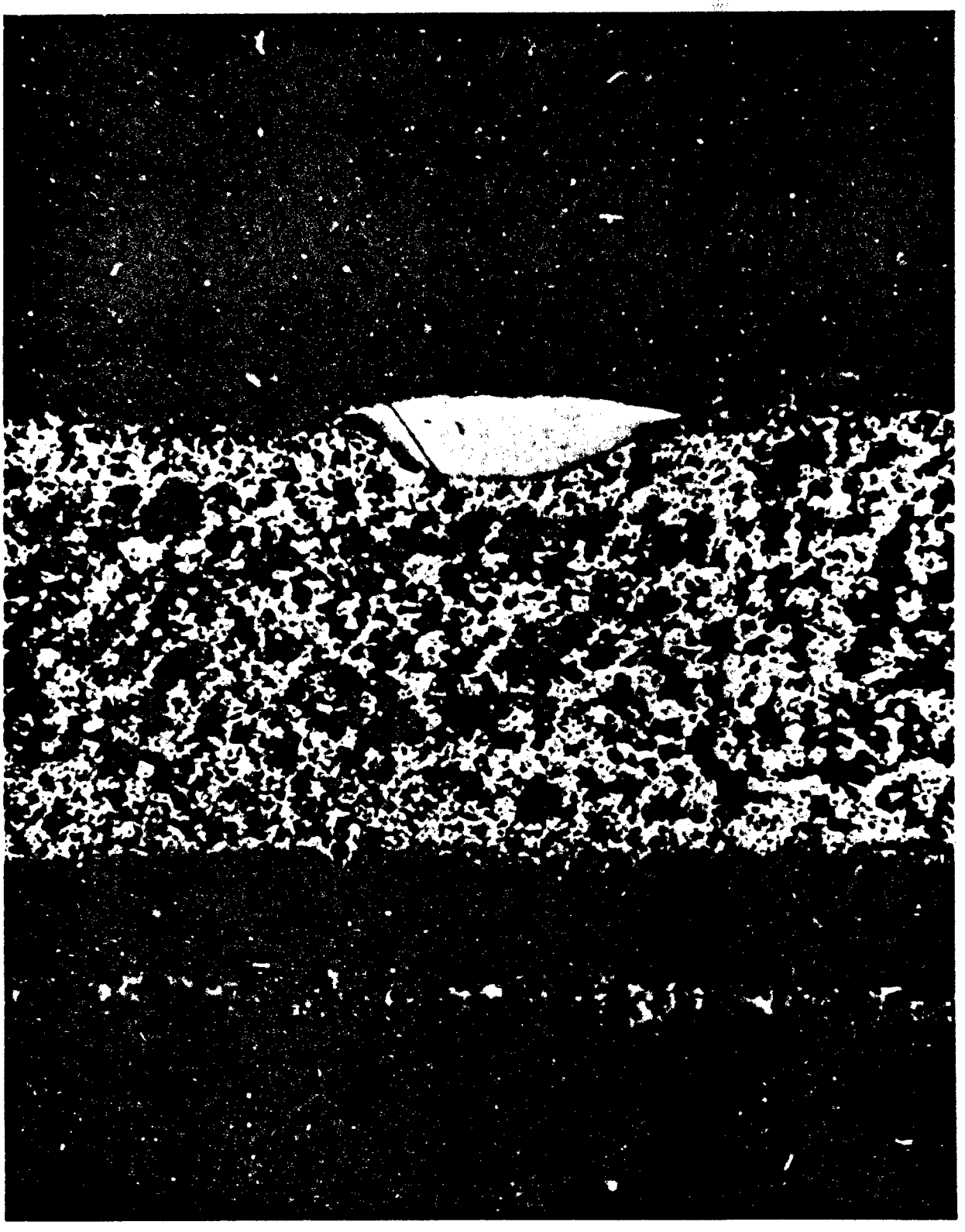

Figure 1 Negative Plate Containing 1% Carbowax with a Molecular Weight Range of 6000 After 132 Cycles 100X

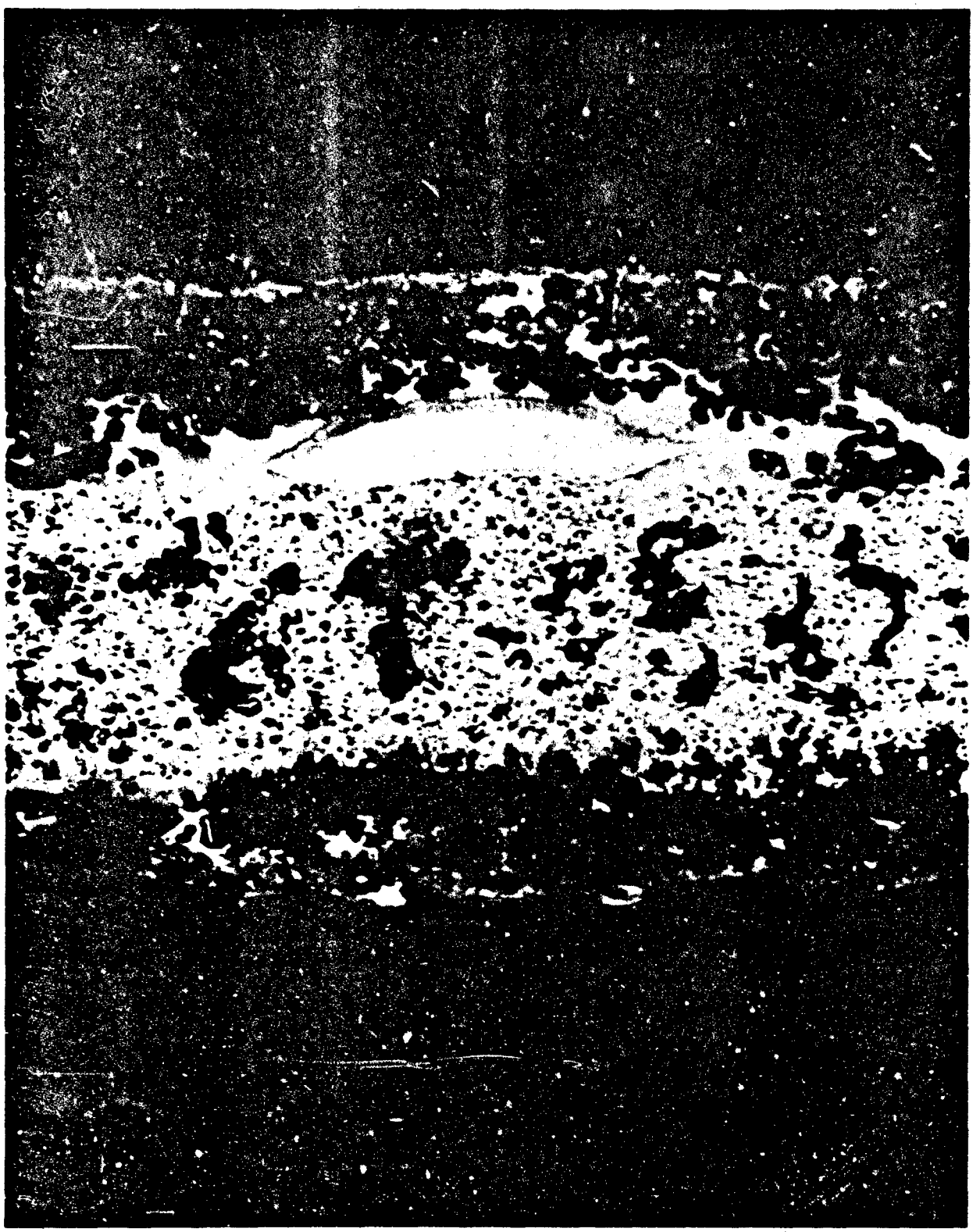

Figure 2 Negative Plate Containing 1% Carbowax with a Molecular Weight Range of 1000 After 200 Cycles. 100X

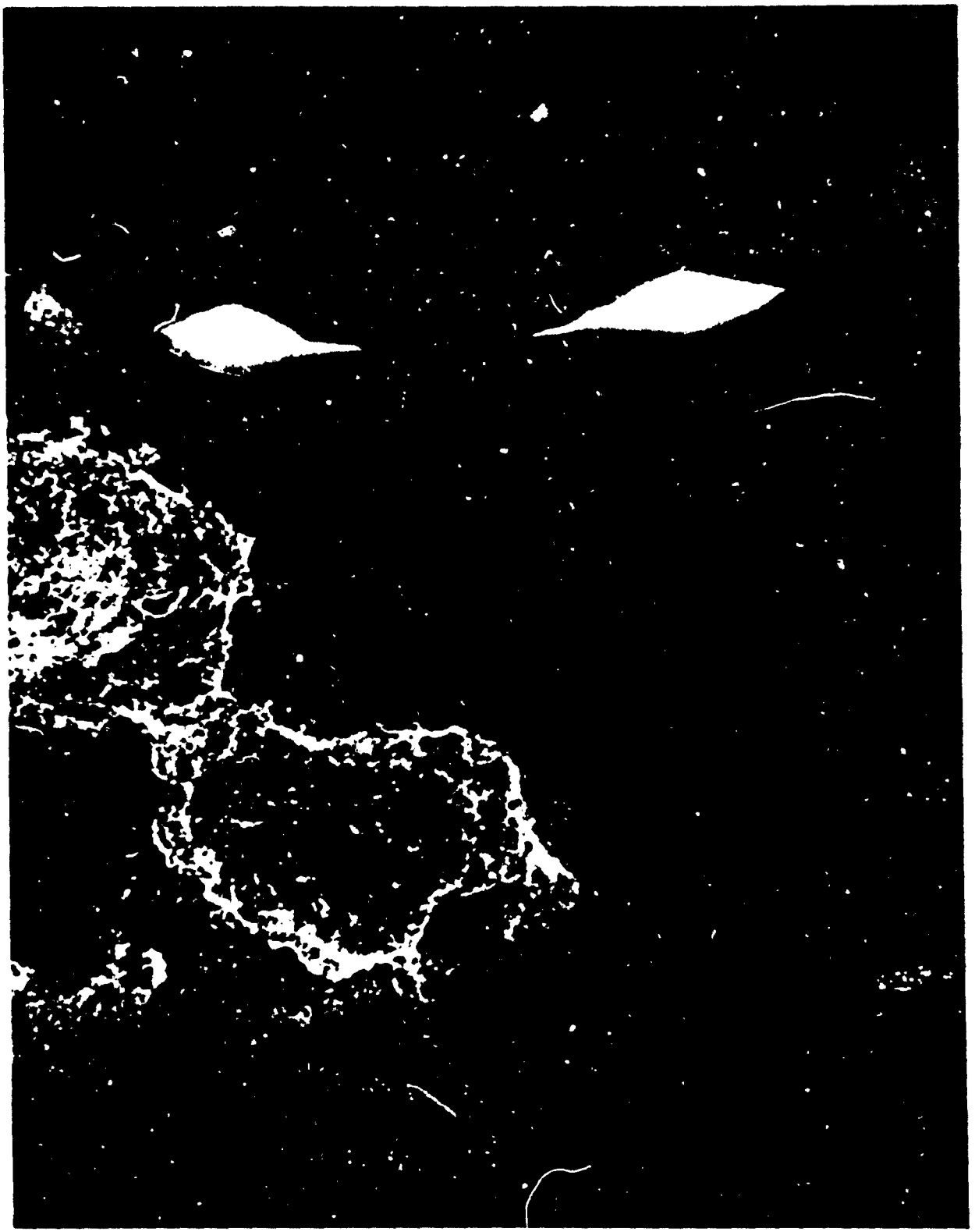

Figure 3 Negative Plate Containing 1% Carbowax with a Molecular Weight Range of 200 After 100 Cycles 100X

Figure 4 Negative Plate Containing 1.1% LSA After 108 Cycles 100X

Figure 5 Negative Plate Containing 1.1% LSA and 5% $ZnSO_4$ After 96 Cycles. 100X

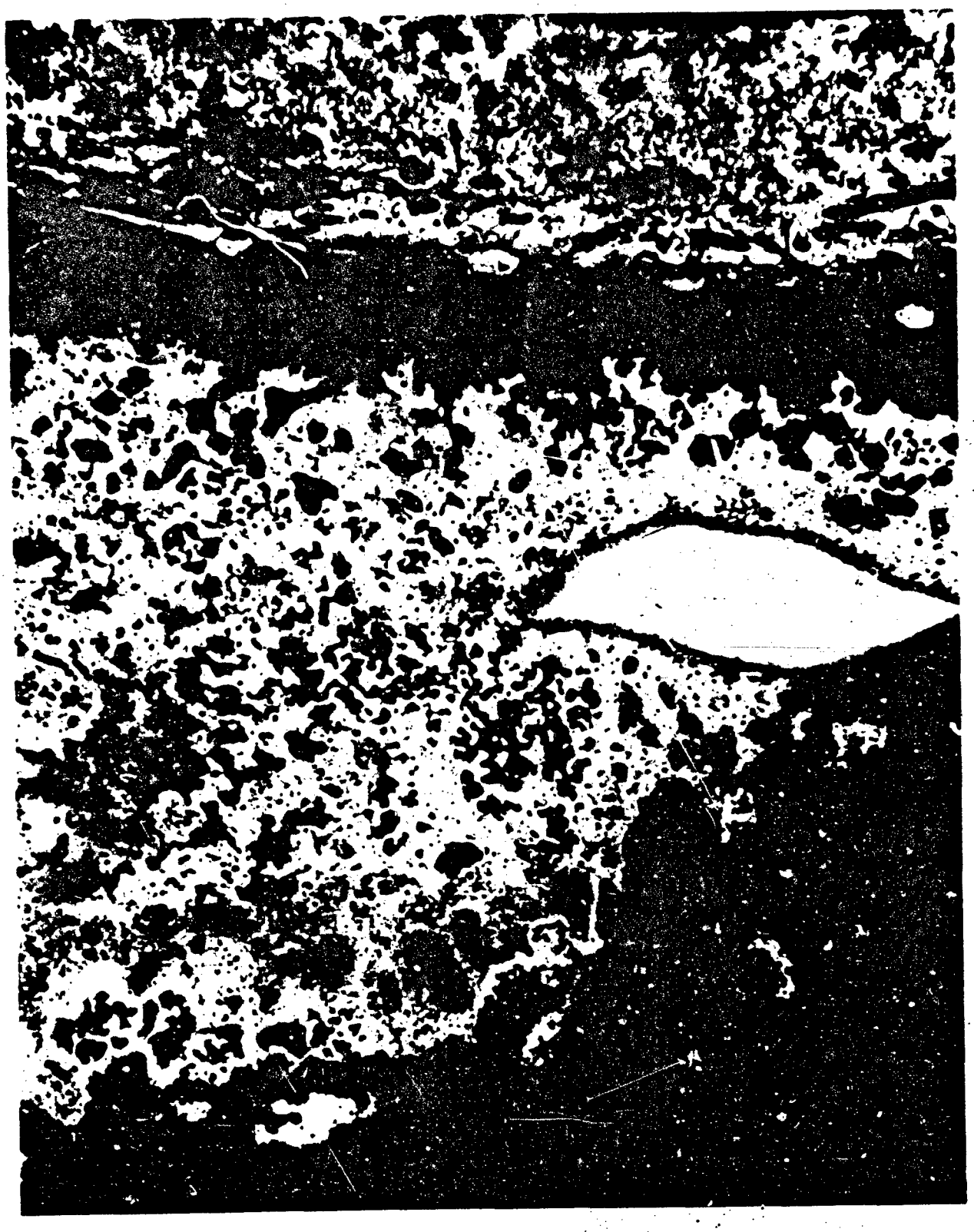

Figure 6 Negative Plate Containing 0.0008% Pb in ZnO 100X

Figure 7 Negative Plate Containing 0.028% Pb in ZnO 100X

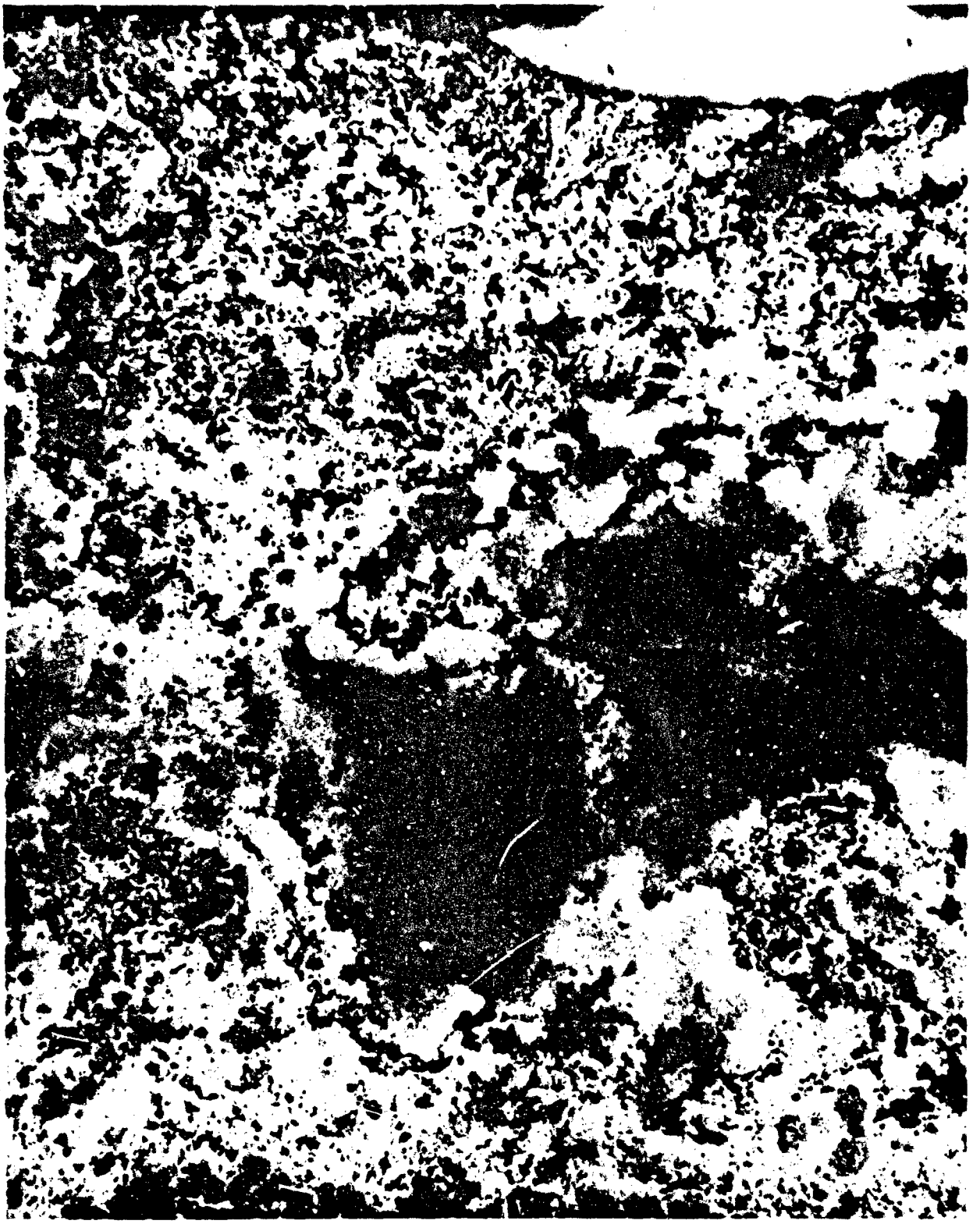

Figure 8 Negative Plate Containing 1.02% Pb in ZnO 100X

Figure 9 Negative Plate Containing 2.42% Pb in ZnO 100X

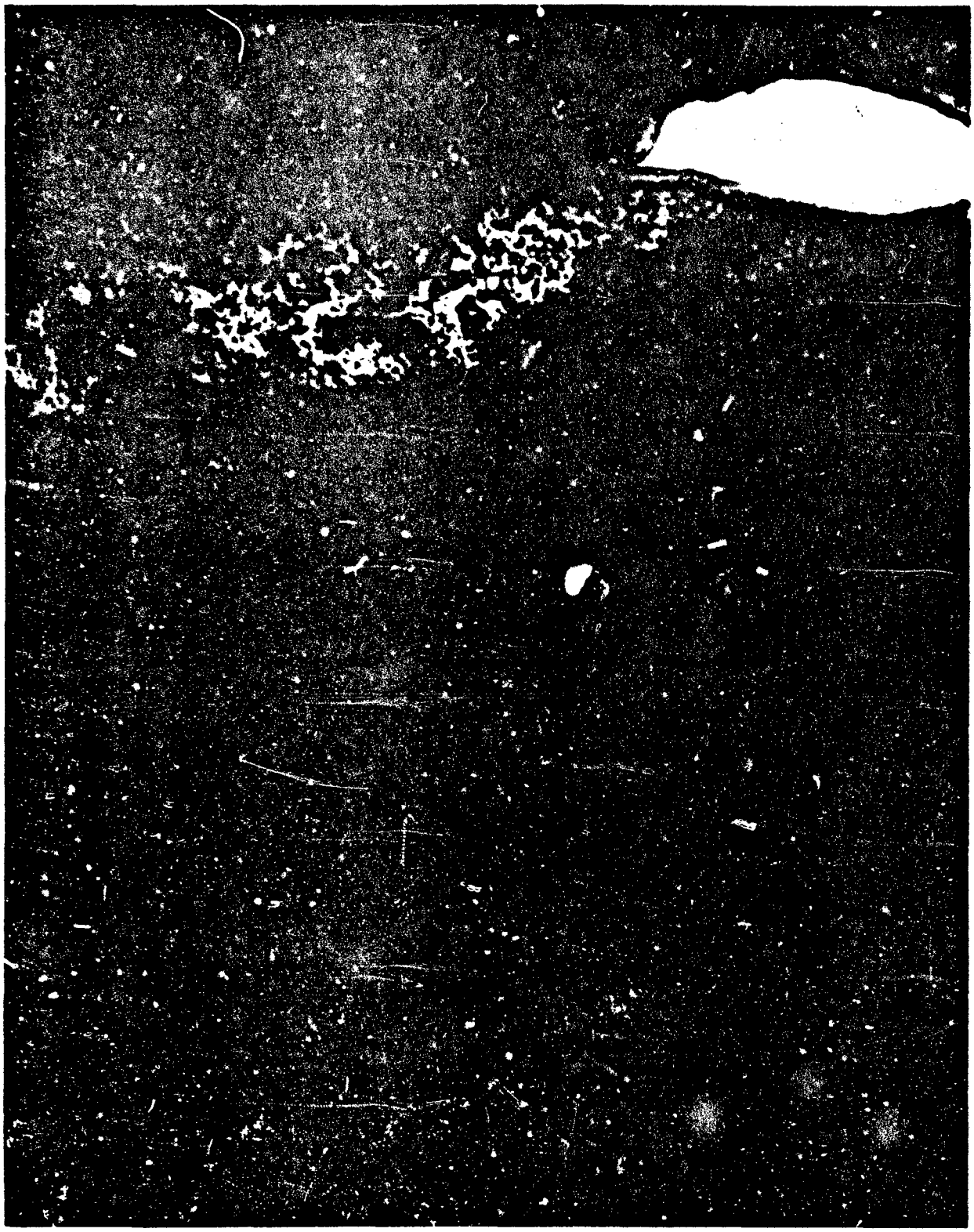

Figure 10 Negative Plate Containing 0.0006% Fe in ZnO 100X

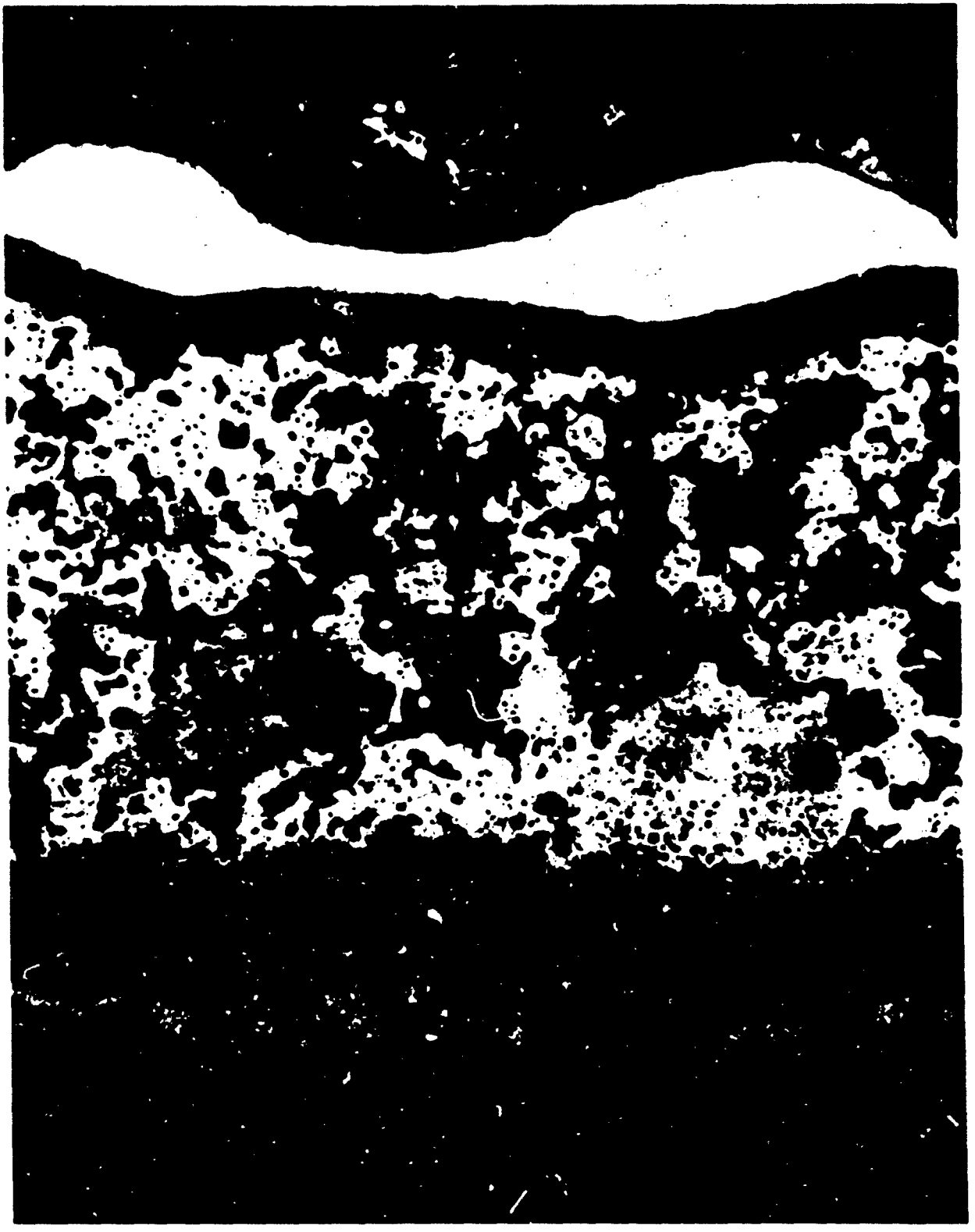

Figure 11 Negative Plate Containing 0.0086% Fe in ZnO 100X

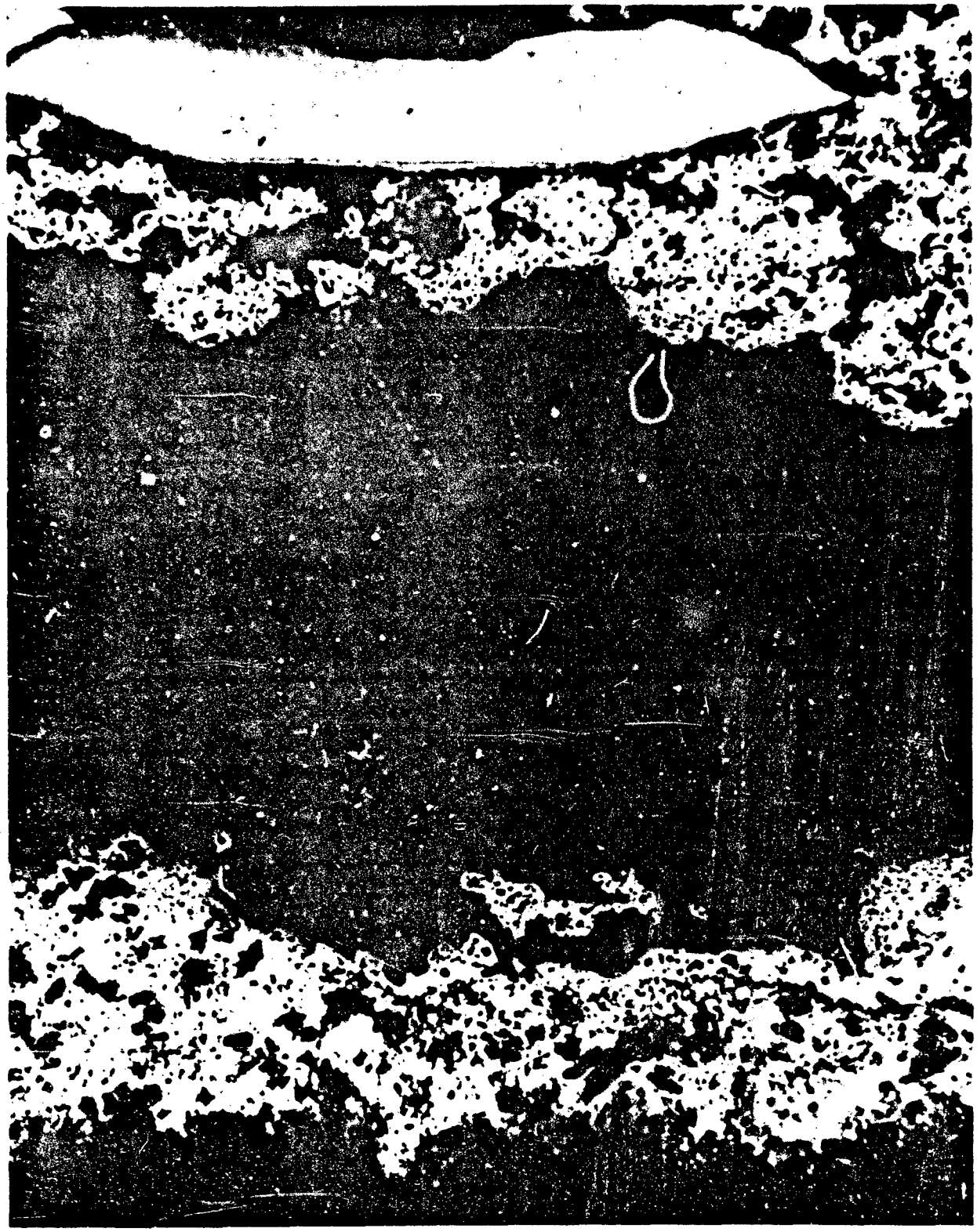

Figure 12 Negative Plate Containing 0.009% Fe in ZnO 100X

Figure 13 Negative Plate Containing 0.26% Pb in ZnO 100X

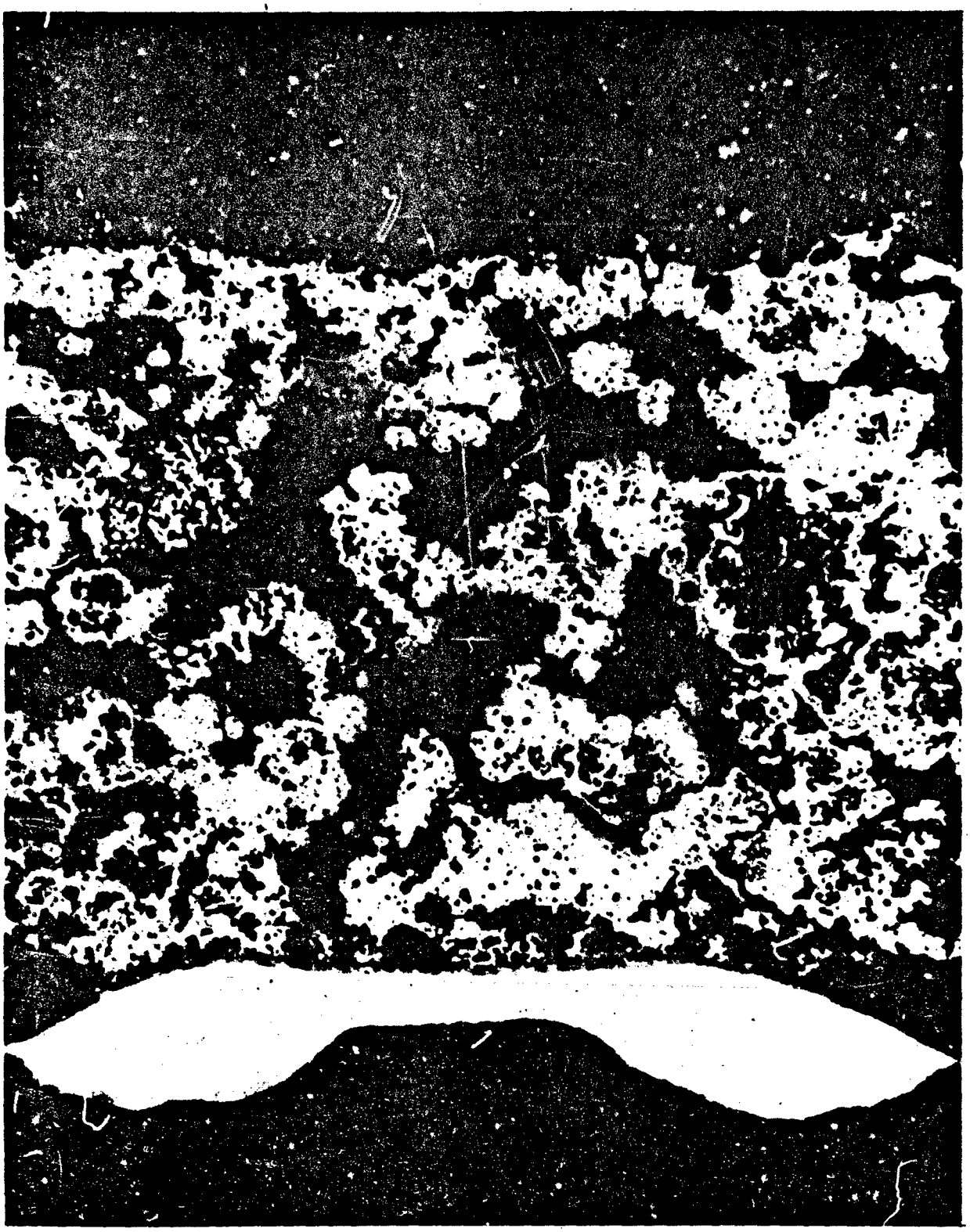

Figure 14 Negative Plate Containing 0.07% Al in ZnO 100X

Figure 15 Negative Plate Containing 0.92% Al in ZnO 100X

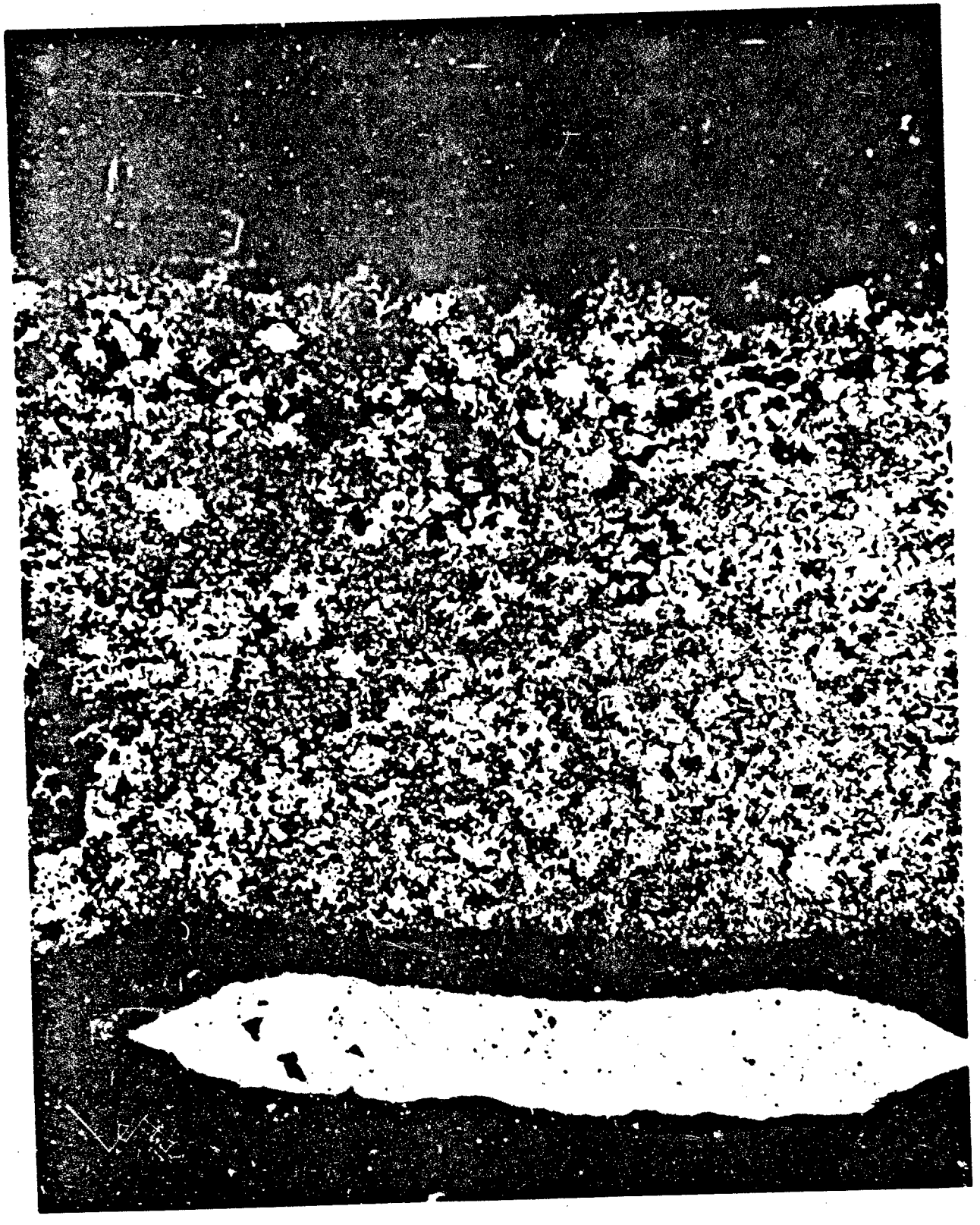

Figure 16 Negative Plate Containing 0.0006% Fe in ZnO 100X

Figure 17 Negative Plate Containing 0.3% Al in ZnO 100X

Figure 18 Control Negative Plate (KADOX-15) After 170 Cycles
100X

Figure 19 Negative Plate Containing Zinc Dust After 168 Cycles
100X

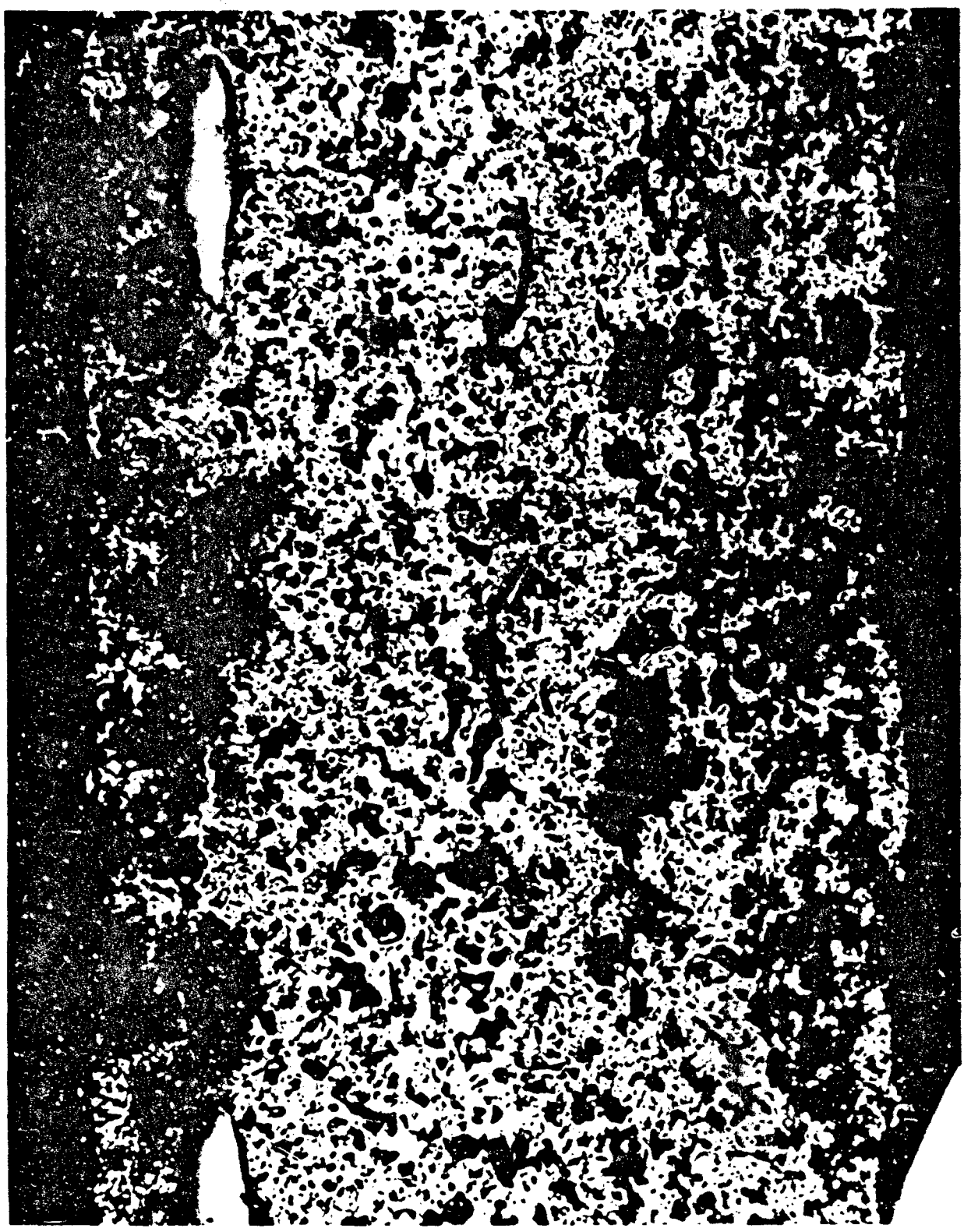

Figure 20 Negative Plate Containing Flaked Zinc Dust After 204 Cycles
100X

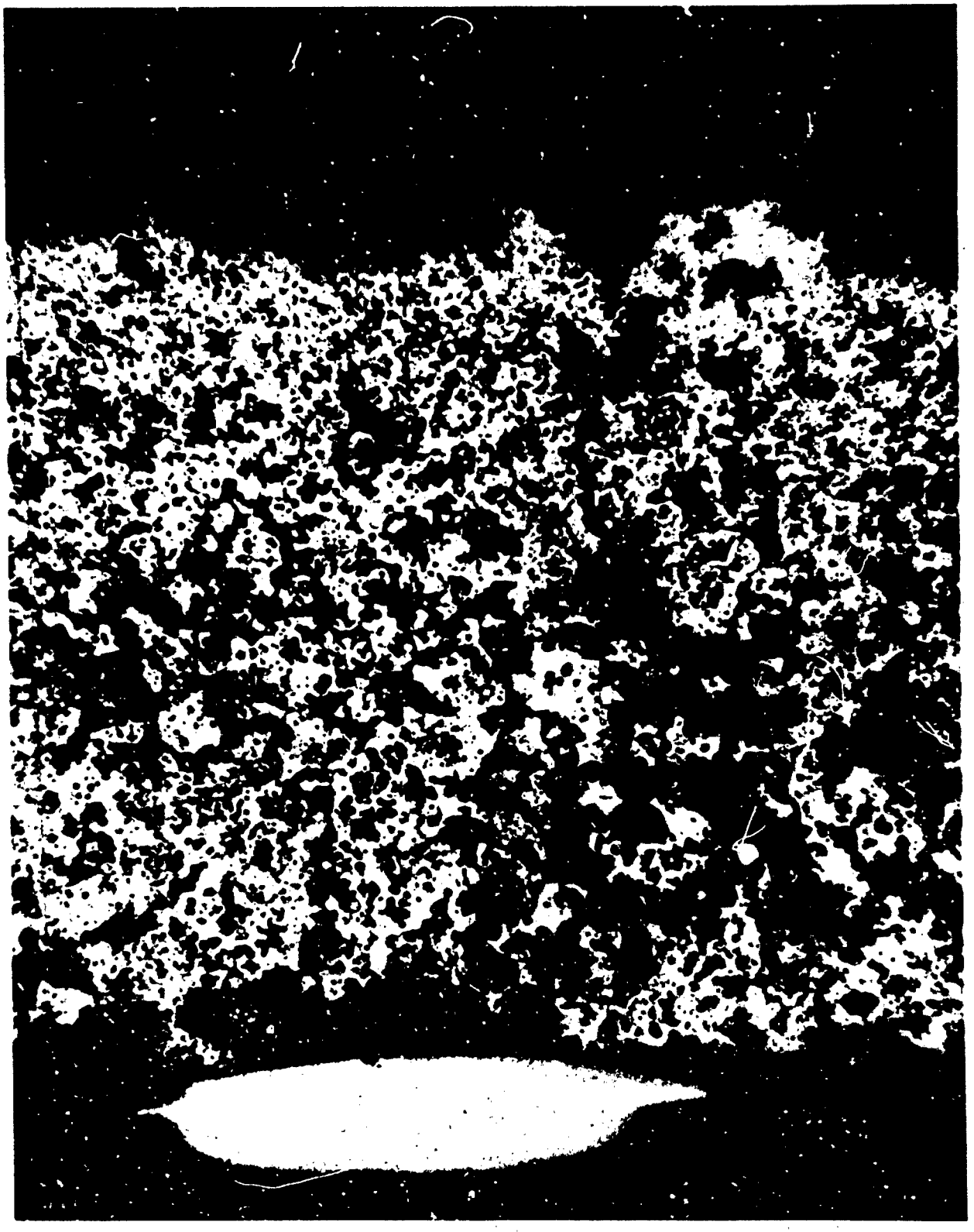

Figure 21 Control Negative Plate (KADOX-15) After 130 Cycles
100X

Figure 22 Preformed Negative Plate Containing ZnO (KADOX-15) After 150 Cycles 100X

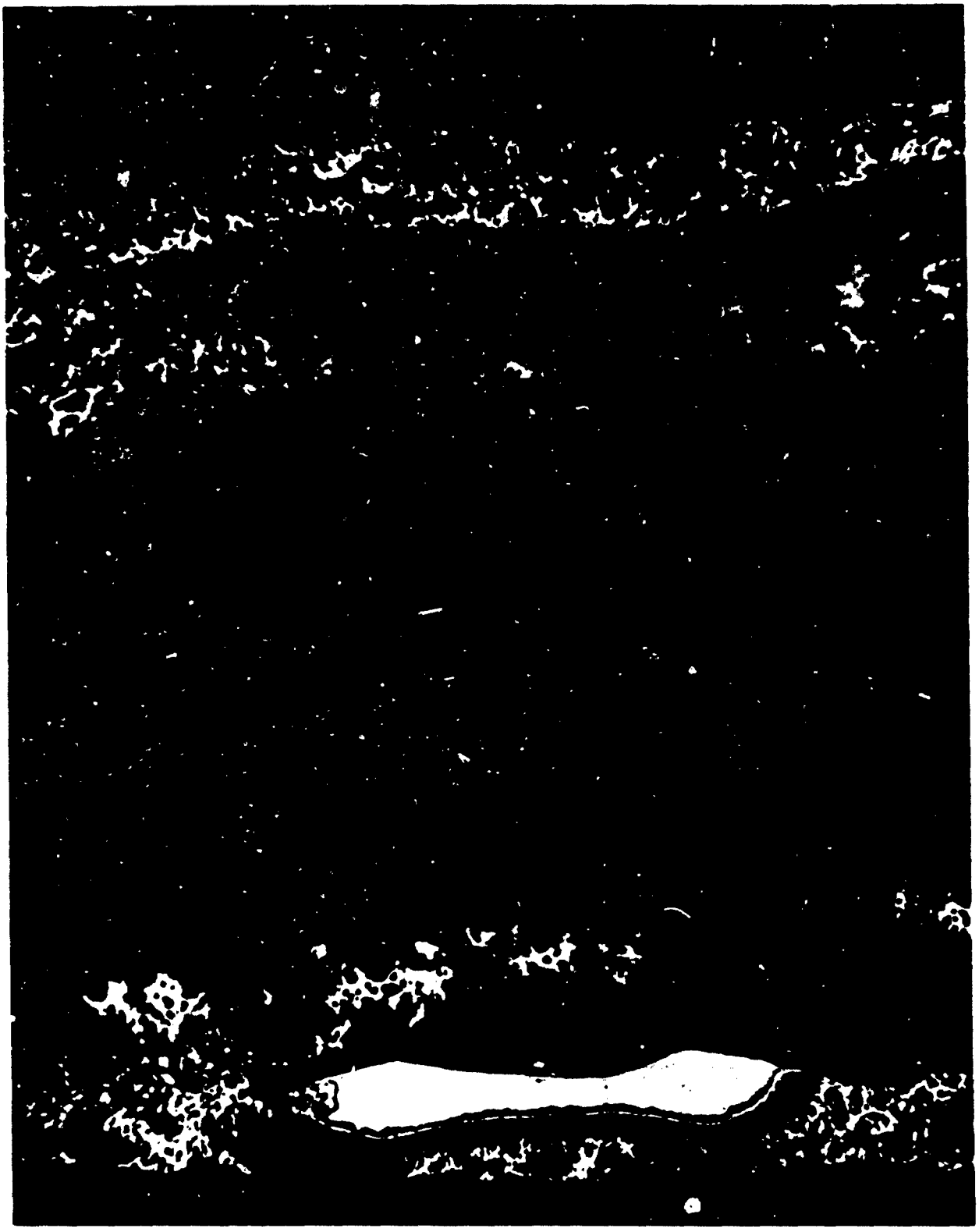

Figure 23 Negative Plate Containing .027% As After 80 Cycles 100X

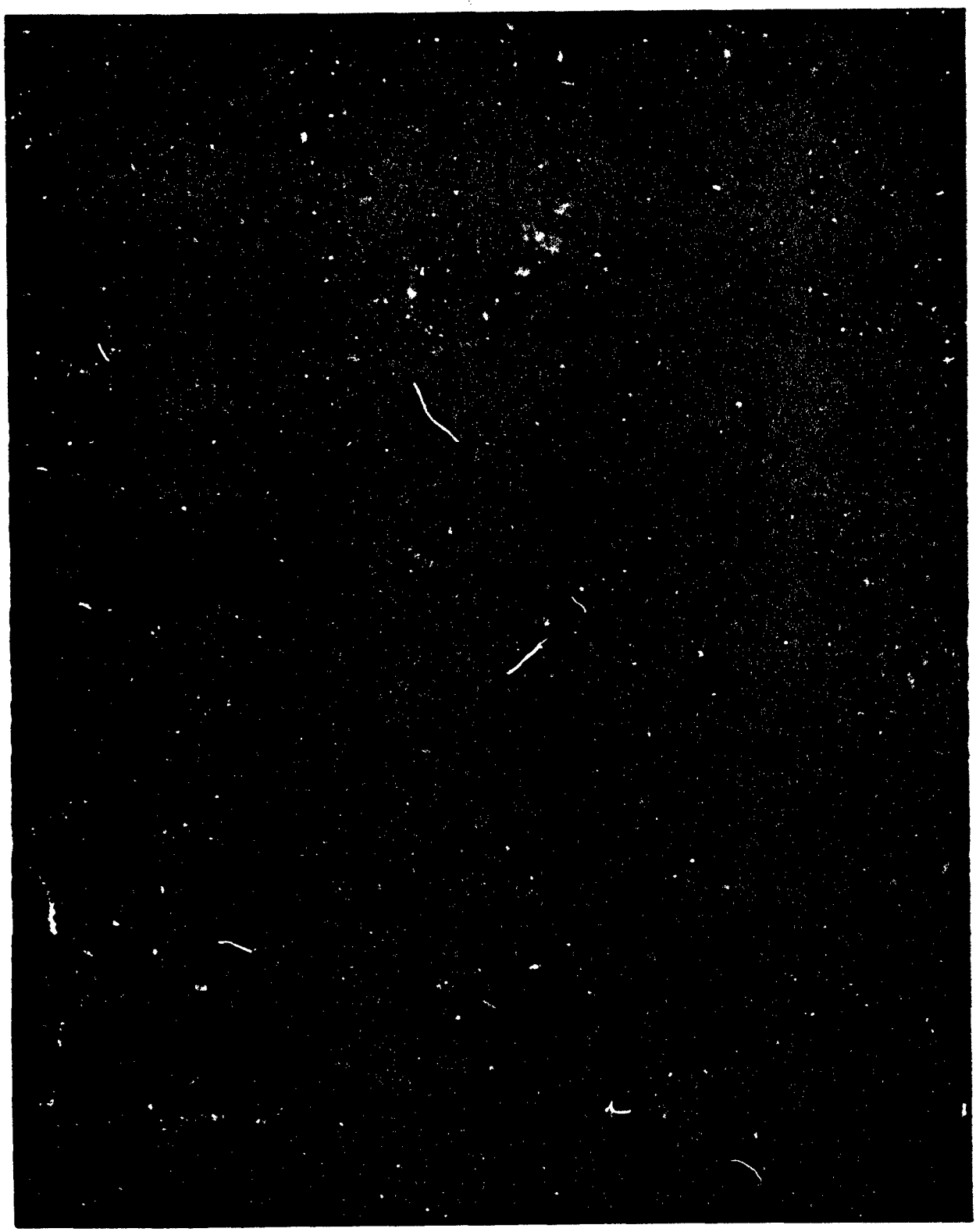

Figure 24 Negative Plate Containing .089% Mn After 130 Cycles
100X

Figure 25 Negative Plate Containing 30% CaO After 84 Cycles
100X

Figure 26 Negative Plate as Control After 84 Cycles
100X

Figure 27 Electronmicrograph of the Surface of VF WP Millipore Material at 150,000 X 100X

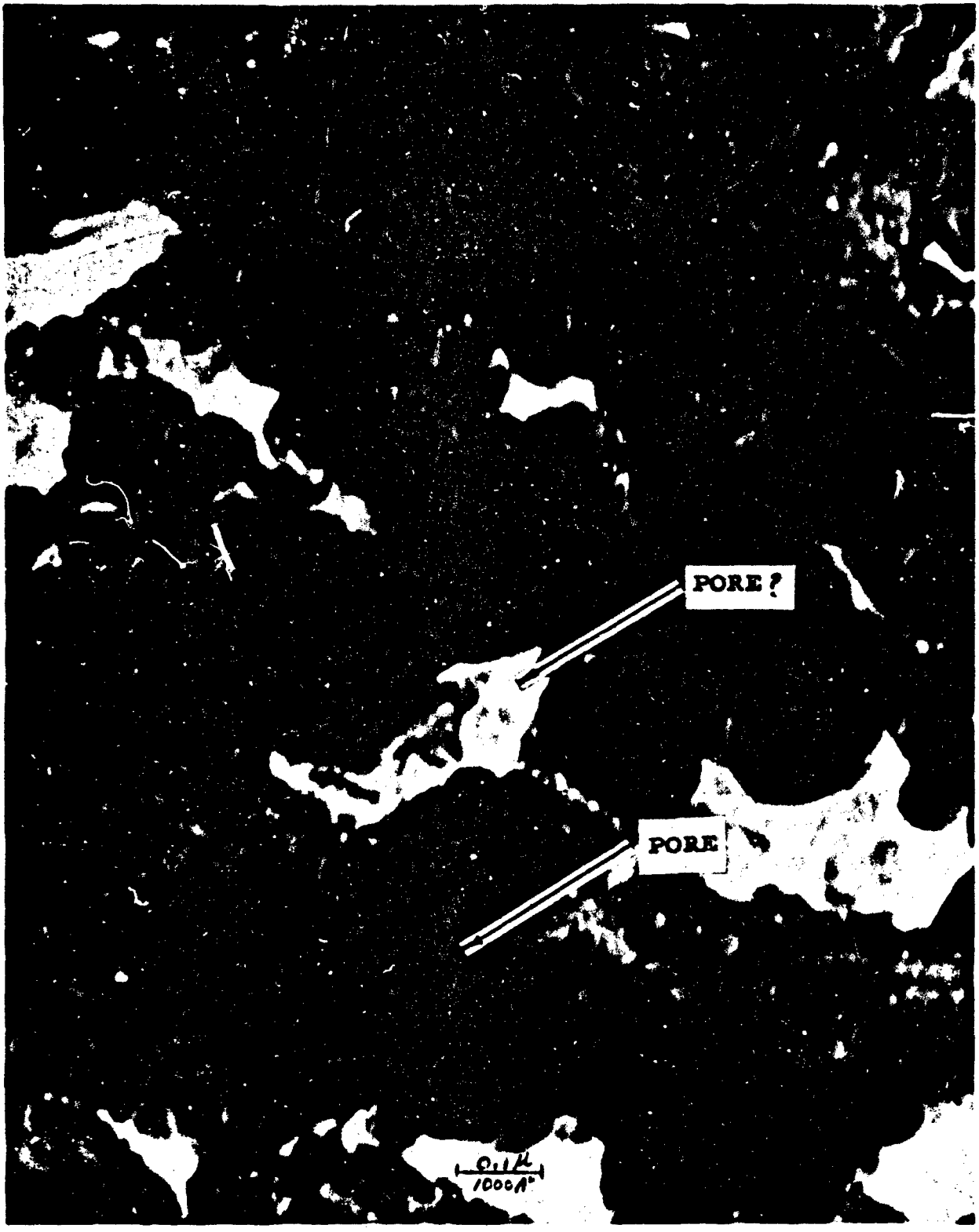

Figure 28 Electronmicrograph of the Surface of VM WF Millipore Material at 150,000 X 100X

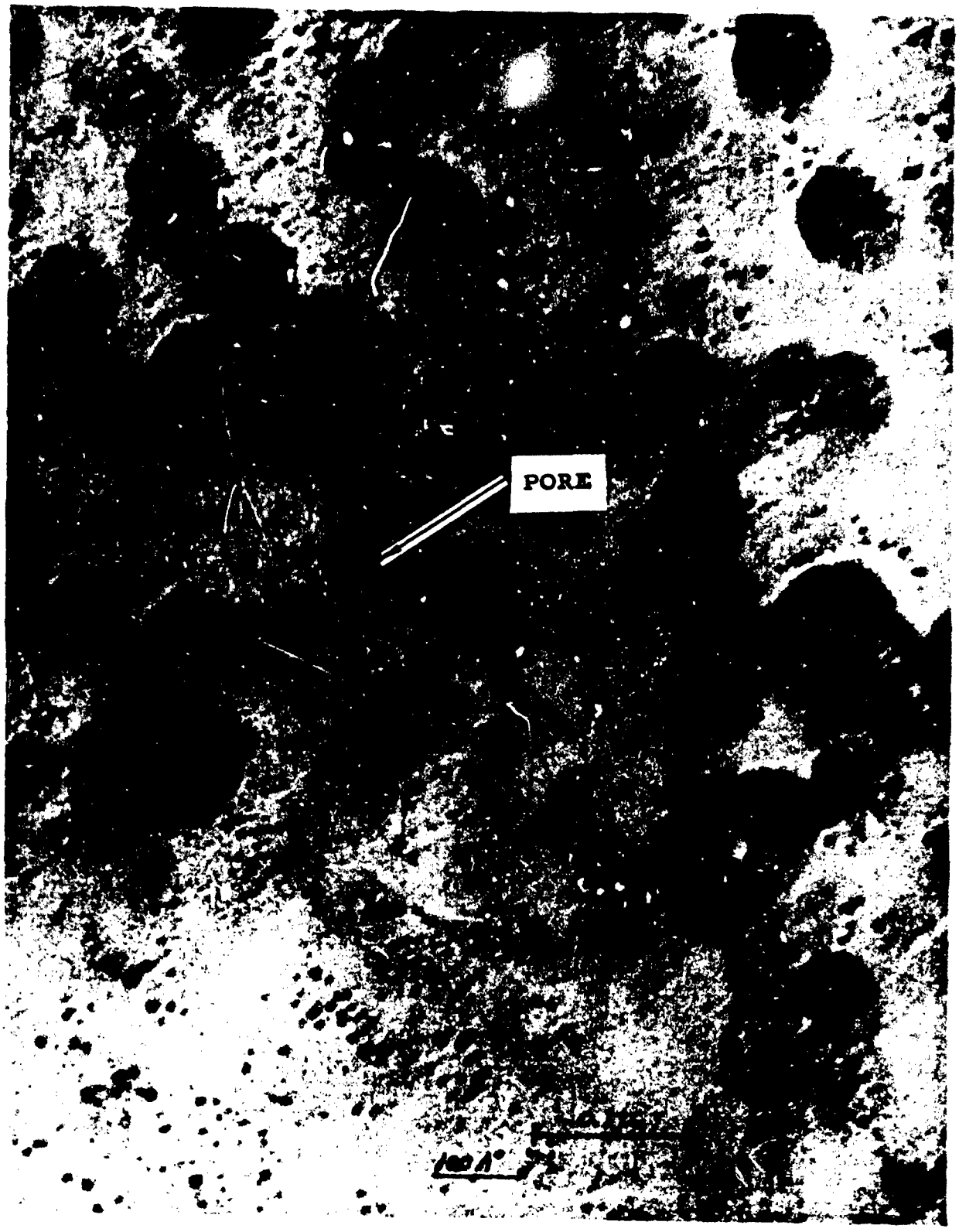

Figure 29 Electronmicrograph of the Surface of Dow Corning Porous Glass at 300,000 X
100X

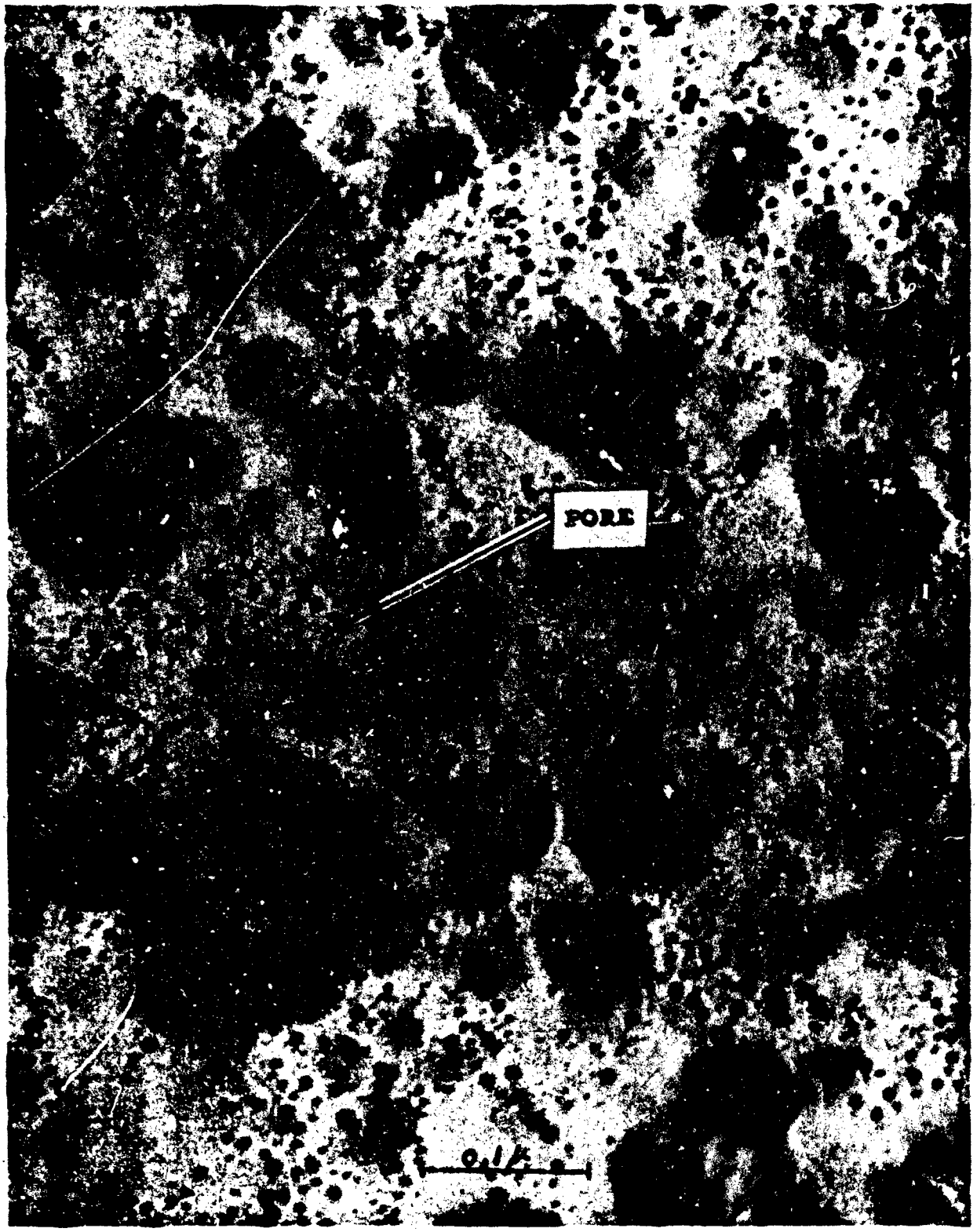

Figure 30 Electronmicrograph of the Surface of 2.2XH Membrane Material by RAI at 61,000 X 100X

Figure 31 Electronmicrograph of the Surface of Dow Corning Porous Glass at 300,000 X 100X

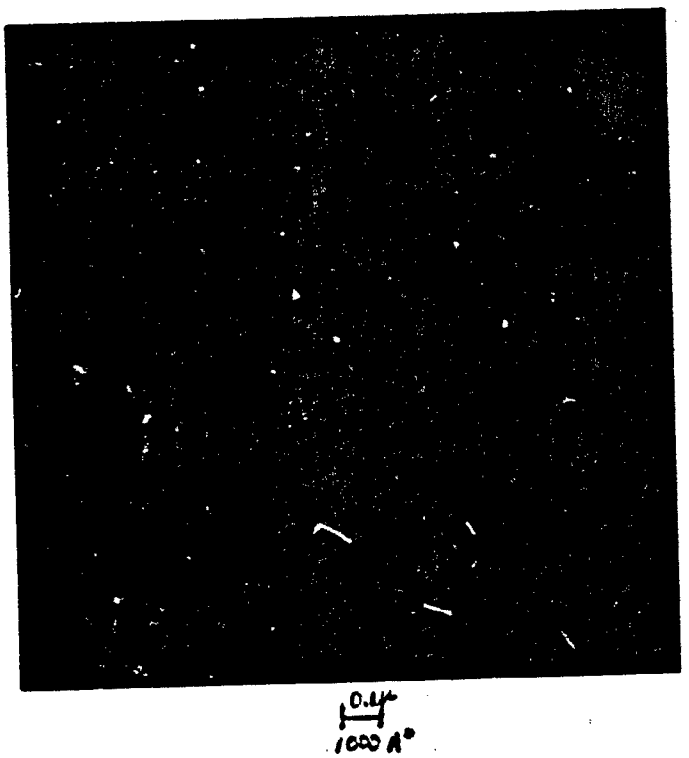

Figure 32 Electronmicrograph of the Surface of 2.2XH Membrane Material by RAI at 61,000 X 100X

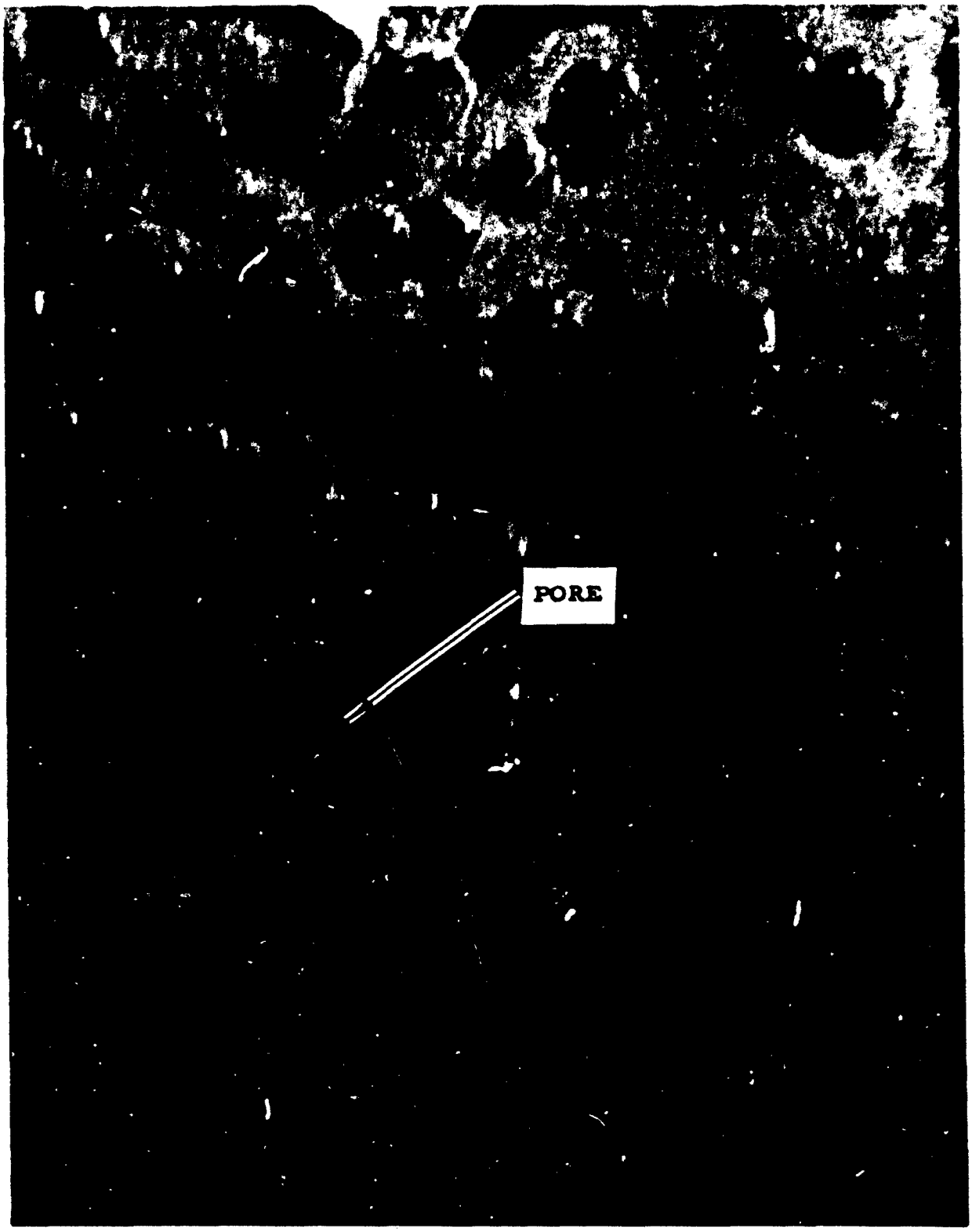

Figure 33 Electronmicrograph of Surface of 2.2XH Membrane Material by RAI at 300,000 X 100X

Figure 34 Electronmicrograph of Surface of 2.2XH Membrane Material by RAI at 300,000 X 100X

Figure 35 Negative Plate with 2:1 Construction After 184 Cycles at 60% DOD. 100X

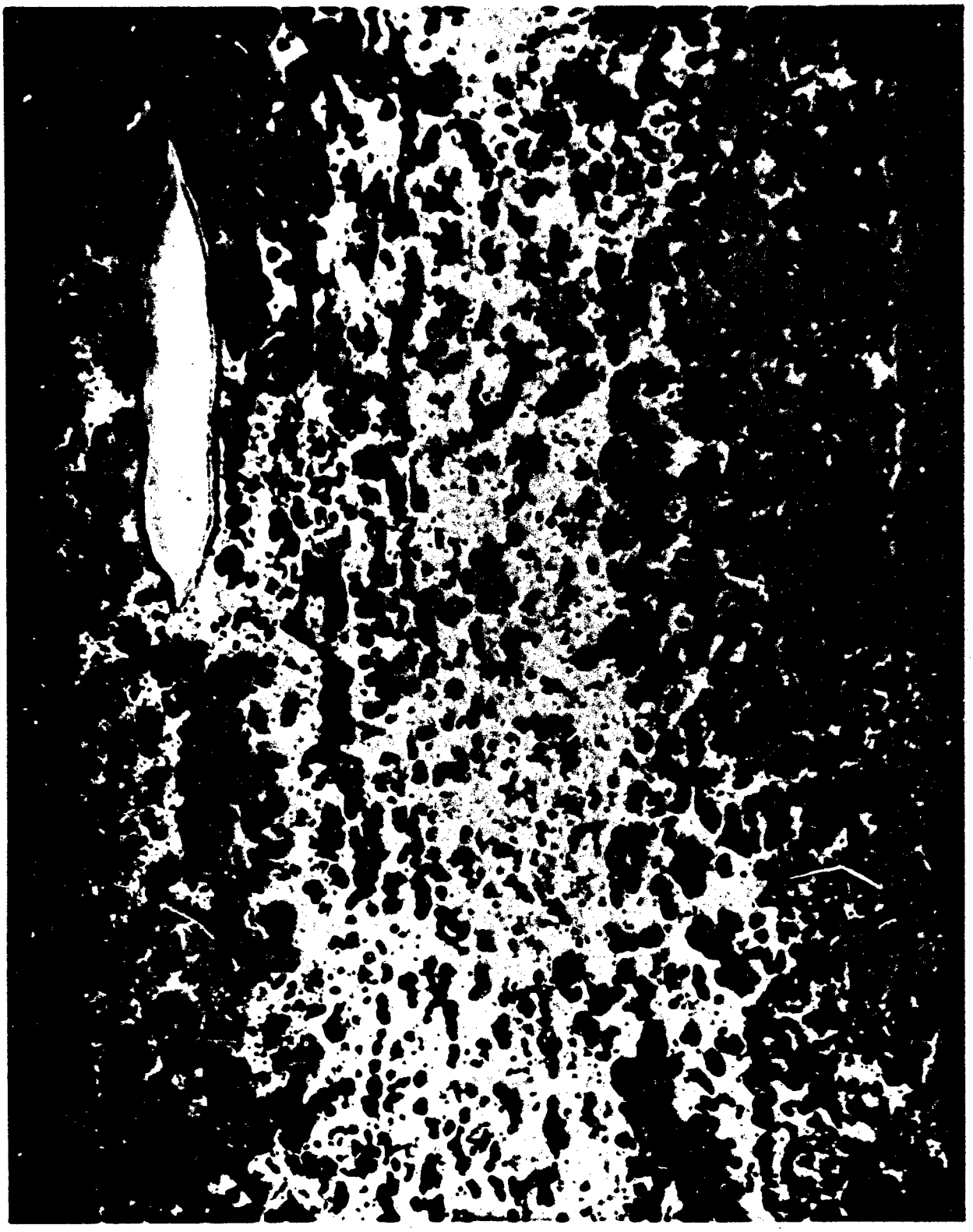

Figure 36 Negative Plate with a 3:1 Construction After 204 Cycles at 60% DOD 100X

Figure 37 Negative Plate With a 4:1 Construction After 220 Cycles at 60% DOD 100X

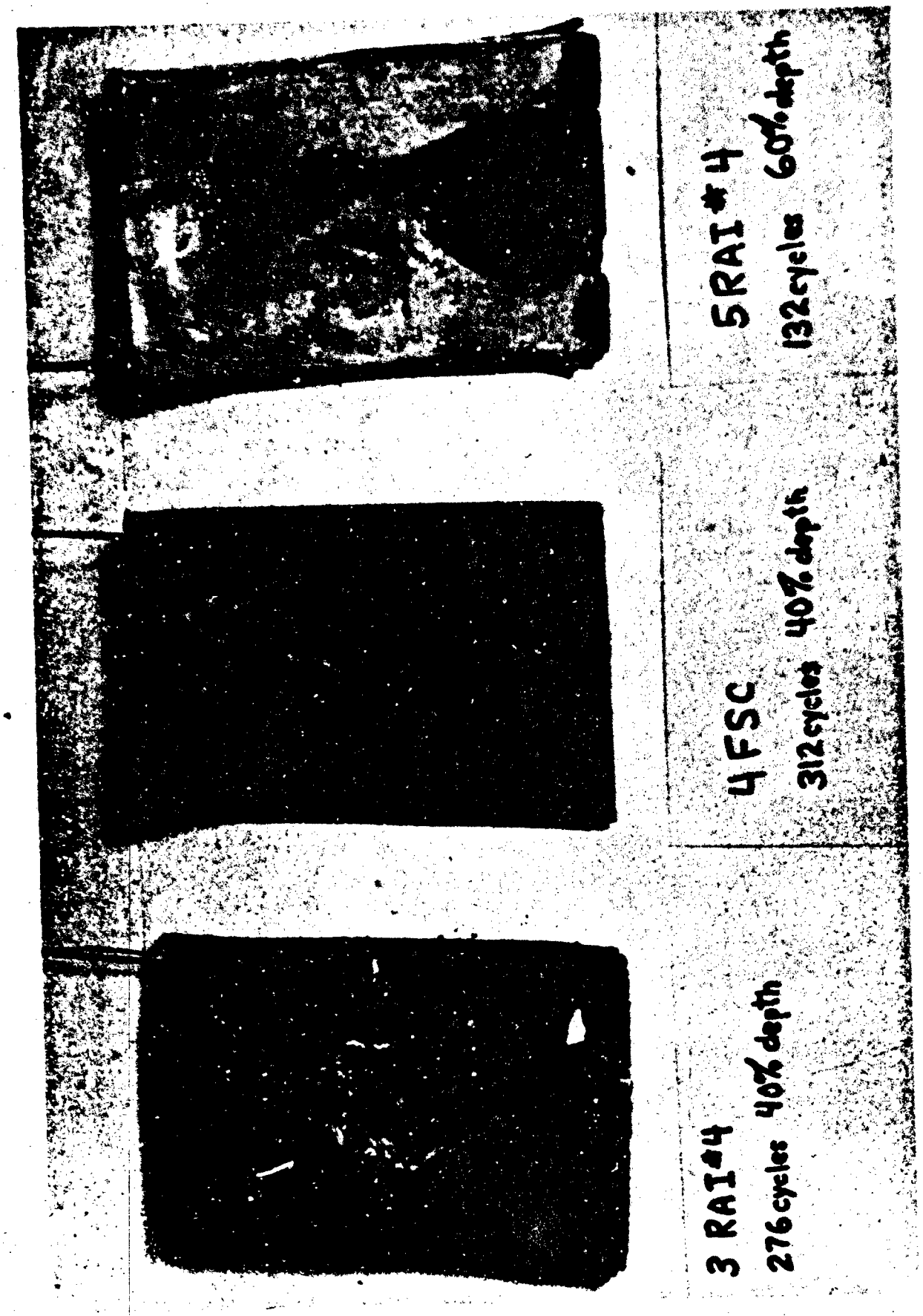

Figure 38 Appearance of the Negative Material After Cycle Failure in the Separator Test 100X

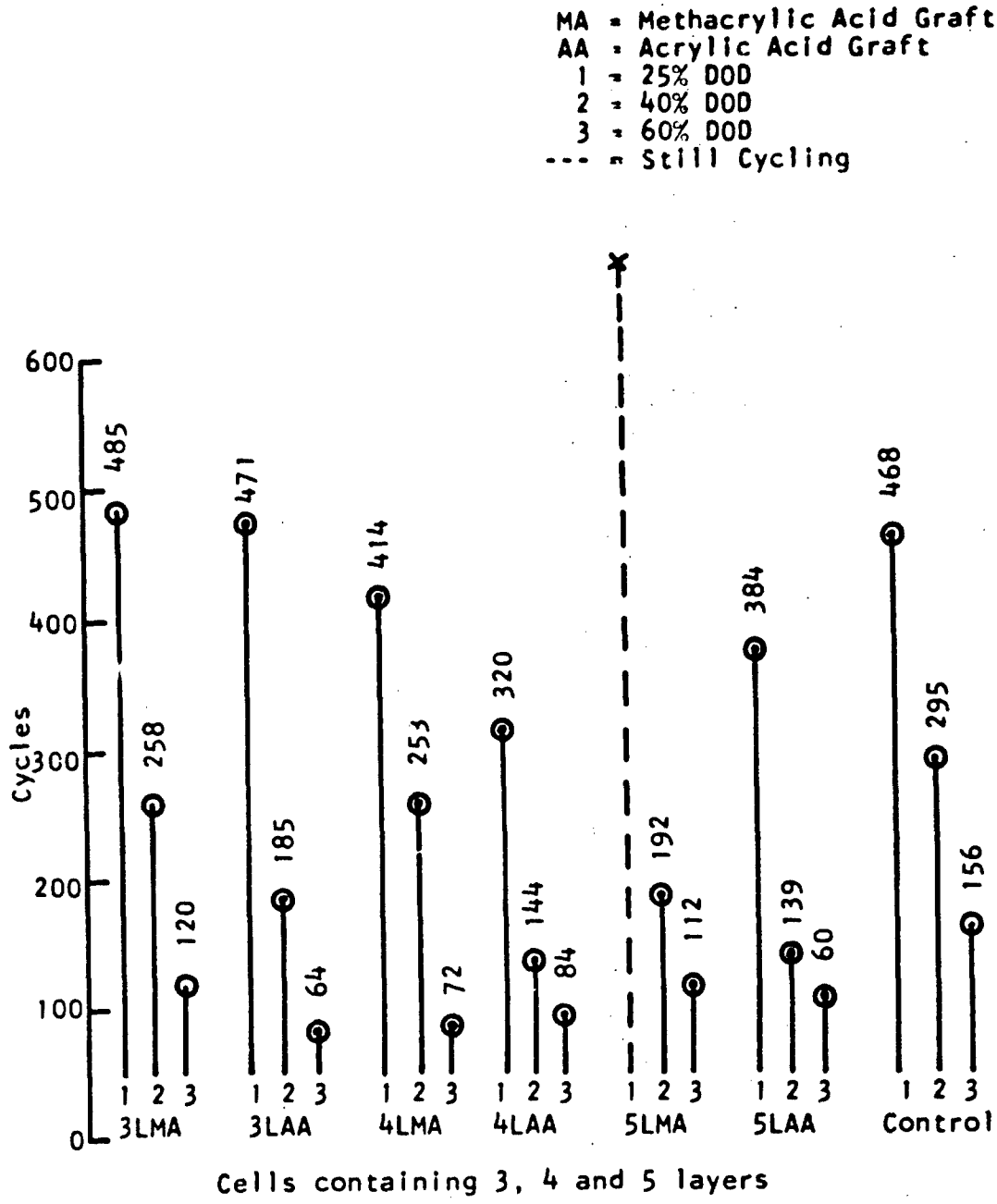

Figure 39 Average number of cycles obtained with RAI membrane in each depth-of-discharge.

APPENDIX I

SURFACE AREA STUDIES OF ZINC ELECTRODES

SURFACE AREA STUDIES OF ZINC ELECTRODES

Summary Report

March 25, 1968

T. P. Dirkse

Calvin College

SURFACE AREA STUDIES OF ZINC ELECTRODES
Summary Report

INTRODUCTION

In the development of zinc electrodes for use in alkaline battery systems, the surface area exposed to the electrolyte is of considerable importance. However, no convenient method is available to measure the surface area of battery electrodes of the type produced by Delco-Remy. These are porous electrodes made by the electrolytic reduction of zinc oxide.

The purpose of the work described here was to develop a method for measuring the surface area of such electrodes. The approach was to determine the time required to passivate a zinc electrode and then relate this time to the surface area.

It is generally agreed that as the zinc electrode discharges (is anodized) a solid product is formed. This product dissolves readily in the KOH electrolyte. When this dissolution is no longer possible, the discharge product deposits on the electrode and forms a film which passivates the electrode. If the anodization is carried out at a high current rate, the dissolving of the discharge product may not take place to an appreciable extent and this product then deposits on the electrode directly. It has been observed that the zinc may become covered with a blue film. This film may be the passivating layer. The color of this film suggests that it is about 500 A. thick. Thus, if the anodization can be carried out so rapidly that no dissolution of the discharge product takes place, then the number of coulombs passed before passivation tells us the amount of discharge product formed on the

electrode. Assuming a thickness of 500 A for the film or layer, we can then calculate the surface area, or at least a relative surface area.

Sheet zinc electrodes were used as reference standards for surface area measurements. KOH concentrations ranging from 1% to 40% wer used and runs were made at 0°, 15°, and 25°C.

EXPERIMENTAL

The sheet zinc electrodes were zinc strips 1.5 x 0.5 inches and 0.02 inches thick. These strips were degreased in etnylene dichloride and then given a slight etch with dilute HCl. Following this they were rinsed thoroughly, dried, and then painted with polystyrene cement so that only an area 0.5 x 0.5 inches was exposed to the electrolyte. They were then stored until ready for use.

The circuit consisted of a 28 volt battery in series with variable resistors to reduce the current to the proper level. A switch turned on the current and an electric timer at the same time.

The cell was a jar 6 x 5 x 3 inches holding about 350 ml of the KOH solution. Two nickel oxide electrodes, 4 x 4 inches, were placed on either side of the cell. A piece of zinc wire served as a reference electrode. The test zinc electrode was placed between the two nickel oxide electrodes. A vacuum tube volt meter was used to measure the potential between the test electrode and the reference electrode. When this potential rose suddenly to more than 2 volts the current and timer were turned off and the electrode

was considered to be passivated.

RESULTS

Effect of Pre-treatment.

During the time the sheet zinc electrodes were stored it is possible that they acquired a small amount of oxide coating. This had to be removed before the electrode could be anodized. Three kinds of pretreatment were used:

1- the electrodes were immersed in the electrolyte for 5 minutes, then treated cathodically at about 35 ma. for one minute, and then allowed to remain on open circuit for another 5 minutes before anodization.

2- the electrodes were placed in the electrolyte for 5 minutes and then anodized.

3- the electrodes were abraded with a 3/0 silicon carbide paper, rinsed with distilled water and allowed to remain in the KOH solution for 5 minutes before the run was started.

These electrodes were all anodized in 10% KOH at 25°C. The results are shown on Figure 1. There appears to be no significant difference. The same results are obtained regardless of the method of pretreatment. In subsequent work, pretreatment #1 was used.

It is likely true that the surface area was not exactly the same after the three types of pretreatment. Abrading should alter the surface area while cathodic current and immersion in the electrolyte would remove surface oxide films by reduction or by dissolving.

Any such difference however, are within the experimental uncertainty of the method being used. Several factors contribute to this uncertainty. The main ones are: (a) lack of reproducibility in exposing exactly a 0.5 x 0.5 inch area to the electrolyte; (b) time lag in switching; and (c) the possibility that some of the discharge product is being dissolved.

Effect of Amalgamation.

Another factor to be considered is that commercial zinc battery electrodes are amalgamated. Evidence is available that amalgamation has the effect of increasing the surface area of the zinc electrode. Consequently, several sheet zinc electrodes were amalgamated by dipping them for 30 seconds in a solution containing 50 gms. of $HgCl_2$ per liter. These were then anodized and compared with non-amalgamated electrodes. The results are shown on Figure 2. It is obvious from Figure 2 that this method cannot distinguish between the surface area of amalgamated and non-amalgamated electrodes, if there is such a difference. Thus in using this method to compare the surface area of porous zinc electrodes with that of sheet zinc electrodes we need not take into account the fact that our sheet zinc electrodes are not amalgamated while the porous electrodes are.

Effect of Surfactants.

Delco-Remy electrodes as currently produced contain about 0.1% of an Emulphogene. This material is a surfactant which has increased the cycle life of the zinc electrodes. The reason for this improvement is as yet not known. Consequently, a few runs were made to determine whether this surfactant would alter the effective

surface area of the electrode as determined by this method.

An excess of Emulphogene BC-610 was added to 10% KOH (the solubility of the Emulphogene is very low). The results of the passivation times are given on Figure 3 together with similar results obtained in 10% KOH containing no Emulphogene. Apparently, the Emulphogene makes no difference in the surface area measurement by this method. Consequently, in making comparisons between Delco-Remy electrodes and sheet zinc electrodes, it is not necessary to make any allowance for the presence or absence of Emulphogene.

Effect of KOH Concentration and Temperature

In view of the assumed mechanism for the passivation of the zinc electrode, both temperature and KOH concentration should have an effect on the passivation times. The rate of dissolution of the discharge product is undoubtedly a function of the temperature. The solubility limit is a function of the KOH concentration. Consequently, at low temperatures and low KOH concentrations the dissolution of the discharge product should be minimized. Then the coulombs needed to passivate the electrode should be a direct measure of the amount of material needed to cover the surface of the zinc electrode with a passivating layer.

Passivation times were measured in a concentration range of 1 to 40% KOH and at 0°, 13°, and 25°C. Figures 4,5, and 6 give the results obtained at each temperature. These results are what would be expected. More coulombs are needed to passivate the zinc electrode as the KOH concentration increases, although the difference between 10 and 20% KOH is not great. The curve in 1% KOH

at 0°C is almost parallel to the base. This suggests that the same number of coulombs are required to passivate the electrode regardless of the current used. That is, the rate of dissolution of the discharge product is approaching zero.

The results are presented differently on Figures 7, 8, 9, and 10. Here the effect of temperature is more clearly seen. As would be expected, more coulombs are needed to passivate the electrode as the temperature increases. This is because the rate of dissolution of the discharge product increases with increasing temperature.

Delco-Remy Electrodes.

Having obtained data about passivation times for sheet zinc electrodes under a variety of conditions, the next step was to determine passivation times for Delco-Remy porous electrodes under some of these same conditions. These electrodes could not be painted with polystyrene cement to expose only a limited surface area to the action of the electrolyte. Consequently, a 0.5 x 0.5 inch section of the electrode was used. This was cut from the upper corner where the lug or tab was attached. In this way, the lug could be used for electrical connection to the active material.

In making these runs several experimental difficulties were encountered. First of all, a considerably higher current was required to give passivation times comparable with those obtained for the sheet zinc electrodes. This higher current rate was more difficult to control and maintain constant throughout the run. Secondly, these electrodes behaved somewhat differently than did the sheet zinc electrodes. For the latter, the voltage rose very abruptly at passivation. There was no difficulty in determining

from the voltage change when the electrode had become passive. The porous electrodes showed a gradual increase in voltage during anodic treatment. The voltage did not rise abruptly. Consequently, it was difficult to determine from the voltage change just when the electrode had become passive. A rather arbitrary standard was finally adopted. The electrode was considered to have become passivated when its voltage showed that it had been polarized to the extent of 4 volts. This, admittedly, is arbitrary and is partly responsible for the rather poor reproducibility encountered in measuring these passivation times.

A third difficulty was encountered in cutting and handling these porous electrodes. During these processes some active material was lost from the electrode area that was to be tested. This also contributed to the lack of reproducibility.

In addition to these experimental difficulties there is another consideration. This method we are describing uses the amount of anodic coulombs as a measure of surface area. This means that only the surface area which is zinc can be measured. It can undergo anodic oxidation. Any surface area which is an oxidized form of zinc, e.g., zinc oxide, zinc hydroxide, zinc carbonate, will not be measured by this method because it cannot be further oxidized. However, if these materials should dissolve in the electrolyte and then expose zinc, this exposed zinc could be oxidized and would be included in any calculated area. This method, then, does not measure total surface area but rather it measures the area available for electrochemical oxidation. And this is not necessarily the area that would be measured, e.g., by the BET method using gas adsorption.

The above considerations are mentioned to help in interpreting the results that were obtained.

The procedure used was as follows. The electrode was placed in the electrolyte at open circuit for five minutes. It was then given a cathodic treatment for one minute at a low current density. Hydrogen was being evolved at the electrode by the end of this minute. Following this the electrode was left on open circuit for another five minutes and then anodized.

After measuring the time to passivation, this time was compared with the time to passivation for a sheet zinc electrode. For example, if the time to passivation for a porous electrode was 10 seconds, then reference was made to sheet zinc electrodes passivated under the same conditions of KOH concentration and temperature, Figures 3-10. From these curves one reads the number of coulombs required to passivate a sheet zinc electrode in 10 seconds. The ratio of this number of coulombs to the number of coulombs required to passivate the porous electrode in 10 seconds under the same conditions is considered to be also the ratio of the surface areas of the two types of electrodes.

These ratios were determined under several conditions and are summarized in Table I

TABLE I

RATIO OF AREA OF DELCO-REMY ELECTRODES TO THAT OF SHEET ZINC

% KOH	Temp, °C	Ratio
40	25	7:1
10	25	10:1
10	13	10:1
10	-3	13:1
1	-3	28:1

The uncertainty of the ratios given in this Table is about ± 20%. It appears to decrease somewhat at lower temperatures and at lower KOH concentrations. It is abvious that the ratio obtained depends on the conditions under which the measurements are made. The ratio increases as the temperature is lowered and as the KOH concentrations are decreased. These are the same conditions under which one would expect the rate of dissolution of the discharge reaction product to be less. Thus, it seems that the less the interference of the dissolving of the discharge product, the higher is the ratio of apparent surface area of porous zinc electrodes to sheet zinc electrodes. This might suggest that the best ratio or the most realistic ratio is the one determined in 1% KOH at 0°C. However, this is merely a guess until an independent method is available which will determine the surface area of the electrochemically active zinc in these porous electrodes. Certainly, a surface area ratio of 30:1 seems more realistic than a ratio of 7:1. Until an independent method is used to determine what the surface area ratio is, this method cannot very well be used to determine such a ratio. If such an independent method would tell us the ratio, then we could select the conditions under which this coulombic method gives the same ratio, and use the method for determining surface area ratios for zinc electrodes. The method is fairly simple and with further work the uncertainty could probably be reduced to about ± 10%.

Surface Area of Failed Electrodes.

Attempts were also made to determine the relative surface area of Delco-Remy porous zinc electrodes which had been removed from cells. These cells had been cycled until failure, and failure

was due to loss of zinc electrode capacity. These electrodes were treated the same way as the fresh zinc electrodes were, and the same difficulties were encountered in making time-to-passivation measurements.

In addition to this there was an added difficulty. This had to do with selecting a representative sample. In most electrodes there was no active material left on the grid in the vicinity of the lug. The active material on these electrodes had, during cycling, been redistributed away from the top of the electrode towards the bottom of the electrode. We were limited to the use of a 0.5 x 0.5 inch segment of the electrode. We eventually selected a sample from the center of the electrode. However, this was not necessarily a representative sample. This certainly had a higher surface area of active material than did a similar sized section near the lug (where there was no active material). Because of this the surface area measurement on such a segment will tell us only the relative surface area of that section and will tell us little, if anything, about the surface area of the total electrode compared to that of a fresh electrode.

These surface area measurements were also made under several conditions and the relative surface areas so determined are given in Table II.

TABLE II

RELATIVE SURFACE AREA OF FAILED ZINC ELECTRODES COMPARED TO SHEET ZINC ELECTRODES

%KOH	Temp. °C	Ratio
40	25	9:1
10	-3	14:1
1	-3	25:1

The uncertainty in these measurements was about ±7%.

Comparing these results with those in Table I it appears that there is not a great deal of difference. The differences are within the experimental uncertainties of each other. The value for the failed electrodes is higher under two conditions, but lower under the third. Thus we may conclude that this method of measurement shows no difference between the relative surface area of a fresh Delco-Remy porous zinc plate and a similar plate which has been cycled to failure. However, as noted earlier, this measurement was made on a segment of the electrode. There were other areas on the grid of these failed electrodes that had no active material. Thus, because the active material still remaining on the grid had a surface area equal to that of a fresh electrode, it is obvious that the total surface area of a failed electrode is less than that of a fresh electrode. To what extent it is less can only be judged by noting what fraction of the grid has no active material on it.

Kinetic Interpretations.

The primary purpose of the work described in this report was to evaluate this method as a means to determine surface areas of zinc electrodes. However, these results can be treated in other ways as well. Because current and time were measured, these values can be used to test various limiting conditions for the electrode reaction.

The times involved in these measurements were rather short and hence it is possible that these electrode reactions were limited and controlled by diffusion of solution species. One common way to check this is to plot current vs. $t^{-\frac{1}{2}}$. If the results show a linear relationship between these two values, then it is likely that

the electrode reaction is diffusion controlled.

Not all of our measurements were amenable to such treatment because the range of time or the range of currents used at a given temperature and in a given KOH concentration were too narrow. Figure 11 is an i vs $t^{-\frac{1}{2}}$ plot for some of the results we obtained where the spread in time and current was sufficiently broad to make the plot meaningful, and where a sufficient amount of data was available. The relationship is reasonably linear. This suggests strongly that these electrode reactions were diffusion controlled. The results do not allow us to infer which ion is the controlling one. It may be diffusion of OH^- ions to the electrode or the diffusion of zincate ions away from the electrode. It may be that both processes are equally significant.

Solution Rates.

If one accepts as valid the general outline for the anodic zinc reaction given earlier in this report, then the results we have obtained may be able to give us an indication of the rate at which the discharge reaction product dissolves under various conditions.

The coulombs-time data given, e.g., on Figure 4 generally show that the number of coulombs accepted by the electrode during electrolytic oxidation increases with increasing passivation times. The increased time allows more of the discharge reaction product to dissolve. Thus more coulombs are needed so that the electrode surface will be covered with undissolved reaction product. The results in 1% KOH at $0^{\circ}C$, however, show no such positive slope. This suggests that under these conditions the rate of dissolution of the reaction product is so slow that all the coulombs accepted by the electrode

are used to coat the surface of the electrode. Thus the number of coulombs needed to bring about passivation is independent of the time allowed for passivation. If this be so, then the number of coulombs required for passivation in 1% KOH at 0°C gives us a direct measure of the surface area (this will be treated later), and of the amount of reaction product needed to coat the surface of the sheet zinc electrodes. The amount required for covering the surface of the sheet zinc electrodes then is 0.1 coulomb.

Later work under these same conditions but over a wider time range showed that at 0°C in 1% KOH the plot of coulombs vs. time also shows a positive slope, Figure 12. The line, however, does extrapolate to 0.1 coulomb for the electrode. This then will be assumed to be the amount of charge needed to cover the surface of the 0.5 x 0.5 inch area of the sheet zinc electrodes. This amounts to 0.1/2 x 96500 or 5.2×10^{-7} moles of zinc oxide or hydroxide. Any additional zinc compound produced during the time to passivation is assumed to have dissolved in the electrolyte.

The rate of dissolution of the zinc reaction product may then be calculated as follows. From Figure 3 a value of 3.8 coulombs is obtained for a passivation time of 10 seconds. Of this, 0.1 coulomb was needed to coat the electrode surface and 3.7 coulombs, the remainder, then represents the amount of discharge product that dissolved or diffused away in the 10 seconds. The 3.7 coulombs corresponds to 19×10^{-6} moles of reaction product. This amount dissolved over a period of 10 seconds which, on a linear basis, corresponds to 19×10^{-7} moles per second as a rate of dissolving. This same procedure has been followed for calculating the dissolution rates under other conditions. The results are summarized in Table III, and on Figure 13.

TAPLE III

RATE OF DISSOLUTION OF ZINC ELECTRODE DISCHARGE PRODUCT

MOLES PER LITER PER SECOND x 10^{+7}

temp → / % KOH	-3 C°	13°C	25° C
1	1	1	2
10	7	8	19
20	10	11	20
30		28	32
40	20	31	35

The results on Figure 13 are given as rate of dissolution per square centimeter of electrode surface.

The dissolution rates are what would be expected. They increase with increasing temperature and with increasing KOH concentration. Whether they are real or not depends on the validity of the assumptions made in calculating them. There is no other way known to us at the moment for checking these results nor are we aware of any other such measurements having been made.

The solubility of the discharge product was studied in still another way. After an electrode became passive it was assumed to be covered with a film or layer of the discharge reaction product, probably zinc hydroxide. This product is soluble in the KOH solution and when it has dissolved the electrode should again be electrochemically active. After being passivated the electrode was allowed to remain on open circuit in the electrolyte for a period of time. It was then treated anodically and the time to passivation

was again measured. When the time to passivation was about the same as that for a fresh electrode in the same solution, the electrode was considered to be electrochemically active.

One such series of trials was carried out in 10% KOH at 25°C using sheet zinc electrodes. It was found that when the electrode remained on open circuit for at least 10 seconds, it had regained its electrochemical activity. For periods of less than 10 seconds the electrode showed some semblance of passivity, i.e., time to passivation was shorter than for a fresh electrode.

A similar experiment was carried out under the same conditions using Delco-Remy porous zinc electrodes. With this electrode it was found necessary to leave the electrode on open circuit at least 3 minutes before electrochemical activity was regained. This added time reflects the increased surface area and the greater congestion in the pores of the electrode. The ratio of these two open circuit times is 3 x 60/10 or 18:1, which is considerably larger than the surface area ratio shown in Table I for these same conditions.

No further work was possible in this area because of time limitations. Until more such work is done no significant conclusions can be drawn from these data.

Dimensions of Surface Film.

It was pointed out earlier that 0.1 coulomb or 5.2×10^{-7} moles of reaction product are required to form the passivating layer over the surface of the electrode. If this film is zinc hydroxide then the weight of the film is $99.4 \times 5.2 \times 10^{-7} = 5.2 \times 10^{-5}$ grams. The handbook density for this substance is given as 3 gm/cc.

This, or course, may not be the density of the actual material in the passivating layer. However, assuming that it is, then the volume of the layer is 1.7×10^{-5} cc. For a surface area of 0.5 x 0.5 inch, this gives a value of 1000 A for the thickness of the film. This assumes a roughness factor of 1. A roughness factor of 2 to 3 is a more realistic figure and this would give a film thickness of 300 to 500A. This may or may not be a realistic value. If the thickness of the film could be determined by an independent method then this could be used to calculate the roughness factor for the sheet zinc surface.

The experimental difficulty involved is in actually observing the passivating film. It dissolves readily in the KOH electrolyte. Furthermore, if removed from the electrolyte, the film may undergo changes in composition.

An alternate way of getting some indication of the thickness of the passivating film is to assume that during passage of current there is film formation and film dissolution, with the latter process being slower than the former. Then, the film gradually thickens as the current is passed and when it has reached a certain thickness the electrode is passivated.

The rate of growth of the film = k x i. The thickness of the film, x, is

$$X = \frac{i \times t \times 99.4}{2 \times 96{,}500 \times 3 \times 1.6} \text{ cm.} \qquad (1)$$

Where i = current

t= time

99.4= mol.wt. of $Zn(OH)_2$

2= mol. wt./equiv.wt. for $Zn(OH)_2$

3= density of $Zn(OH)_2$

1.6= surface area of the sheet zinc electrodes

96,500 = the Faraday

The rate of dissolution of the film, k_d, is constant at a given temperature in a given KOH concentration. This is expressed as moles/sec. To change this value to a corresponding film thickness we change this to a corresponding weight and volume and divide by the density.

$$X' = \frac{k_d \times t \times 99.4}{3 \times 1.6} \text{ cm.} \qquad (2)$$

The thickness at any time X_t then is $X - X'$ or

$$X_t = \frac{i \times t \times 99.4}{2 \times 96{,}500 \times 3 \times 1.6} - \frac{k_d \times t \times 99.4}{3 \times 1.6}$$

or

$$X_t = \frac{t \times 99.4}{3 \times 1.6} \left[\frac{i}{193{,}000} - kd\right] = 20.6\ t \left[\frac{i}{193{,}000} - k_d\right] \qquad (3)$$

For equation (3) we have values for i and t and estimated values for k_d.

An attempt has been made to solve equation (3) for the thickness of the layer from the time-current data we have obtained. However, the two terms in the brackets, i.e., 1/193,000 and k_d are so nearly equal in value, that the difference between them is less than the experimental uncertainty in either one. Consequently, this approach has to be abandoned for the calculation of the thickness of the passivating film until more precise data become available.

T. P. Dirkse

T. P. Dirkse

December 28, 1965

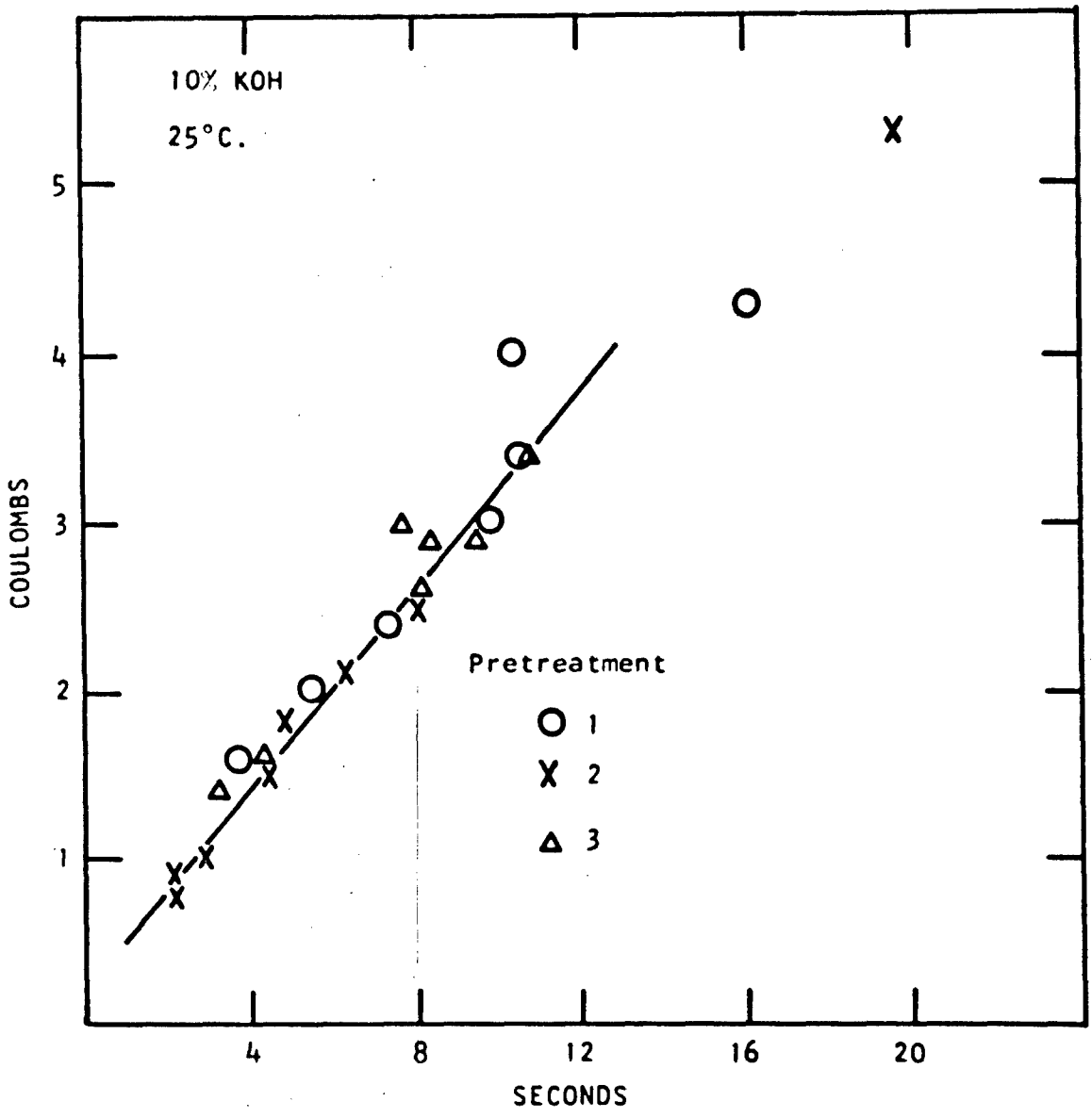

Figure 1 Passivation times for sheet zinc electrodes as a function of the method of pretreatment.

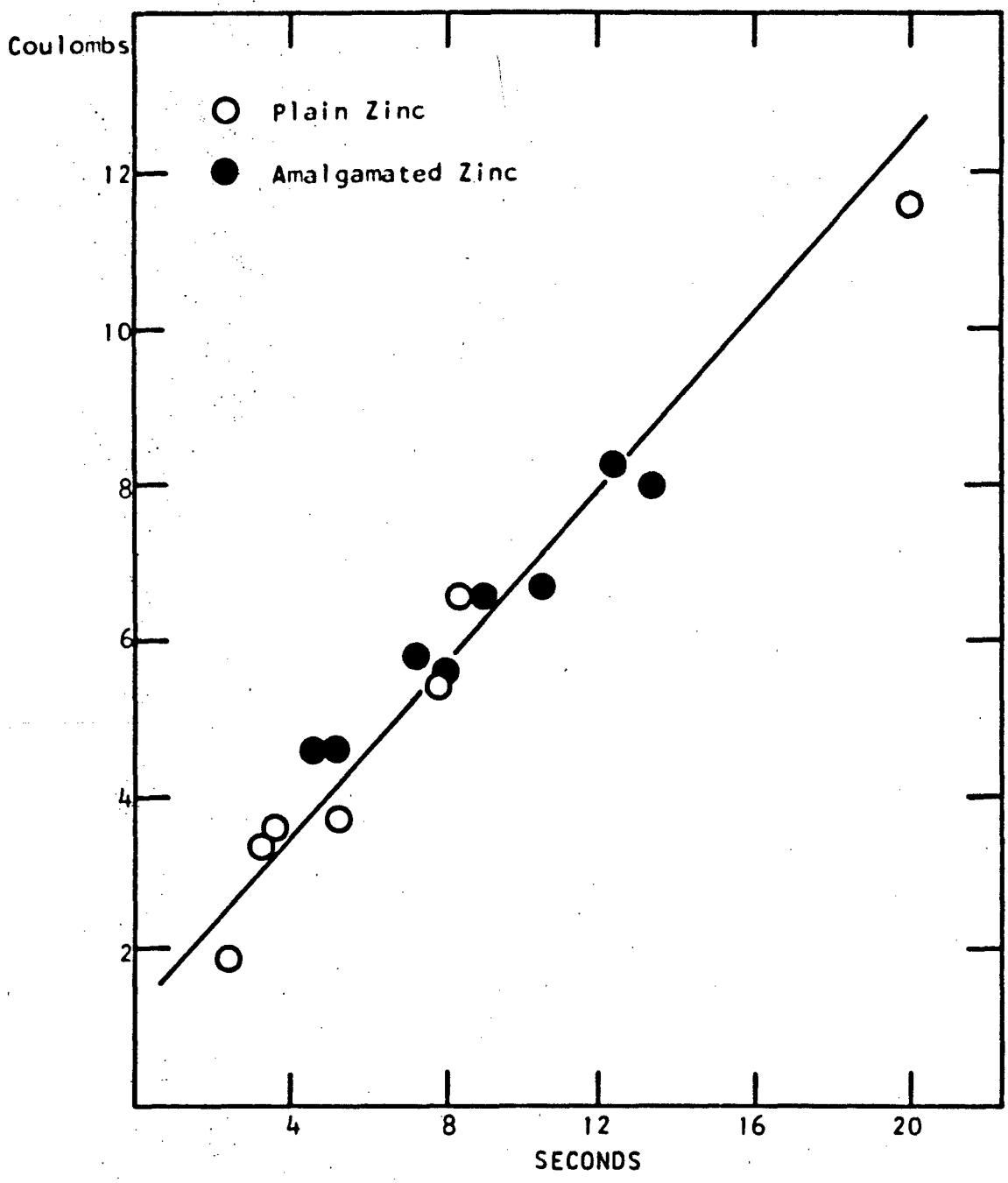

Figure 2 Effect of amalgamation on passivation times for sheet zinc electrodes in 40% KOH at 25°C.

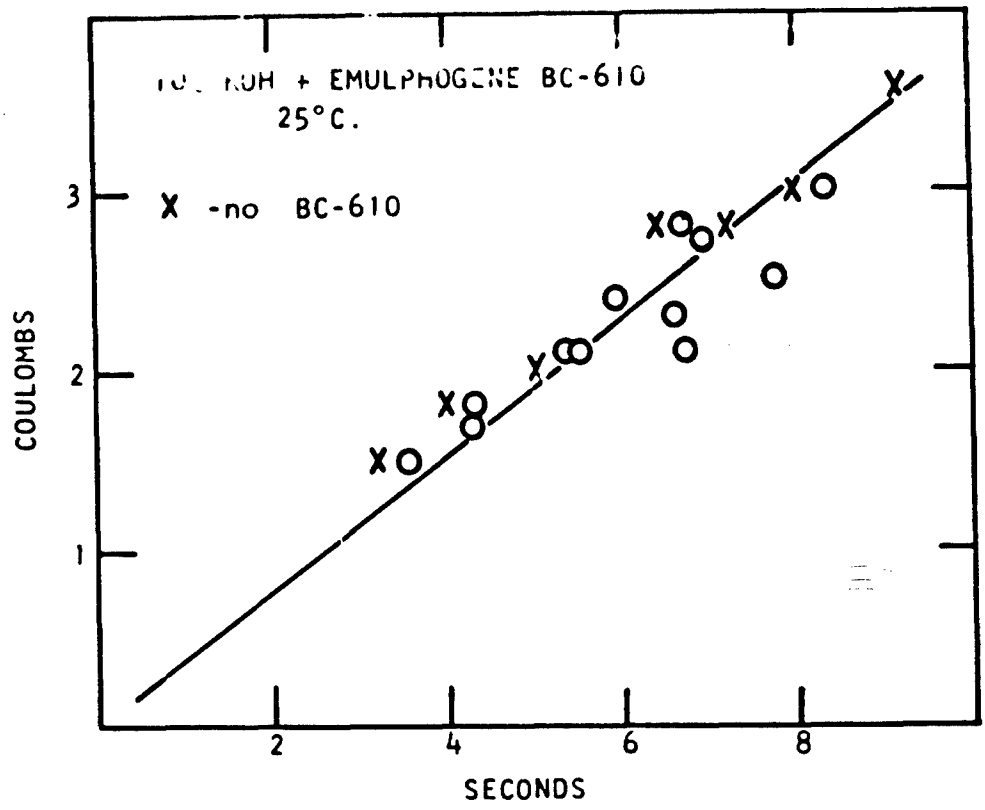

Figure 3 Effect of amalgamation on the passivation times for sheet zinc electrodes.

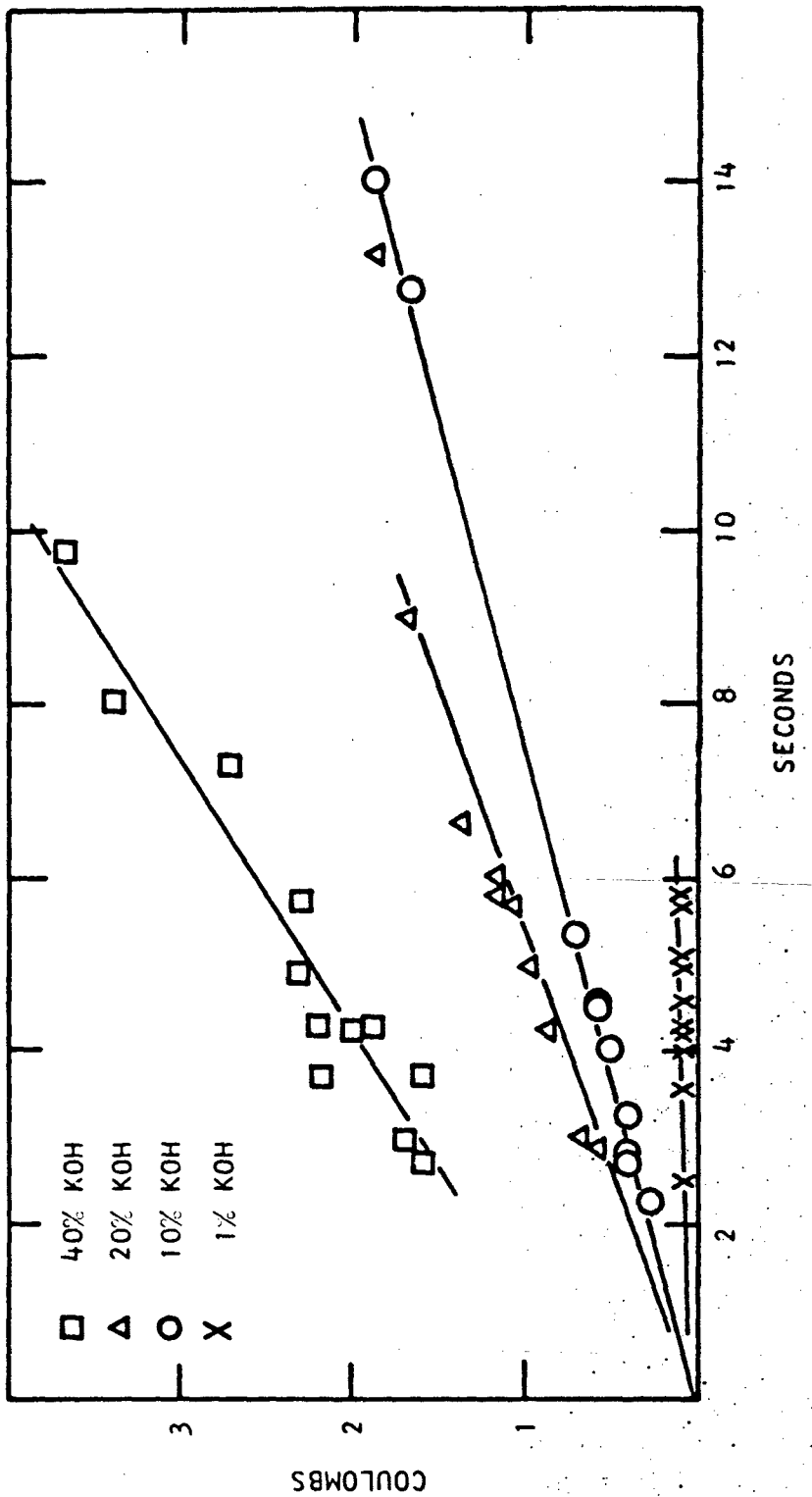

Figure 4 Passivation times for zinc electrodes at 0°C.

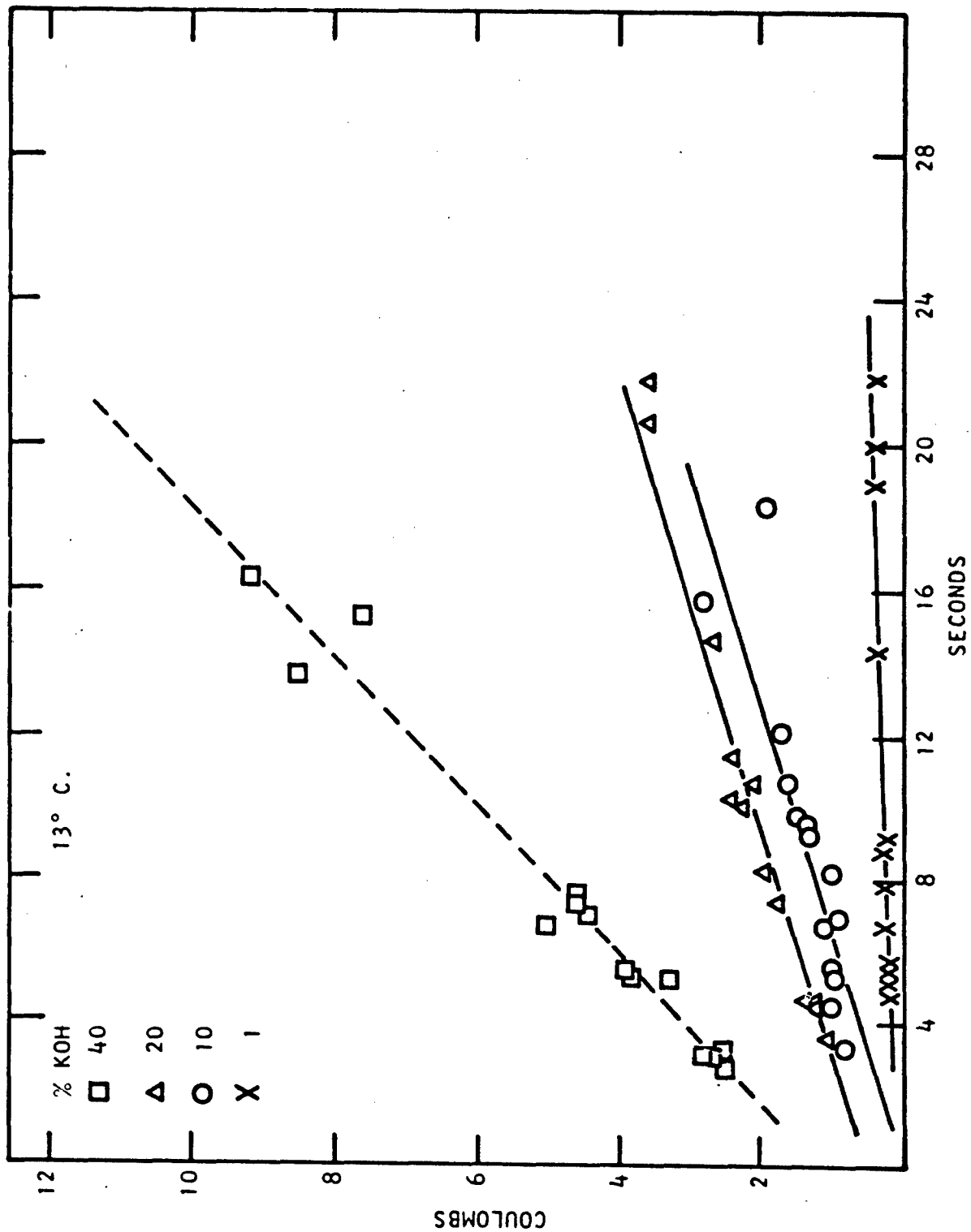

Figure 5 Passivation times for sheet zinc electrodes at 13°C.

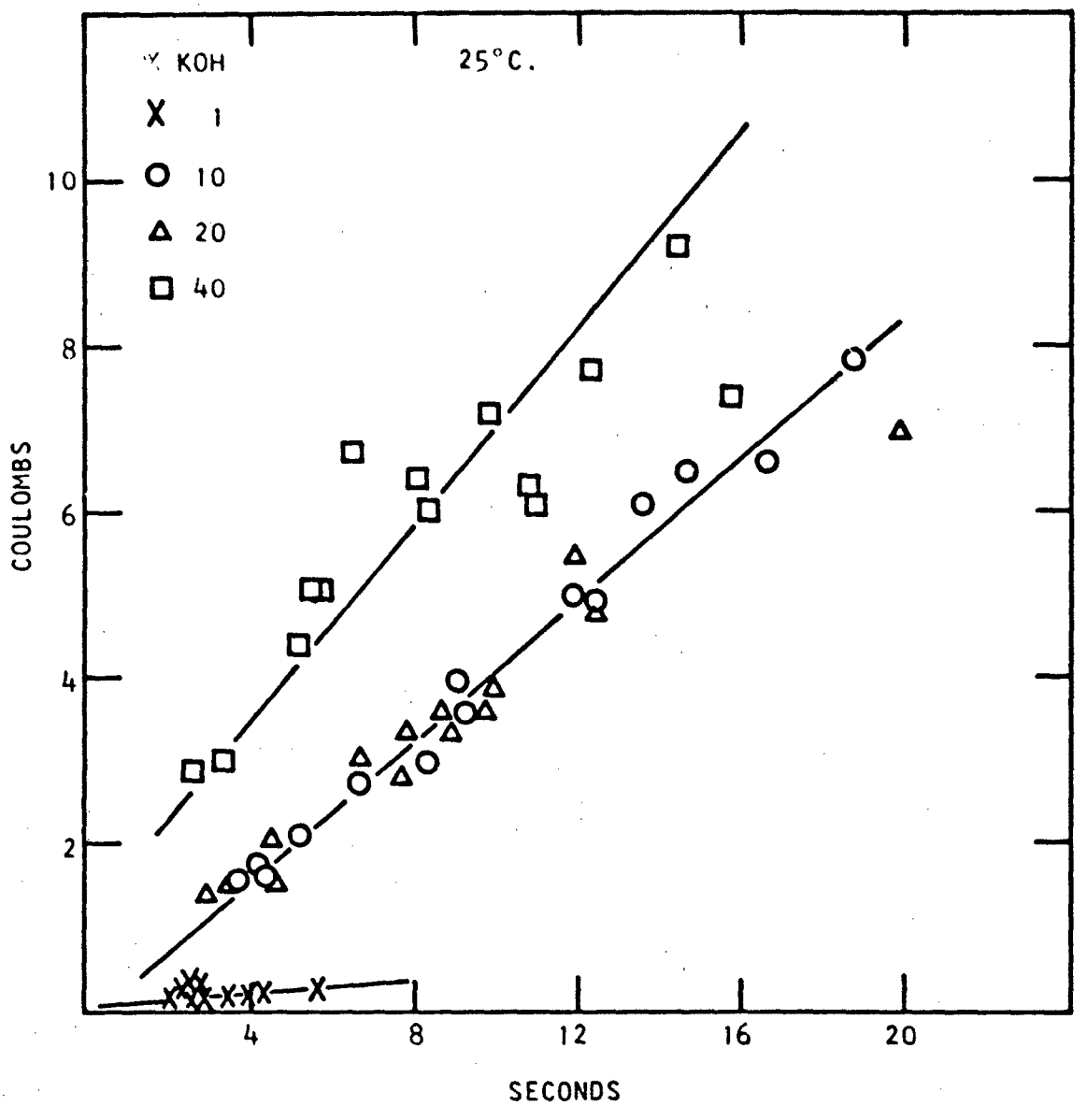

Figure 6 Passivation times for sheet zinc electrodes at 25°C.

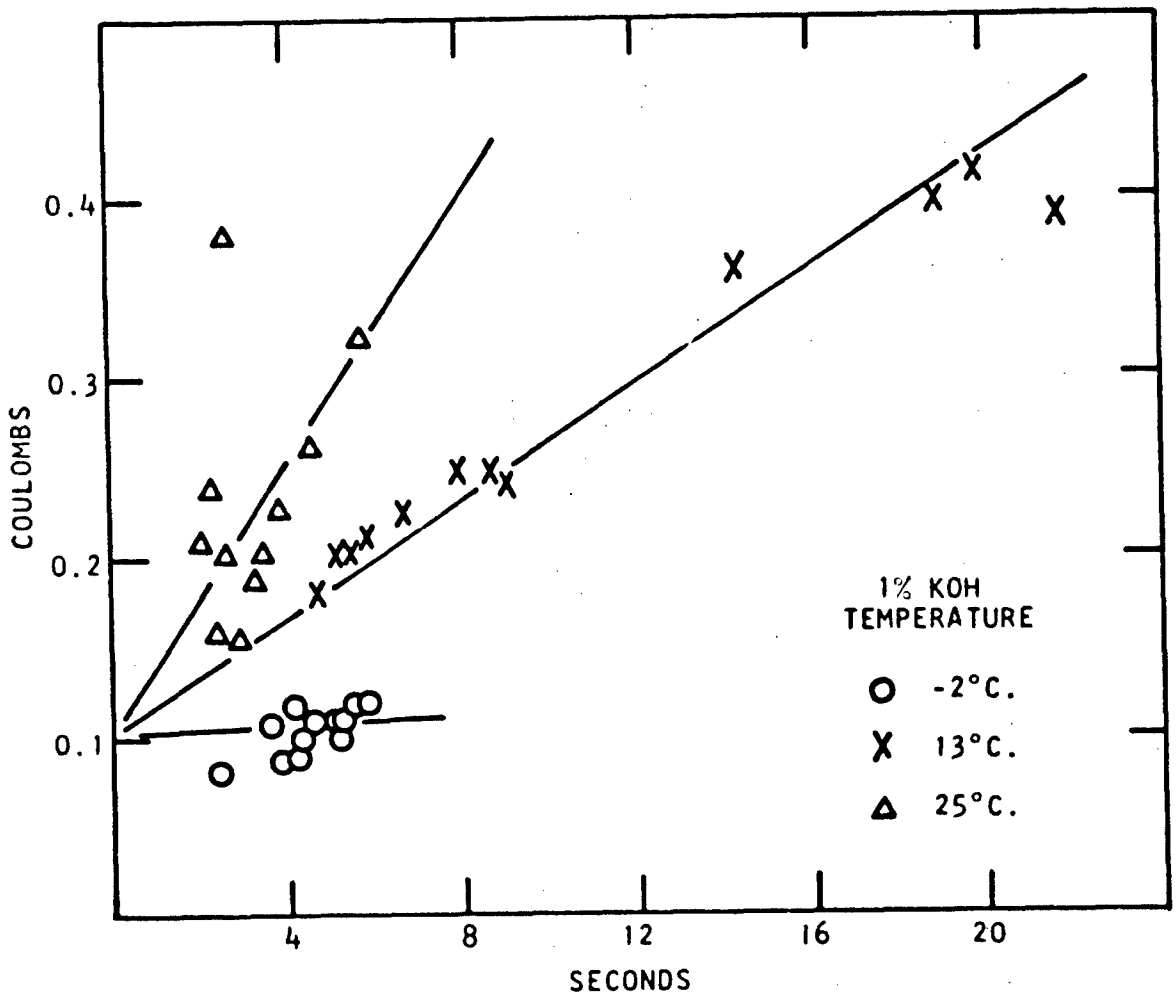

Figure 7 Passivation times for sheet zinc electrodes in 1% KOH

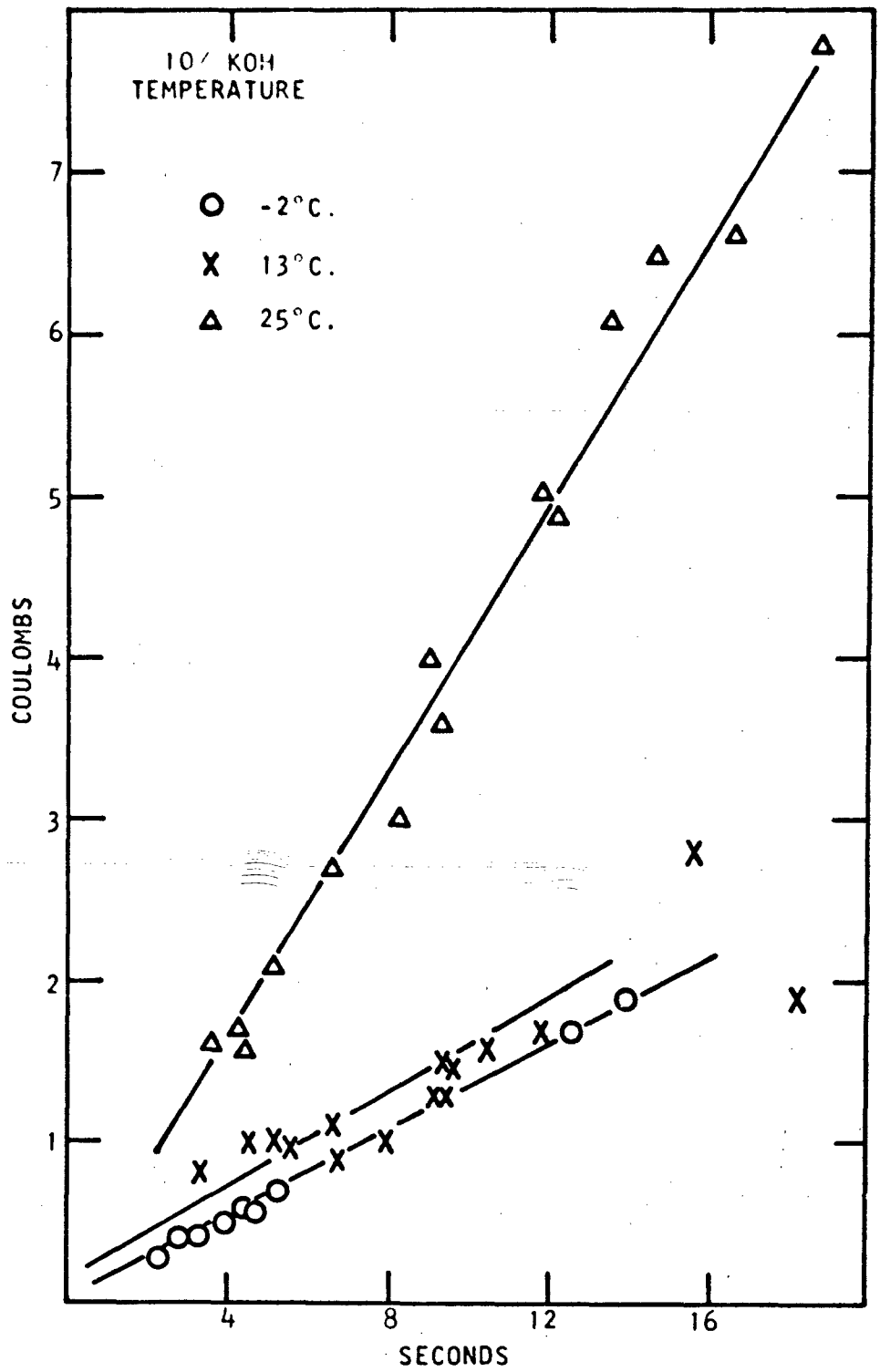

Figure 8 Passivation times for sheet zinc electrodes in 10% KOH.

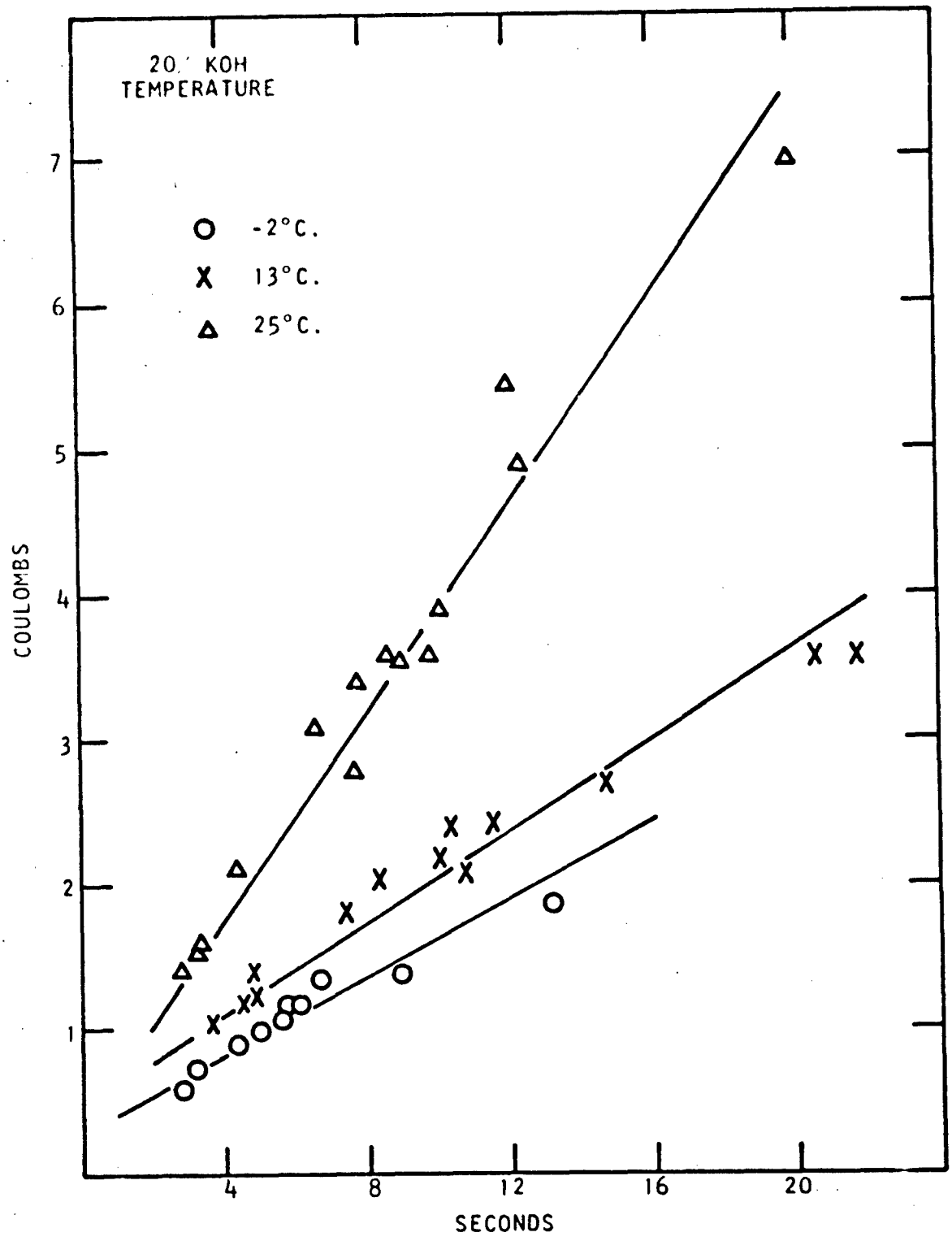

Figure 9 Passivation times for sheet zinc electrodes in 20% KOH

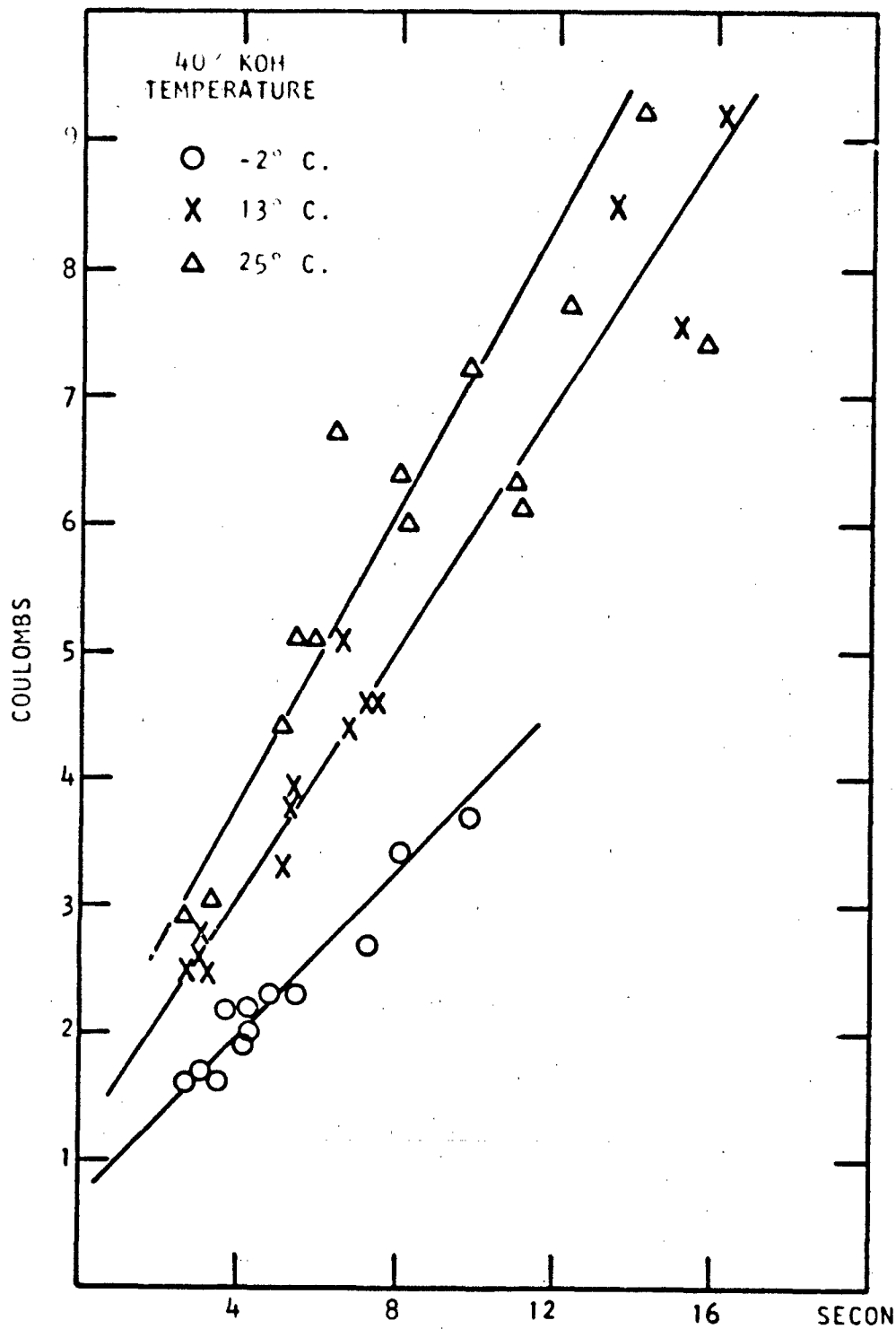

Figure 10 Passivation times for sheet zinc electrodes in 40 ' KOH

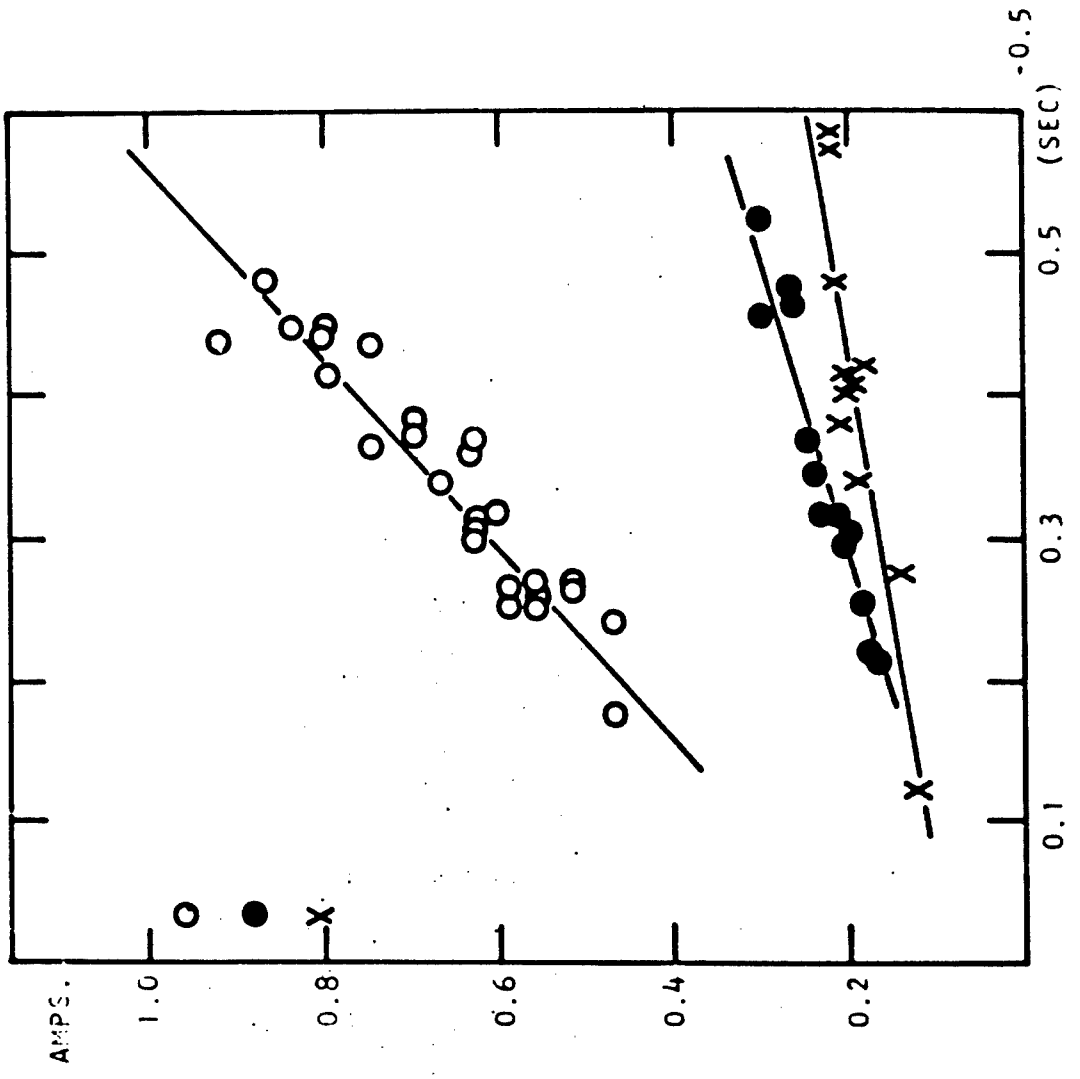

Figure 11 Current vs. $t^{-1/2}$ plots for sheet zinc electrodes

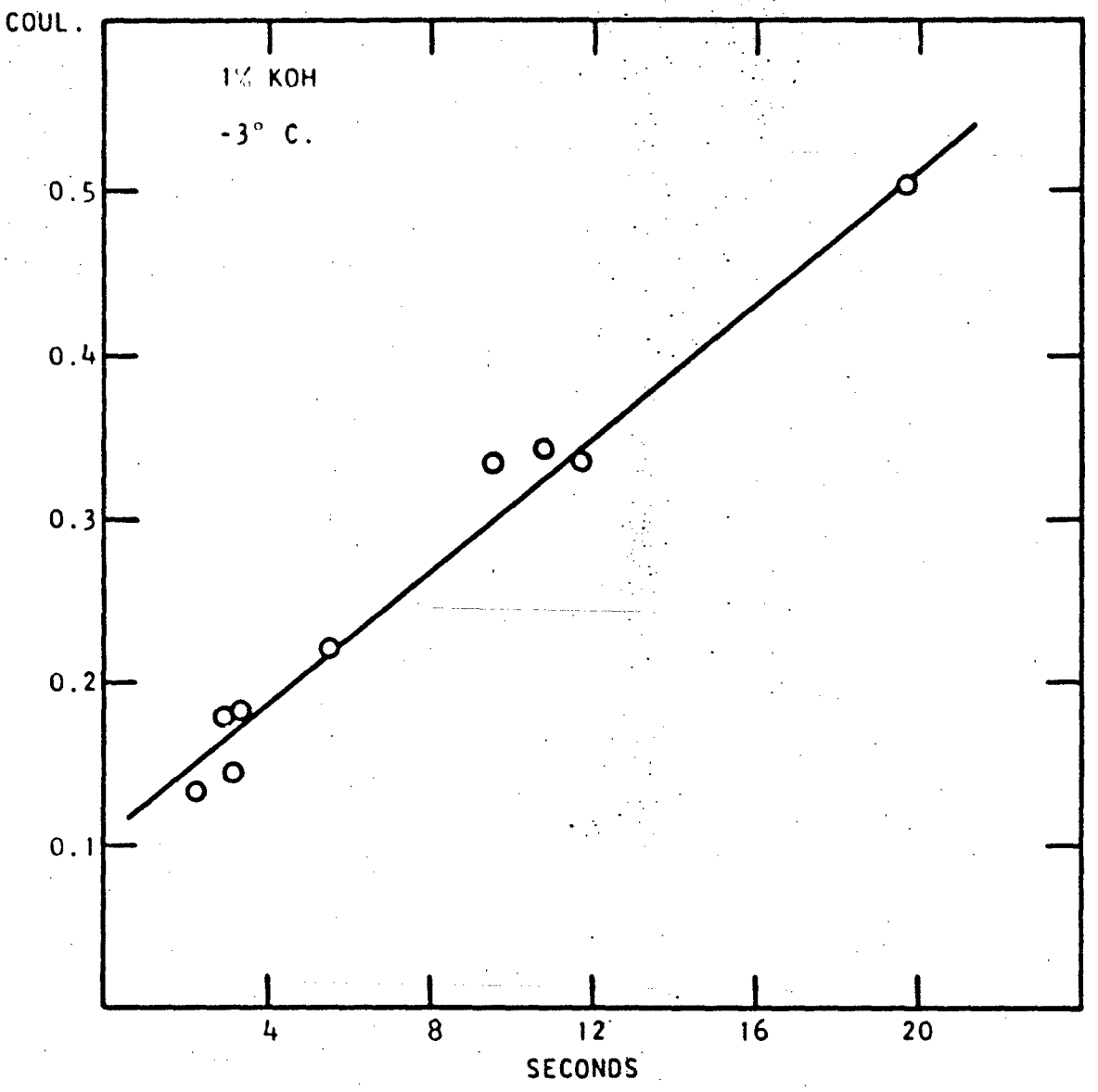

Figure 12 Time-to-passivation data for sheet zinc electrodes

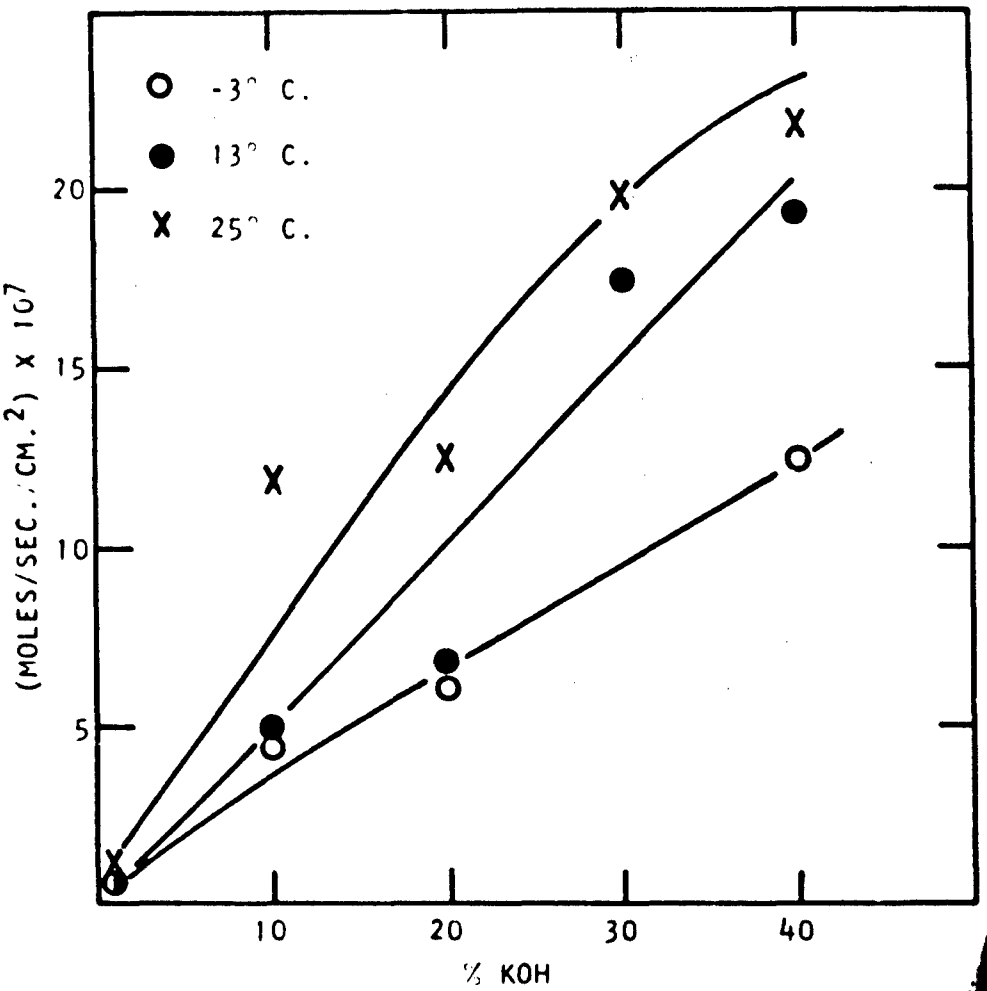

Figure 13 Calculated dissolution rates for th zinc discharge reaction product.

APPENDIX II

PREPARATION AND CHARACTERIZATION OF SPECIAL ZINC OXIDES FOR EVALUATION IN SILVER OXIDE-ZINC SECONDARY BATTERIES

Purchase Order D-R115475
Under Contract No. AF33(615)-3487

PREPARATION AND CHARACTERIZATION OF SPECIAL ZINC OXIDES FOR EVALUATION IN SILVER OXIDE-ZINC SECONDARY BATTERIES

Sixth Quarterly Technical Progress Report

Covering the Period

15 January 1968 to 15 April 1968

Dated

23 April 1968

Prepared by

D. O. Carpenter

G. E. Snow

FOREWORD

This report was prepared by The New Jersey Zinc Company, Palmerton, Pennsylvania on Delco-Remy Division of General Motors Corporation Purchase Order D-R115475 under Air Force Contract No. AF33(615)-3487. The work was directed by Drs. C. E. Barnett and L. J. Reimert.

NOTICE

Foreign announcement and distribution of this report is not authorized. Release to the Clearinghouse for Federal Scientific and Technical Information, CFSTI (formerly OTS) is not authorized. The distribution of this report is limited because it contains technology identifiable with items on the Strategic Embargo Lists excluded from export or reexport under U.S. Export Control Act of 1949 (63STAT.7), as amended (50 USC APP 2020.2031), as implemented by AFR 400-10.

This report is being published and distributed prior to Air Force review. The publication of this report, therefore, does not constitute approval by the Air Force of the findings or conclusions contained herein. It is published for the exchange and stimulation of ideas.

TABLE OF CONTENTS

LIST OF TABLES

LIST OF FIGURES

V. Appendix - Electron Micrographs

ABSTRACT

Previous results have indicated that Fe and Pb impurities in ZnO substantially affect the cycle-life of the Zn electrode in Silver Oxide/Zn secondary batteries, Fe having a detrimental effect and Pb a beneficial effect. To study the role of impurities in more detail, samples of ZnO with varying Fe or Pb contents have been prepared, as well as two samples with added Al.

I. Introduction

The objective of this project has been to prepare and characterize a variety of zinc oxides for evaluation (by Delco-Remy) in silver oxide/zinc secondary batteries. The Fifth Quarterly Technical Progress Report (24 January 1968) contained a summary of the electrode evaluation data obtained by Delco-Remy. The data indicated improved electrode performance for 0.25 wt. % Pb-doped ZnO, possible improvements for Al-doped ZnO, and decreased performance with 0.07 wt. % Fe-doped ZnO. During the past quarter, samples have been prepared in an attempt to more clearly define the effects of these impurities, especially the minimum Fe content having a detrimental effect and the optimum Pb content for beneficial effects.

II. Sample Characterization Tests

The samples were characterized by the following tests: (1) air permeability particle size, (2) nitrogen adsorption surface area, (3) electron micrographs, (4) qualitative spectrographic and, where necessary, chemical analysis for specific impurities. Due to the detrimental effects observed for Fe, all samples were analyzed for Fe. Since much of the Fe normally present in undoped ZnO is regarded as "tramp" material resulting from atmospheric contamination, quantitative analytical results are complicated by sampling problems.

See the First Quarterly Technical Progress Report (31 January 1967) for a description of the characterization tests.

III. Description of Impurity-doped Zinc Oxides

The impurities were introduced by 600°C. air atmosphere calcination of an intimate admixture of a French Process ZnO and an oxide of the impurity. See the Second Quarterly Technical Progress Report (19 April 1967) for more information on doping of ZnO.

Characterization test data are given in Tables 1 and 2. The samples cover the approximate range 0.0003 to 0.01 wt. % Fe and 0.0008 to 2.4 wt. % Pb. Sample 243-135-1 was doped with both Fe and Pb with the thought that the Pb might counteract the adverse effects of Fe. Sample 243-131-2A is an uncalcined blend of iron oxide and ZnO which may give an indication of whether or not Fe must be in solid solution to cause detrimental effects.

X-ray diffraction evaluations of samples 243-107-2 and -3 suggest that not all of the Pb went into solid solution with the ZnO. The electron micrographs and surface area data for samples 243-139-1 and -2 show that very little of the Al entered the ZnO lattice. If the electrode evaluation results seem to warrant it, the question of impurity solid solution in the case of Pb and Al can be investigated more thoroughly.

IV. Future Program

The future program will depend on Delco-Remy's electrode evaluations currently in progress for the previously described samples.

V. Appendix

Electron micrographs at 25,200X are shown for each of the previously described samples.

TABLE 1

Characterization Test Data for Pb-, Fe-, and Al-doped ZnO Samples

Sample No.	Air Permeability Particle Size, μ	N_2 Adsorption Surface Area, M^2/G	Dopant Content (Wt. %) Fe	Pb	Al
243-127-2(1)	0.46	2.7	0.0003(2)	0.0008(2)	--
243-107-4	0.47	2.7	0.0003(2)	0.028	--
243-107-2	0.38	3.4	0.0003(2)	1.02	--
243-107-3	0.37	3.5	0.0004(2)	2.42	--
243-131-1	0.46	2.6	0.0006	--	--
243-131-2A(3)	0.36	3.5	0.0086	--	--
243-131-2B	0.46	2.6	0.0092	--	--
243-135-1	0.42	2.9	0.010	0.26	--
243-139-1	0.46	2.7	0.0010(2)	--	0.07
243-139-2	0.36	4.4	0.0008(2)	--	0.92

(1) Base ZnO calcined at 600°C. in air.
(2) Impurity present in the base ZnO.
(3) Not calcined.

TABLE 2

Qualitative Spectrographic Analysis Data for Pb-, Fe-, and Al-doped ZnO Samples

Element	243-127-2	243-107-4	243-107-2	243-107-3	243-131-1	243-131-2A	243-131-2B	243-135-1	243-139-1	243-139-2
Zn	vs	vs	vs	vs	vs	vs	vs	vs	vs	vs
Pb	vf-f	w	w-m	m	vf-f	vf-f	f-w	w-m	f+	f
Si	f-w	f-w	f-w	f-w	f	f	f	f	f	f
Fe	vf	vf	vf	vf	vf	f	f	f	xf-vf	xf-vf
Cu	vf-f	vf-f	vf	vf-f	xf-vf	vf	xf-vf	xf-vf	xf-vf	xf-vf
Al	vf	vf	vf	vf	vf	vf	vf	vf	w	w-m
Cd	xf	xf	xf	xf	xf	xf	xf	xf	xf	xf
Mg	xf	xf	xf	xf	xf	xf	xf	xf	xf	xf
B	xf	Trace	Trace	Trace	Trace	Trace	--	--	--	--
Bi	--	--	--	xf	--	--	--	--	--	--
Mn	Trace	Trace	Trace	Trace	Trace	xf	xf	xf	--	--
Sb	Trace	Trace	Trace	Trace	Trace	Trace	Trace	Trace	Trace	Trace

Legend:

vs - very strong
m - moderate
w - weak
f - faint
vf - very faint
xf - extremely faint

Figure 1. Sample 243-127-2 - French Process ZnO
Calcined 600°C. in Air
Particle Size = 0.46μ
Magnification = 25,200X

Figure 2. Sample 243-107-4 - French Process ZnO + 0.028% Pb
Calcined 600°C. in Air
Particle Size = 0.47μ
Magnification = 25,200X

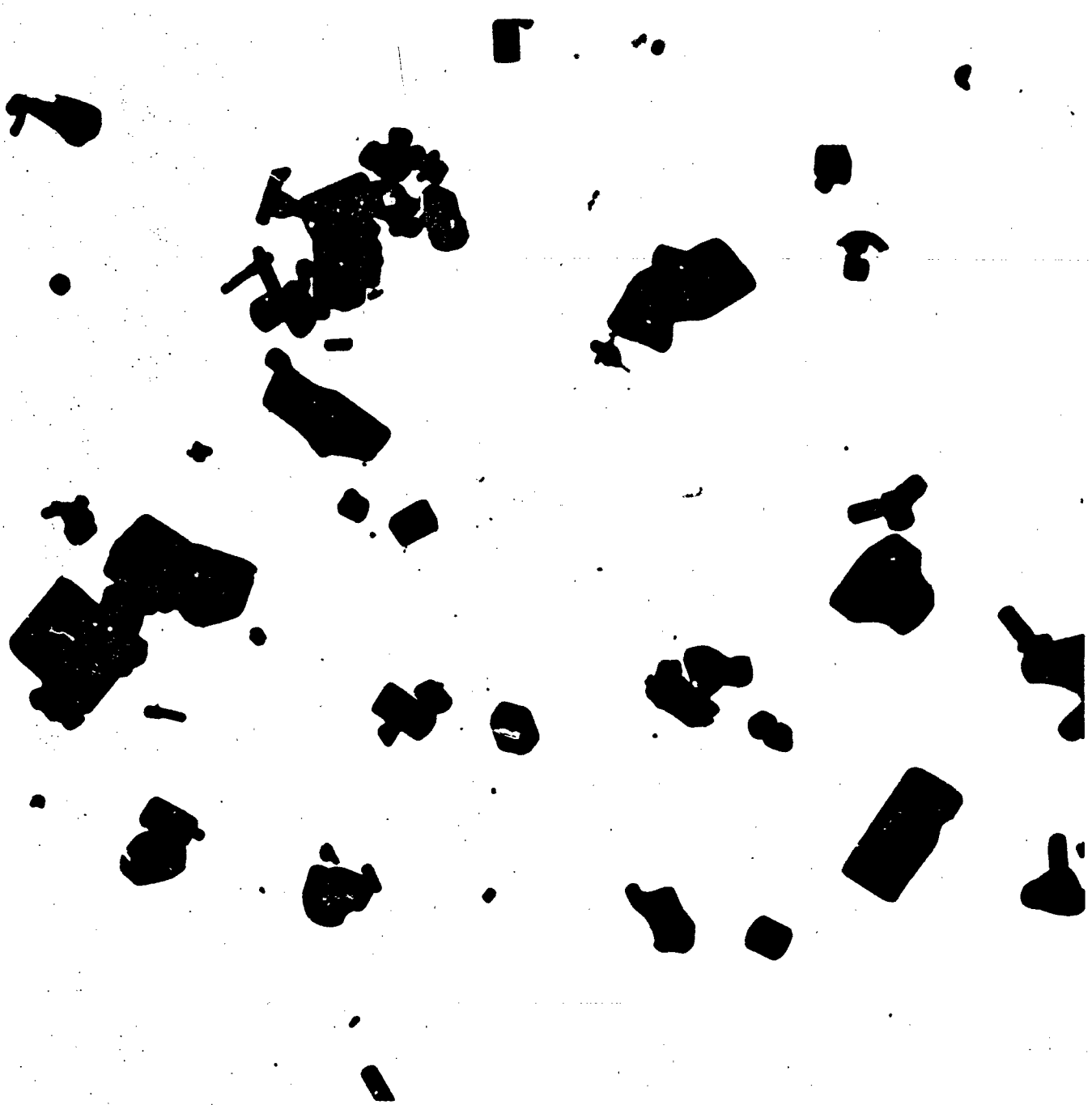

Figure 3. Sample 243-107-2 - French Process ZnO + 1.02% Pb
Calcined 600°C. in Air
Particle Size = 0.38μ
Magnification = 25,200X

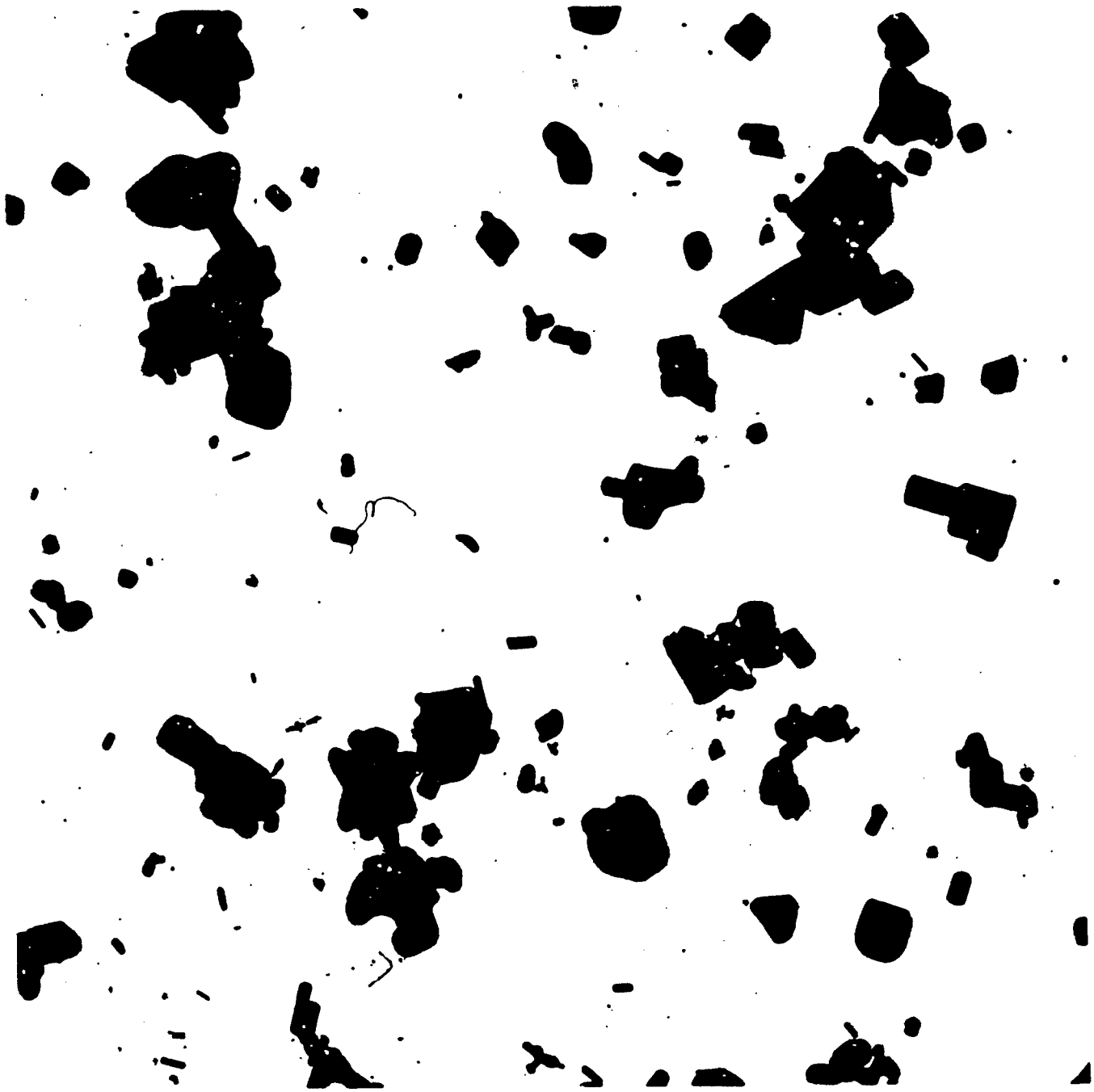

Figure 4. Sample 243-107-3 - French Process ZnO + 2.42% Pb
Calcined 600°C. in Air
Particle Size = 0.37μ
Magnification = 25,200X

Figure 5. Sample 243-131-1 - French Process ZnO + 0.0006% Fe
Calcined 600°C. in Air
Particle Size = 0.46μ
Magnification = 25,200X

Figure 6. Sample 243-131-2A - French Process ZnO + 0.0086% Fe
Not Calcined
Particle Size = 0.36μ
Magnification = 25,200X

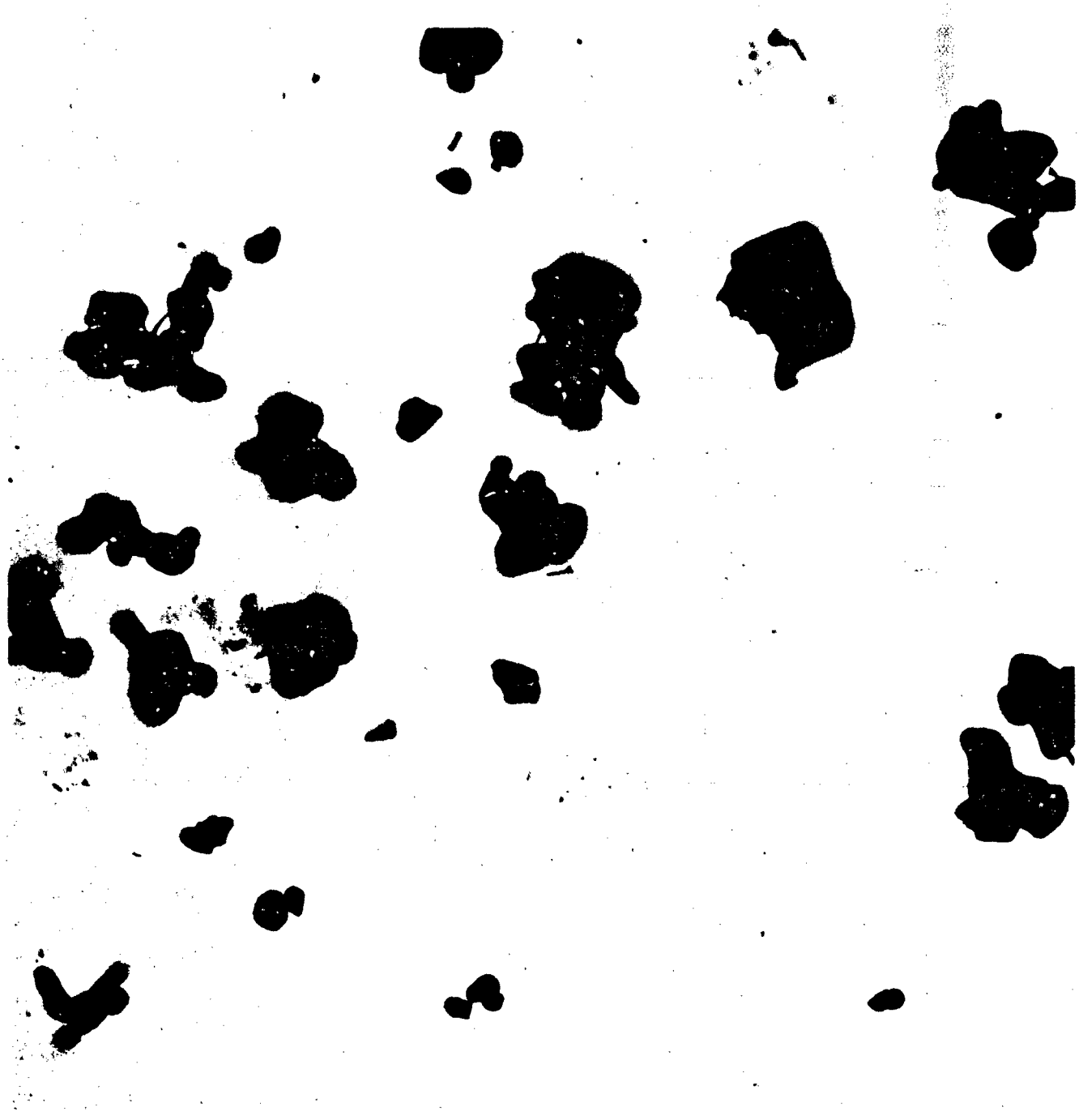

Figure 7. Sample 243-131-2B - French Process ZnO + 0.0092% Fe
Calcined 600°C. in Air
Particle Size = 0.46μ
Magnification = 25,200X

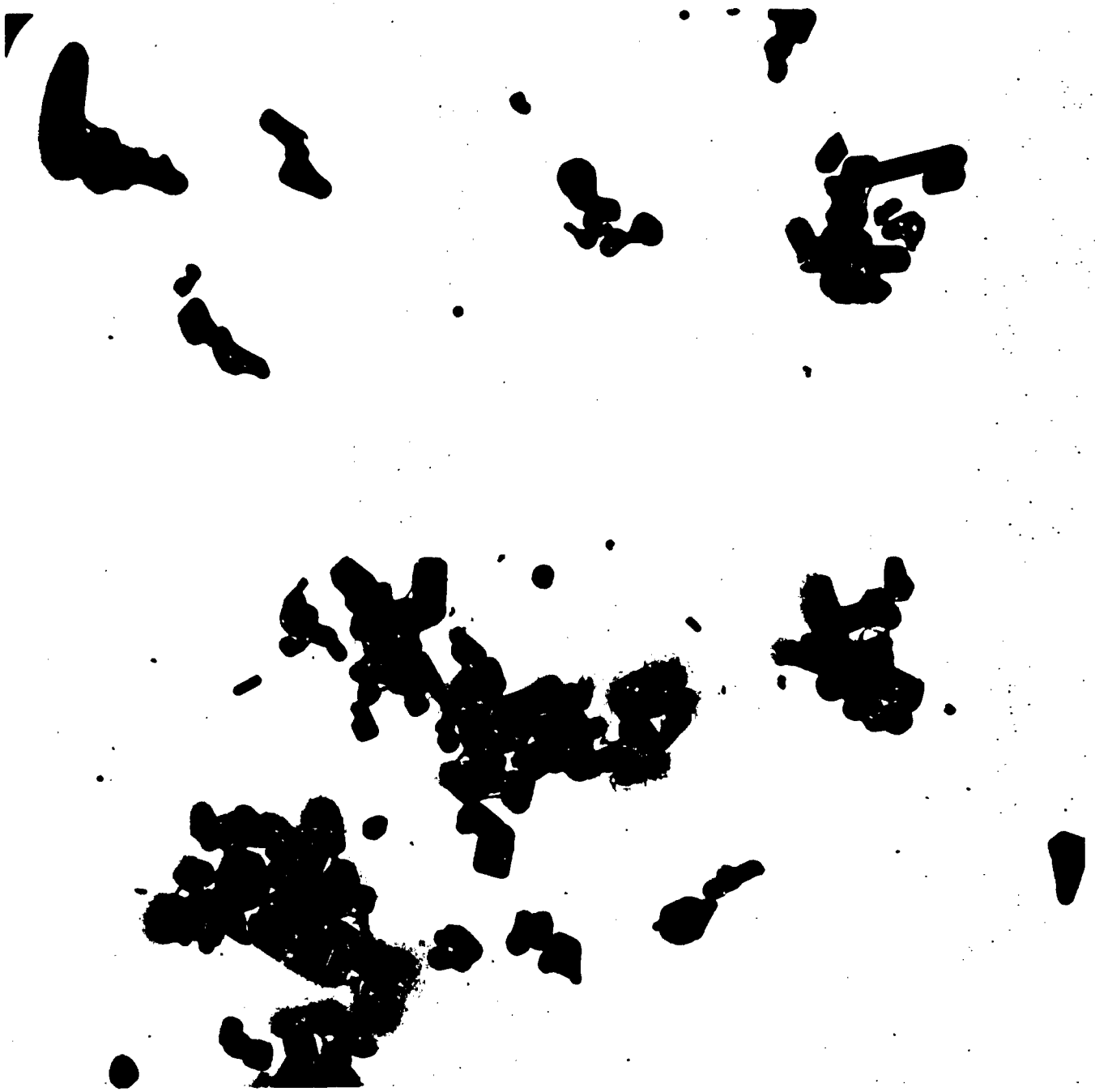

Figure 8. Sample 243-135-1 - French Process ZnO +
0.010% Fe + 0.26% Pb
Calcined 600°C. in Air
Particle Size = 0.42 μ
Magnification = 25,200X

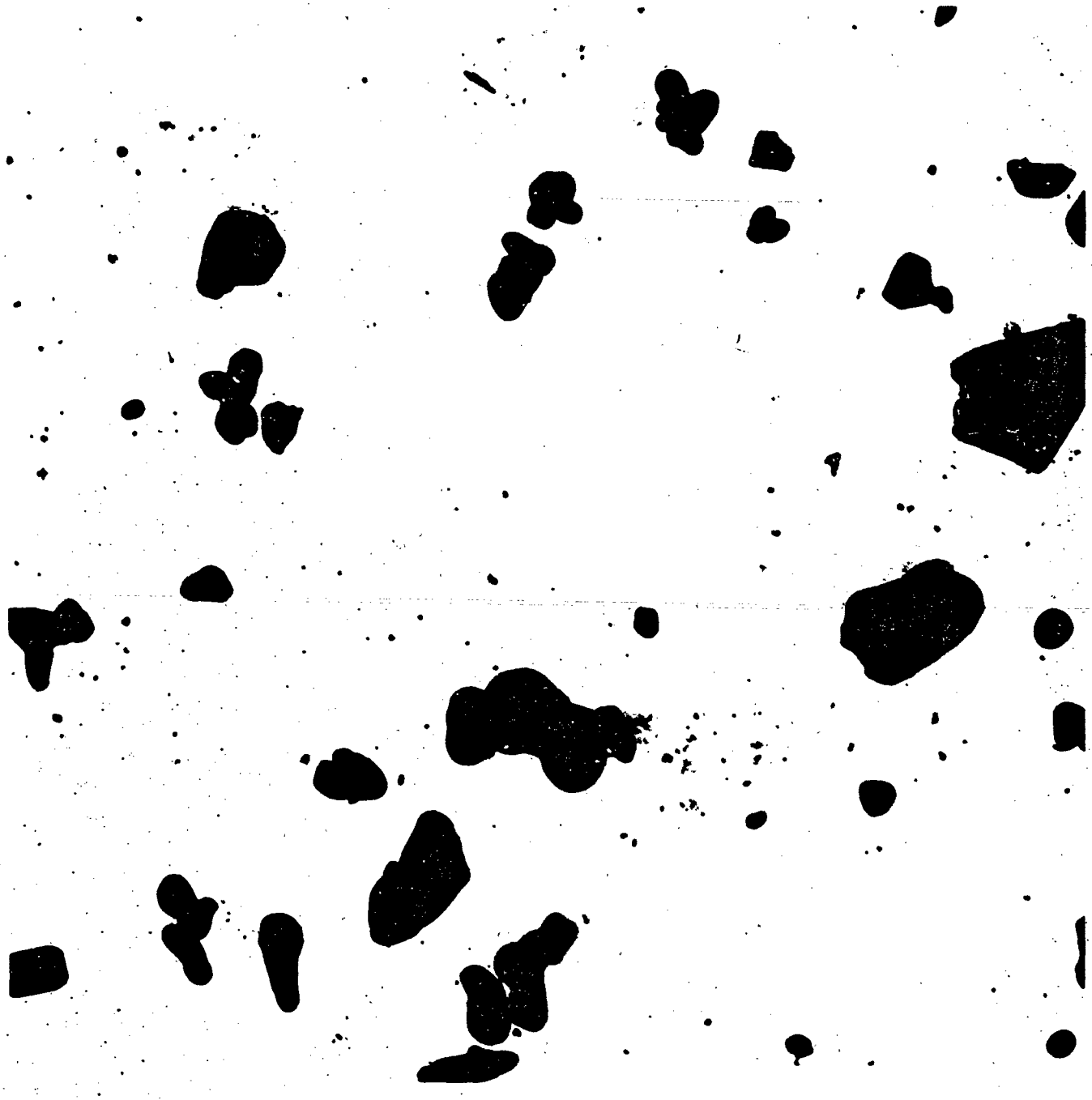

Figure 9. Sample 243-139-1 - French Process ZnO + 0.07% Al
Calcined 600°C. in Air
Particle Size = 0.46μ
Magnification = 25,200X

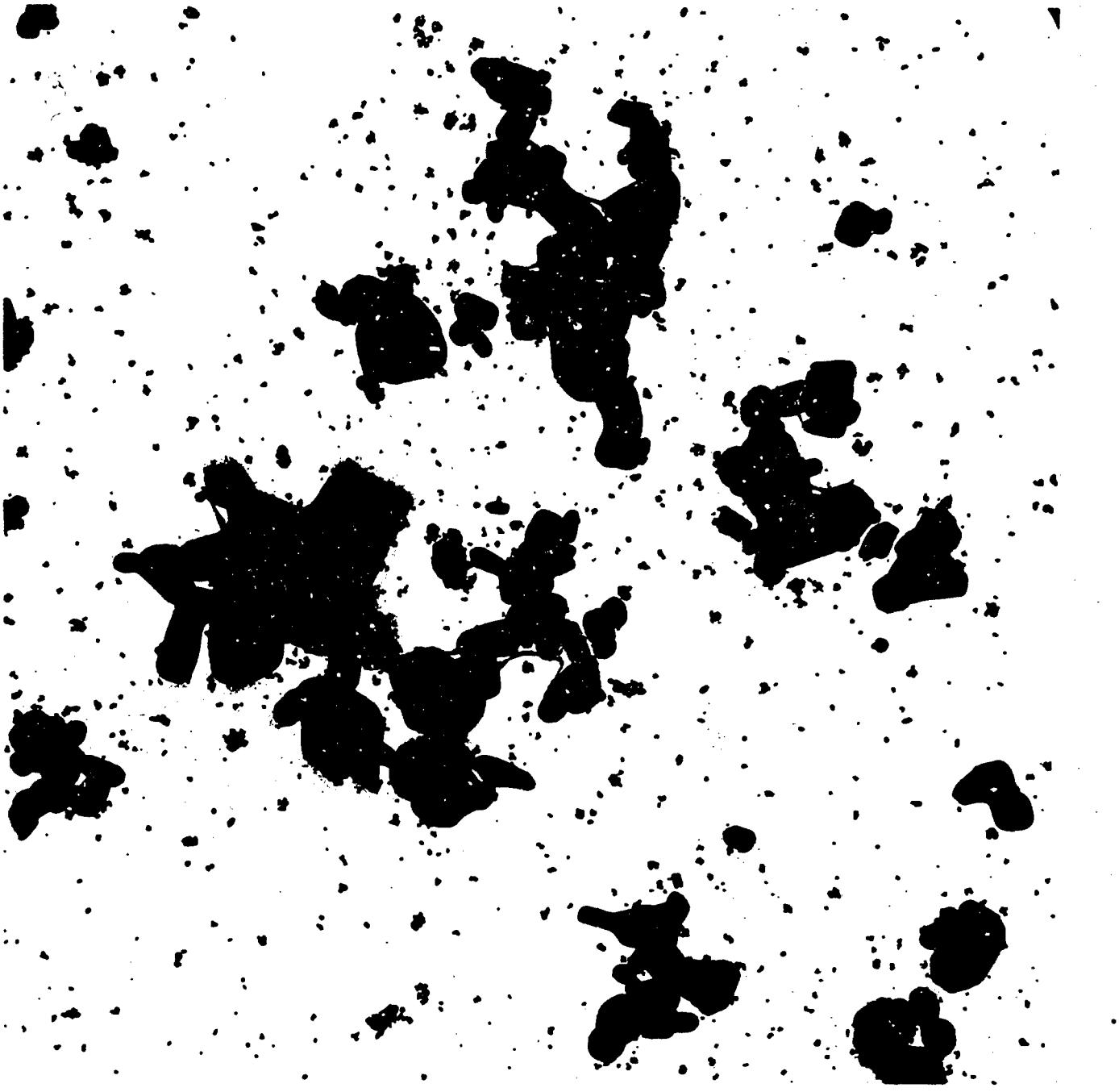

Figure 10. Sample 243-139-2 - French Process ZnO + 0.92% Al
Calcined 600°C. in Air
Particle Size = 0.36 μ
Magnification = 25,200X

APPENDIX III

ADSORPTION OF ORGANIC MATERIALS ON ZINC ELECTRODES

ADSORPTION OF ORGANIC MATERIALS ON ZINC ELECTRODES

Sixth Quarterly Technical Progress Report

Covering the Period

15 January 1967 to 14 April 1967

Purchase Order D-R 120111

Under Contract AF 33(615)-3487

Prepared by

Dewitt A. Payne

Hiroyasu Tacnikawa

Allen J. Bard

The University of Texas

Austin, Texas

Introduction

The capillary electrometer has been calibrated and measurements are now being made to determine the absolute values of the amount of Emulphogene adsorbed on mercury from KOH solution.

Measurements are being made on pure zinc and zinc amalgam electrodes in pure KOH to elucidate the reaction mechanisms and rate constants so that the effect of organic adsorption may be determined. Evidence accumulated so far points to this mechanism.

$$Zn + 2OH^- \rightleftarrows Zn(OH)_2^- + e$$

$$Zn(OH)_2^- \rightleftarrows Zn(OH)_2 + e$$

$$Zn(OH)_2 + 2OH^- \rightleftarrows Zn(OH)_4^{--} \quad \text{(fast)}$$

Both electron transfer steps appear to have similar rate constants. Preliminary measurements also show that addition of Emulphogene slows down both charge transfer steps. Measurement at a rotating zinc disk electrode indicates that both the cathodic and anodic overvoltages increase but the limiting current is about the same.

It has been possible to measure differential capacity at a pure zinc electrode and it was found that addition of Emulphogene lowered the differential capacity, but only at much higher concentrations of BC-720 than with a mercury of zinc amalgam electrode.

Experimental

A Lippmann capillary electrometer is being used to obtain electrocapillary data. The capillary was drawn from 1/2 millimeter capillary tubing and attached to a mercury reservoir which in turn is connected to a

pressurizing system. Coarse pressure adjustment is obtained by filling the system from a tank of water pumped nitrogen. Excess nitrogen is released through a fine needle valve. When the approximate pressure is reached, the system is closed and final adjustment is made with a large brass bellows in the system.

The capillary was calibrated with 0.1 N KCl solution using a 0.1 N calomel reference electrode with no liquid junction. The data used to calibrate the capillary was from Devanathan and Peries (1). The KCl solution was purified with activated charcoal and then electrocapillary curves were measured until there was agreement over the whole curve between our measured data and the data from the literature to at least 0.1 dyne/cm. KOH solutions are also purified with charcoal before addition of Emulphogene. Conductivity water from a Barnstead still was used to prepare solutions.

99.9999% pure zinc metal from Eagle-Picher was obtained and an electrode was constructed by casting the metal in a pyrex capillary under 10^{-6} mm Hg vacuum. When the glass had cooled, it was broken away from the resulting metal rod, a length of which was sealed in a teflon sleeve and made into a rotating disk electrode similar to the one previously described. The rates of the electrode reactions at the zinc and zinc amalgam electrodes were made with the instrument and cell previously described using both chronocoulometry and chronoamperometry. Preparation of zinc amalgam has been described previously.

Results

We have measured electrocapillary curves for mercury in 1 M KOH at several different concentrations of Emulphogene BC-720. We will soon have

enough data to determine surface concentrations of Emulphogene. Computer programs described previously will be employed in the analysis of the data.

Initial measurements of the rate of zinc ion reduction were made in 1 M KOH with millimolar Zn(II) at a mercury drop electrode using the chronocoulometric technique with large potential steps (2). In this technique a potential step is applied to the hanging drop electrode, and the total number of coulombs which pass, Q, are recorded as a function of time, t. The equation governing the variation of Q with t is (2):

$$Q = \frac{K}{\lambda^2}\left(\exp y^2 \operatorname{erfc} y + \frac{2y}{\sqrt{\pi}} - 1\right) \qquad (1)$$

where

$$K = nFAk_a^{\circ}\left[C_o\, e^{-\alpha nf(E-E^{\circ})} - C_R\, e^{(1-\alpha)nf(E-E^{\circ})}\right] \qquad (2)$$

$$y = \lambda t^{1/2}$$

$$\lambda = k_a^{\circ}\left[\frac{e^{-\alpha nf(E-E^{\circ})}}{\sqrt{D_o}} + \frac{e^{(1-\alpha)nf(E-E^{\circ})}}{\sqrt{D_R}}\right] \qquad (4)$$

$$f = F/RT$$

A plot of Q vs. $\sqrt{t}$ becomes linear for y>5, and shows an intercept on the $\sqrt{t}$ axis, $\sqrt{t_i}$, such that

$$\lambda = \sqrt{\pi}/2\sqrt{t_i} \qquad (6)$$

and allows the determination of λ. A plot of ln λ vs. E, in regions where one or the other terms in (4) are negligible shows a slope of $-\alpha nf$ or $(1-\alpha)nf$, and allows determination of α. A plot of log λ vs. E for a mercury drop electrode and zinc(II) in KOH is shown in Figure 1. These measurements produced values of αn, the charge-transfer coefficient-electron product, which were much lower than we had expected from the work previously published. Our measured product for the cathodic reaction was about 0.59. With 1mM

zinc amalgam in 1 M KOH, the anodic reaction was measured and for large potential steps, (1-α)n was about 0.37. Anodic steps in the presence of Emulphogene gave a value of about 0.34, but the potential stepped to had to be much more positive than without Emulphogene, indicating a much smaller apparent rate constant. Chronoamperometric measurements were made with high concentrations of Zn(II) or zinc amalgam and smaller potential steps. αn for the cathodic reaction was the same as for large potential steps, but for small anodic steps (1-α)n increased sharply to a value of 1.05. Also, the apparent rate constant of the anodic reaction was increased by increasing the KOH concentration, but the cathodic reaction rate was not affected.

It was impossible to obtain kinetic data from rotating disk data because of non-reproducibility. Rotating disk polarograms did show some general characteristics. Addition of Emulphogene caused half wave potentials to shift, but did not seriously affect the limiting current. Addition of Emulphogene also appeared to change the nature of the surface deposit. With no Emulphogene the deposit was rough and hard, but with Emulphogene a soft black deposit formed which could be wiped off revealing a relatively smooth surface underneath.

Cyclic voltammetric experiments experiments with a zinc amalgam electrode were undertaken to elucidate the electrochemical behavior further (Figure 2). These measurements showed some unusual effects. If a cyclic potential sweep was done on a fresh zinc amalgam drop in pure KOH with the initial sweep direction anodic, an extremely large distorted anodic current peak was observed. When the sweep direction was reversed, the cathodic current peak was much smaller than the anodic peak. Further sweeps produced anodic and cathodic peaks of about the same height and about the same size as the initial cathodic

peak. However, if the drop was allowed to stand in a stirred solution for several minutes prior to an experiment, the initial large anodic peak was much smaller, and similar to the cathodic peak height obtained on reversal. Differential capacity measurements at pure mercury drops in these solutions indicated a low concentration of organic material (perhaps a trace of Emulphogene) was present, and that slow adsorption of the organic substance was responsible for the anomalous behavior. It was found that stirring the solution greatly speeded up the achievement of adsorption equilibrium.

The effect of Emulphogene adsorption on a pure zinc (99.9999%) electrode was studied by performing cyclic voltammetric (Figure 3) and differential capacity (Figure 4) measurements. The differential capacity data at the pure zinc electrode indicates that Emulphogene BC-720 is adsorbed. Rotating disk electrode data indicates that adsorption of BC-720 only affects the charge-transfer apparent rate constants as adsorption does not seem to alter the limiting diffusion current.

Discussion

Hampson et. al. (3) in their extensive work on the alkaline zinc electrode indicate that the zinc charge transfer reaction occurs in two steps at the solid zinc electrode.

$$(ZnOH)^-_{ad} \rightarrow (ZnOH)_{ad} + e$$

$$(ZnOH)_{ad} + OH^- \rightarrow Zn(OH)_2 + e$$

Our experimental evidence does not support the possibility of specific adsorption of any zinc species on the mercury or zinc amalgam electrode; however, our present experimental evidence does support a mechanism involving consecutive electron transfer steps. First, there is the low value of αn and

(1-α)n for large potential steps. These values indicate that there is only one electron in the rate determining charge transfer step. Second there is the sharp change in the value of (1-α)n for the anodic reaction between small potential steps and large steps (Figure 1). Taken together these results suggest a consecutive electron transfer mechanism.

Since for the limit of large potential steps, the first electron added (or removed) becomes the rate controlling step; and the cathodic reaction rate constant is unaffected by KOH concentration while the anodic reaction is affected we propose the following mechanism:

$$Zn + mOH^- \rightarrow Zn(OH)_m^{1-m} + e$$

$$Zn(OH)_m^{1-m} \rightarrow Zn(OH)_m^{2-m} + e$$

$$Zn(OH)_m^{2-m} + (4-m)OH^- \rightarrow Zn(OH)_4^{2-}$$

From the data of previous experimenters, m is probably equal to 2. No quantitative figures for the rate constants of the two steps are given because m has not been absolutely determined, and because there may have been some distortion of the anodic figures from the organic contamination previously noted. We plan to perform the anodic experiments again in carefully purified and tested solutions and make quantitative measurements of the rate constants.

Literature Cited

(1) M.A.V. Devanathan and P. Peries, Trans. Faraday Soc., 50, 1236 (1954).

(2) J. H. Christie, G. Lauer and R. A. Osteryoung, J. Electroanal. Chem., Chem., 7, 60 (1964).

(3) N. A. Hampson, Ph.D. Thesis, University of London, 1966. J. P. G. Farr, and N. A. Hampson, J. Electroanal. Chem. 13, 433 (1967). J. P. G. Farr and N. A. Hampson, Trans. Faraday Soc., 62, 3493 (1966).

List of Figures

Fig. 1 Log Lambda vs. Potential

(Lambda is proportional to the sum of the anodic and cathodic rate constants. The slope of the log plot is proportional to the charge transfer coefficient)

. points = Hg drops in Zn(II) 1 and 2 M KOH
θ points = Zn(Hg) in 1 M KOH
X points = Zn(Hg) in 2 M KOH

Fig. 2 Cyclic Potential Scan

1 mM Zn(Hg), 1 M KOH, 0.032 cm^2 area, 50 mV/sec sweep rate
Potential in volts vs. sat. Ag, AgCl, current in microamps
line 1 first cycle
line 2 second cycle

Fig. 3 Cyclic Potential scan

pure zinc (99.9999%) in 10 M KOH
Potential in volts, Current in microamps
a no Emulphogene
b 2×10^{-2} g/ml BC-720

Fig. 4 Differential Capacity
Pure zinc in 10 M KOH
1 no Emulphogene
2 2×10^{-3} g/ml BC-720
3 4×10^{-3}
4 10^{-2}
5 2×10^{-2} g/ml BC-720

fig.1

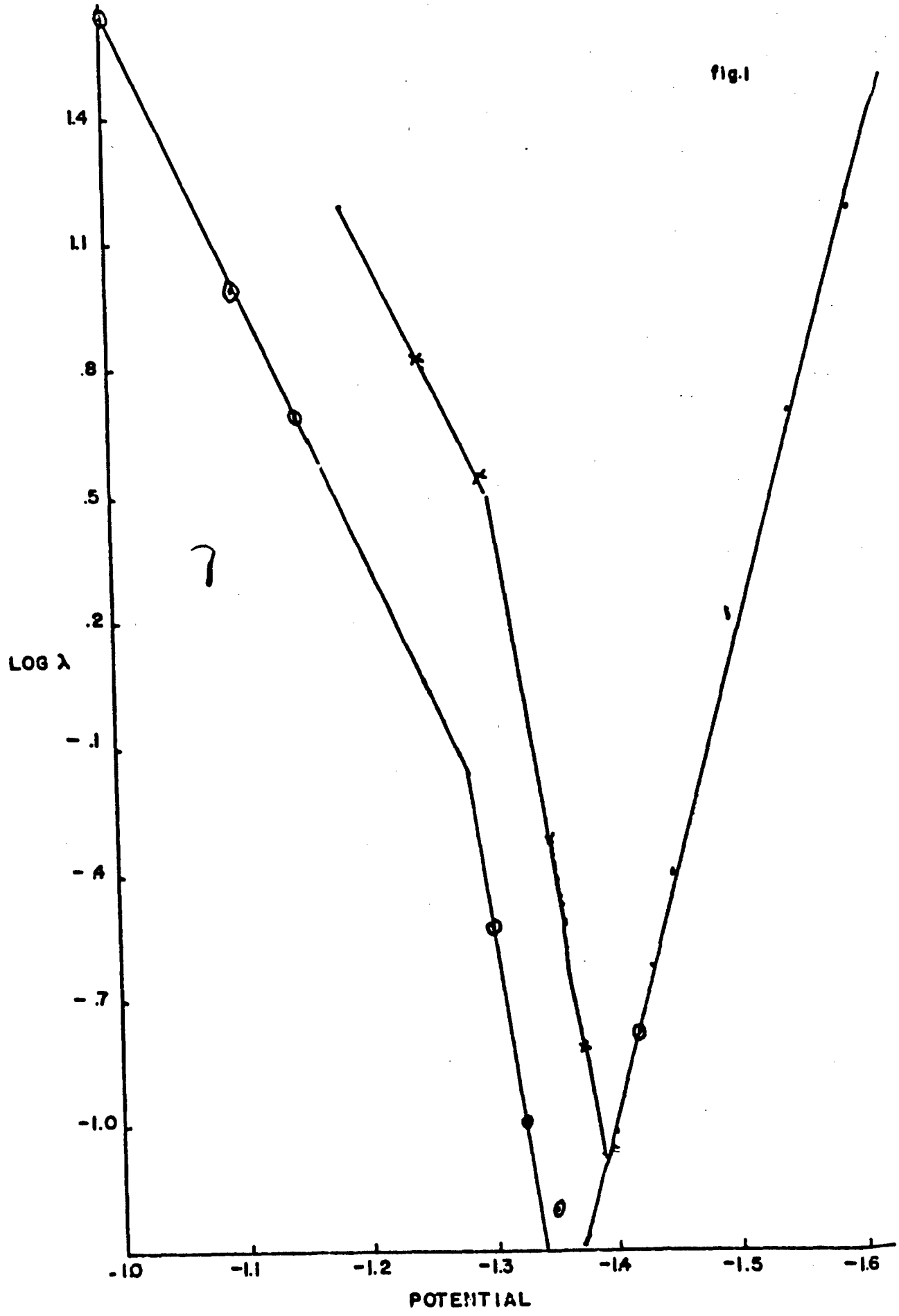

fig. 2

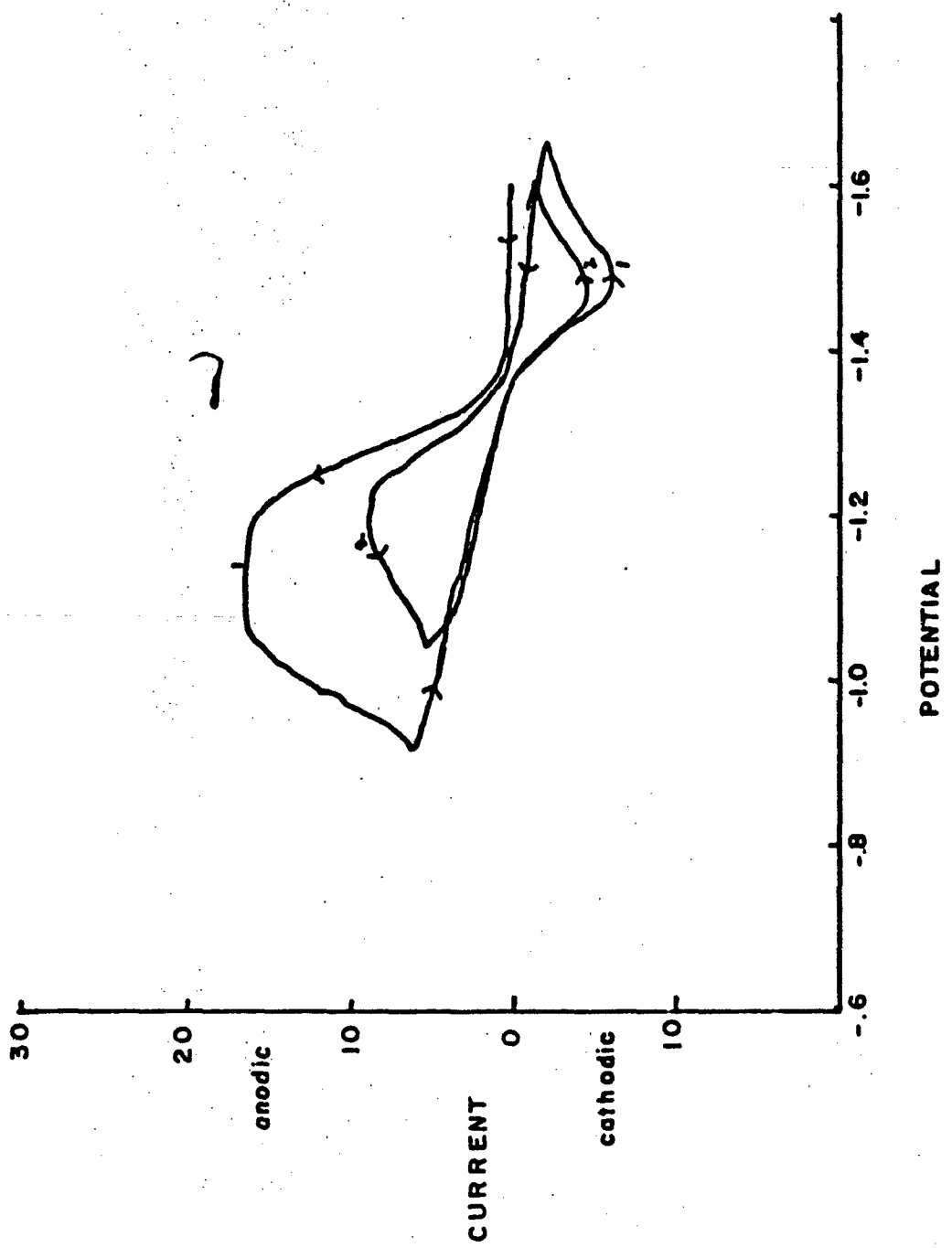

fig.3

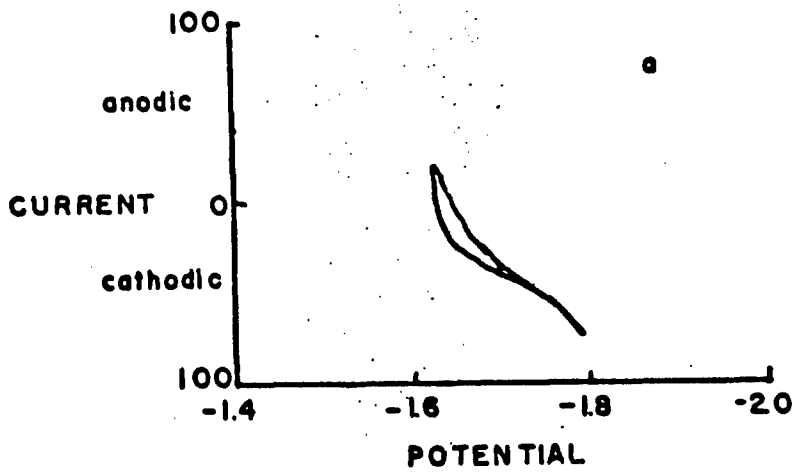
100
anodic
CURRENT
0
cathodic
100
-1.4
-1.6
-1.8
-2.0
POTENTIAL
a

7

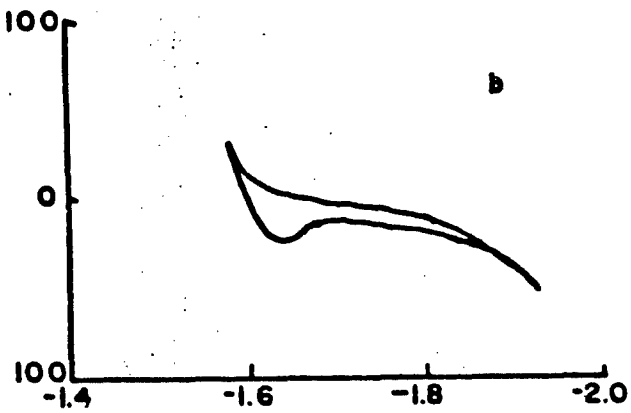
100
0
100
-1.4
-1.6
-1.8
-2.0
b

fig. 4

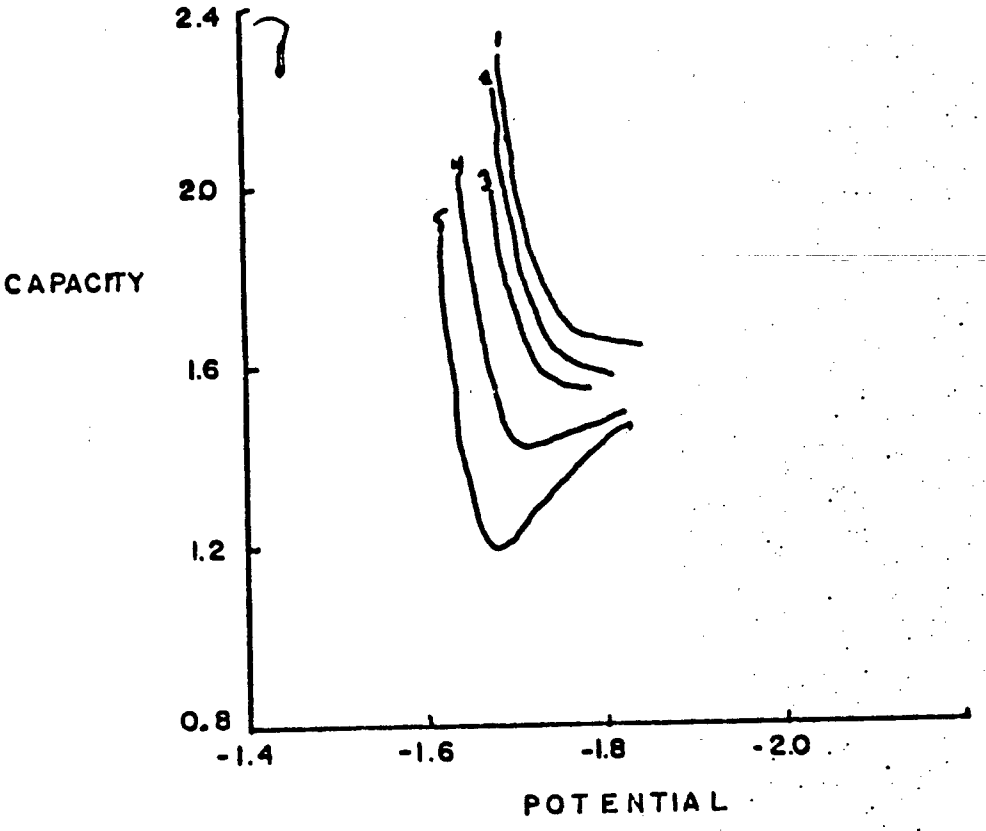

APPENDIX IV

INFLUENCE OF MEMBRANE TRANSPORT CHARACTERISTICS ON ELECTROLYTE CONCENTRATION AND CONSEQUENT PLATE PERFORMANCE

THIRD QUARTERLY REPORT

March 1968 - May 1968

INFLUENCE OF MEMBRANE TRANSPORT CHARACTERISTICS ON ELECTROLYTE CONCENTRATION AND CONSEQUENT PLATE PERFORMANCE

By

A. H. Remanick, M. Shaw and W. I. Nelson

D-R 196419
Contract No. AF 33(615)3487

Prepared for
Delco - Remy
Division of General Motors
Anderson, Indiana
46011

Whittaker CORPORATION
NARMCO RESEARCH & DEVELOPMENT DIVISION
3540 Aero Court · San Diego, California 92123

SUMMARY

In the investigation of the charge characteristics of cadmium plates, it has been found that the most critical factor is the decrease of charge acceptance at lower temperatures. Variation in concentration changes indicate better charge acceptance at higher concentration.

The study of the discharge characteristics of zinc plates indicates a marked change in capacity as a function of concentration. The capacity-concentration relationship appears to exhibit a maximum in 5.0 m KOH at 30° C. At 0° C, the maximum has shifted to 5.0 m KOH.

I. INTRODUCTION

Whittaker Corporation is presently engaged in a program intended to mathematically describe the various operational and design factors influencing the characteristics of silver-zinc and silver-cadmium batteries. Although other studies of plate characteristics exist, the available data is not readily amenable to mathematical reduction. Furthermore, the range of conditions within these studies is not sufficiently wide.

Previous work has described the charge and discharge characteristics of silver plates. In addition, the discharge characteristics of cadmium plates were also investigated. During the present period, work on the charge acceptance of cadmium plates has been completed. In addition, investigation of the discharge characteristics of zinc plates was initiated.

II. RESULTS

A. Cadmium Plate Charge Acceptance

As detailed in previous reports, a standard method of plate formation is necessary in order to avoid apparent changes due to differences in plates. Conditions for plate preparation are charge at 30 ma/in^2 and discharge at 60 ma/in^2 in 8.0 m KOH at 30° C. The charge cutoff voltage is 1.05 v vs Hg-HgO, while the discharge cutoff is 0.75 v. To establish consistent characteristics of the pressed powder plates, it was necessary to cycle them at least ten times. Results of the last two standard cycles were used for test comparisons. Charge tests were carried out at current densities of 15, 30, 60, and 120 ma/in^2, at temperatures of 30°, 0°, and -20° C. Electrolyte concentrations were 2.5, 5.0, 8.0 and 10.7 m KOH at the two high temperatures, while 5.0, 8.0 and 10.7 m KOH were used at -20° C. Duplicate cells were run under all conditions. Test results are presented in Tables I, II, and III.

B. Zinc Plate Discharge

As anticipated, study of the electrolyte concentration effect on zinc electrode characteristics did not proceed as facilely as the corresponding silver and cadmium plate studies. This was due to the high solubility of zincate ion in alkaline electrolyte. The attendant reduction of zincate at the counterelectrode would invalidate any data thereby derived. Further-

TABLE I

CADMIUM PLATE CHARGE, 30° C

C. D. ma/in^2	Conc. m	V_i Volts	Accep. %
15	2.5	0.925	97.5
15	5.0	0.930	100.0
15	8.0	0.924	101.0
15	10.7	0.922	102.0
30	2.5	0.923	81.8
30	5.0	0.932	86.7
30	8.0	0.926	101.0
30	10.7	0.928	102.0
60	2.5	0.946	82.7
60	5.0	0.944	88.1
60	8.0	0.934	97.4
60	10.7	0.936	97.8
120	2.5	0.962	57.6
120	5.0	0.961	67.3
120	8.0	0.944	81.3
120	10.7	0.945	77.8

V_i = Initial stable plateau voltage

$$\% \text{ Acceptance} = \frac{\text{amp-hrs in (test charge)}}{\text{amp-hrs in (standard charge)}} \times 100$$

TABLE II

CADMIUM PLATE CHARGE, 0° C

C. D. ma/in^2	Conc. m	V_i Volts	Accep. %
15	2.5	0.952	40.7
15	5.0	0.949	62.4
15	8.0	0.942	78.8
15	10.7	0.934	85.0
30	2.5	0.958	21.2
30	5.0	0.963	41.7
30	8.0	0.951	71.4
30	10.7	0.940	78.9
60	2.5	0.973	7.1
60	5.0	0.976	21.4
60	8.0	0.961	61.5
60	10.7	0.949	70.2
120	2.5	1.007	6.0
120	5.0	0.997	16.1
120	8.0	0.981	45.1
120	10.7	0.962	59.4

V_i = Initial stable plateau voltage

$$\% \text{ Acceptance} = \frac{\text{amp-hrs in (test charge)}}{\text{amp-hrs in (standard charge)}} \times 100$$

TABLE III

CADMIUM PLATE CHARGE, -20° C

C. D. ma/in^2 (a)	Conc. m	V_i Volts	Accep. %
15	5.0	1.005	1.9
15	8.0	0.987	20.8
15	10.7	0.974	27.8
30	5.0	0.000	00.0
30	8.0	1.016	10.1
30	10.7	0.986	16.3

V_i = Initial stable plateau voltage

$$\% \text{ Acceptance} = \frac{\text{amp-hrs in (test charge)}}{\text{amp-hrs in (standard charge)}} \times 100$$

(a) At current densities of 60 and 20 ma/in^2, no cells exhibited charge acceptance below the standard cutoff.

more, the physical relationship of the zinc plate in an open test cell is sufficiently different from that in a silver-zinc battery, so as to invalidate any plate evaluation by this method. On the other hand, it has been demonstrated that in the tightly wrapped configuration of a typical battery, there is a definite concentration change during cell operation. In order to achieve some compromise in which excess electrolyte would be available for the test cell, and yet provide a method for providing sufficient plate integrity, the plate was wrapped with two types of separators. The first wrap was a polypropylene felt. Use of this type of material was not expected to inhibit electrolyte diffusion because of the essentially macroscopic pores in the material. Furthermore, the relatively large void volume provided excess electrolyte. Several layers of Visking V-7 membrane were then wrapped around the plate. The entire plate stack was placed in the test cell under slight compression.

Although the membrane will absorb electrolyte, resulting in a change of initial concentration because of the ratio of membrane to electrolyte used, this is generally less than one unit in molality. The problem of zincate diffusion and absorption by the membrane must also be considered. The absence of zinc deposition at the counterelectrode indicates that sufficient membrane is available to stop zincate diffusion. Furthermore, the charge-discharge characteristics of the plates are reasonably uniform under a standard charge-discharge regimen. It appears, therefore, that zincate

absorption does not markedly alter the plate characteristics. Physical examination of the cell pack after a few cycles has indicated that the described methods apparently maintain sufficient plate integrity for the few cycles necessary for each plate standardization and test. Since initial testing indicated a marked difference between plates, four plates were tested under each set of experimental conditions.

A standard formation procedure consisted of discharge at 60 ma/in^2 followed by three charge-discharge cycles at the same current density. A final charge at 60 ma/in^2 prepared the plates for the test discharge. Formation was accomplished at 30° C.

The concentration of electrolyte used for the plate formation was the same as that used in the tests. This is in opposition to the procedure used for the silver and cadmium plates which were formed in 8.0 m KOH and then tested in the appropriate electrolyte. The physical condition of the plate after formation did not allow removal of the original electrolyte. Sufficient electrolyte was present in the cell to negate changes of concentration due to hydrogen and oxygen removal at the counterelectrode during the charge-discharge cycle. Discharge was cutoff at 1.10 v vs Hg-HgO. This is about 250 mv below the ocv.

Results of the discharge tests at 60, 120, and 240 ma/in^2 at 30° C and 0° C for concentrations of 2.5, 5.0, 8.0, and 10.7 m KOH are presented in Tables IV and V. Testing at-20° C is in progress.

TABLE IV

ZINC PLATE DISCHARGE, 30° C

C. D. ma/in^2	Conc. m	V_i Volts	Regulation 50 mv %	Regulation 100 mv %	Capacity %
60	2.5	1.275	49	75	96.9
60	5.0	1.318	22	79	94.9
60	8.0	1.336	18	62	92.4
60	10.7	1.345	22	41	90.9
120	2.5	1.266	71	95	61.5
120	5.0	1.270	36	75	82.3
120	8.0	1.286	22	50	68.3
120	10.7	1.279	25	54	76.4
240	2.5	1.200	56	96	35.1
240	5.0	1.212	62	95	49.6
240	8.0	1.260	53	69	38.3
240	10.7	1.232	65	88	40.3

V_i = Initial plateau voltage

$$\% \text{ Regulation } 50 \text{ mv} = \frac{\text{amp-hrs out (to 50 mv below } V_i)}{\text{Total amp-hrs out}} \times 100$$

$$\% \text{ Regulation - 100 mv} = \frac{\text{amp-hrs out (to 100 mv below } V_i)}{\text{Total amp-hrs out}} \times 100$$

TABLE V

ZINC PLATE DISCHARGE, 0° C

C. D. ma/in^2	Conc. m	V_i Volts	Regulation 50 mv %	Regulation 100 mv %	Capacity %
60	2.5	1.243	74	92	46.0
60	5.0	1.278	24	77	76.9
60	8.0	1.278	27	46	56.0
60	10.7	1.287	47	64	47.5
120	2.5	1.251	50	84	9.0
120	5.0	1.250	30	68	33.9
120	8.0	1.267	40	67	28.2
120	10.7	1.273	29	59	23.3
240	2.5	1.151	93	(a)	2.8
240	5.0	1.210	51	92	13.3
240	8.0	1.201	51	85	11.6
240	10.7	1.180	65	(a)	6.3

V_i = Initial plateau voltage

$$\% \text{ Regulation - 50 mv} = \frac{\text{amp-hrs out (to 50 mv below } V_i)}{\text{Total amp-hrs out}} \times 100$$

$$\% \text{ Regulation - 100 mv} = \frac{\text{amp-hrs out (to 100 mv below } V_i}{\text{Total amp-hrs out}} \times 100$$

(a) V_i too low to measure 100 mv decrease before cutoff

III. DISCUSSION

A. Cadmium Plate Charge Acceptance

There is a similarity between the charge acceptance of cadmium plates and the results of the discharge tests previously reported. Thus, there is a marked decrease in charge acceptance as a function of increasing current density and decreasing temperatures as well as concentration. The most marked effect is that of temperature. This is reflected in complete lack of charge acceptance at -20° C for current densities of 60 and 120 ma/in^2.

At 30° C, concentration effects begin to appear immediately after changing current densities from 15 to 30 ma/in^2. The most pronounced effect occurs between 2.5 and 5.0 m, although the percent acceptance is measurably decreased between 5.0 and 8.0 m. Little difference was noted between current densities of 30 and 60 ma/in^2. Increasing the current density to 120 ma/in^2 causes a marked decrease at all concentrations. Again, the most noticeable decrease is at 2.5 m KOH.

The results at 0° C resemble those at 30° C, in that a marked decrease in charge acceptance occurs at 2.5 m KOH. In addition, increasing the current density causes an almost complete loss of acceptance at 2.5 M KOH.

At -20° C, the effect of current density is considerably more pronounced. No charge acceptance occurs at all at 60 or 120 ma/in^2. At 15 or 30 ma/in^2, the total capacity is essentially zero in 5.0 m KOH, while a marked decrease in capacity occurs at 8.0 m and 10.7 m KOH.

We have not detailed the percent regulation of the cadmium plates, defined as

$$\text{Percent regulation} = \frac{\text{amp-hrs in (to 50 mv above } V_i)}{\text{Total amp-hrs in}} \times 100$$

since in all cases, the voltage rise during the major portion of the charge test was relatively low. In all cases, percent regulation on charge was at least 85%.

As stated previously, charge acceptance was terminated 150 mv above ocv. This value was chosen since it represented an inflection point in the charge curve. In some of the tests at low temperature, charging was allowed to rise above this point, since the acceptance to 150 mv above ocv was rather brief. As expected, mixed potential due both to the plate reaction and oxygen evolution was observed. This potential was not fixed, and rose during the measurements from 1.3 v to 1.6 v (vs Hg-HgO). Although some charging of the cadmium plates occurred, the total acceptance was rather erratic under these conditions.

B. Zinc Plate Discharge

The zinc plates used in the tests exhibited about a thirty percent variation

in total capacity. This was not unexpected from pressed powder zinc plates. Some plates exhibited relative characteristics quite different from those within a certain test group. This usually occurred with plates having a lower capacity. Data obtained from these plates was disregarded if it differed significantly from that obtained from the other three plates within the test run. Even with those plates having reasonably similar nominal capacities, some data scatter was evident, particularly at the higher current densities. Percent capacity variation was usually within ten percent, although variation in percent regulation sometimes exceeded this value. Data was not used in those cases where the regulation differed markedly from that of other plates within the test group.

Since it was necessary to carry out the plate formation standardization in the same concentration as used for the tests, it may be argued that the discharge tests may not only reflect the changes due to the test variations, but also the variation due to concentration of the forming electrolyte. However, the similarity of the discharge data obtained at 60 ma/in^2 at 30° C, implies that concentration does not alter the discharge characteristics under these conditions. Since the plates were charged at 60 ma/in^2, it is probable that the concentration during charge may not affect the discharge characteristics. This does not imply that the charge characteristics are independent of concentration, but does indicate that under the conditions employed (60 ma/in^2, 30° C), little effect is expected. Further clarification of this point can be expected

after the charge tests are completed.

In contrast to the discharge of silver and cadmium plates, the discharge curves for zinc plate exhibit a greater slope, necessitating a lower cut-off voltage. Also, in order to more adequately describe the shape of the discharge curve, it was necessary to determine the percent regulation at both 50 mv and 100 mv below the initial voltage. The lack of a stable plateau also necessitated a more arbitrary choice of the initial voltage. This was usually chosen at a point where the initial slope became constant.

The results at 30° C indicate that there is an apparent maximum in percent capacity at 5.0 m KOH. This is evidenced primarily at 60 ma/in^2 although it is also demonstrated at 120 ma/in^2. Better regulation is indicated at the lower concentrations, although this may be partially due to the fact that the initial voltage loss is greater at the lower concentrations, such that a flatter discharge from a lower initial voltage is indicated. Although still prevalent, this effect is not as significant for the percent regulation at 100 mv below V_i.

Comparison of the results at 0° C indicates a decrease of capacity under all conditions, the decrease being dependent on temperature and current density. A maximum in percent capacity is again evident, but at a concentration of 5.0 m KOH. Increasing the current density causes a substantial loss of capacity at 0° C. The change of V_i is relatively

uniform under all conditions, although the variation in percent regulation appears not to follow the pattern shown at 30° C. It is not unlikely that this is an artifact of changes in initial voltage.

BEST AVAILABLE COPY

Security Classification

DOCUMENT CONTROL DATA - R&D

(Security classification of title, body of abstract and indexing annotation must be entered when the overall report is classified)

1. ORIGINATING ACTIVITY (Corporate author) Delco-Remy Division General Motors Corporation Anderson, Indiana	2a. REPORT SECURITY CLASSIFICATION Unclassified 2b GROUP

3. REPORT TITLE

Silver-Zinc Electrodes and Separator Research

4. DESCRIPTIVE NOTES (Type of report and inclusive dates)

Technical Report 3 September 1968

5. AUTHOR(S) (Last name, first name, initial)

J. A. Keralla

6. REPORT DATE 3 September 1968	7a. TOTAL NO. OF PAGES	7b. NO. OF REFS
8a. CONTRACT OR GRANT NO. AF33(615)-3487 b. PROJECT NO. 3145 c. Task No. 314522 d.	9a. ORIGINATOR'S REPORT NUMBER(S) 9b. OTHER REPORT NO(S) (Any other numbers that may be assigned this report) AFAPL-TR-68-115	

10. AVAILABILITY/LIMITATION NOTICES

Foreign announcement and dissemination of this report by DDC is not authorized.

11. SUPPLEMENTARY NOTES	12. SPONSORING MILITARY ACTIVITY Aero Propulsion Laboratory, Air Force Systems Command, Wright-Patterson AFB, Ohio

13. ABSTRACT

Carbowaxes in a molecular weight range of 1000 give comparable cycle life with Emulphogene BC-610. As carbowaxes are linear polyethyleneoxide polymers and as Emulphogenes contain a polyethylene oxide chain, it is surmised that the polyethyleneoxide structure is active in promoting cycle life.

The addition of .25% Pb in ZnO tends to reduce agglomeration of the formed zinc and to prolong cycle life.

The limit of .010% Fe in ZnO is tolerable for satisfactory cycle life.

The use of CaO in the negative material to produce insoluble sites for zincate stoppage is not satisfactory.

Some evidence of pore sizes of various separator membranes have been found through electron microscope studies.

Increasing the stoichiometric ratio of formed zinc is not practical in terms of redesigning the present cell because of increased volume with a small increase in cycle life.

The 90 Mrad precrosslinked Bakelite 0602 polyethylene base, radiation grafted methacrylic acid membrane is suitable for use as a separator in secondary silver-zinc batteries.

DD FORM 1 JAN 64 1473

UNCLASSIFIED

Security Classification

BEST AVAILABLE COPY